

Stony Brook University



OFFICIAL COPY

The official electronic file of this thesis or dissertation is maintained by the University Libraries on behalf of The Graduate School at Stony Brook University.

© All Rights Reserved by Author.

Role of Fluid Shear Modulation on Bone Cell Metabolism during High-Frequency Oscillatory Vibrations

A Dissertation Presented

by

Gunes uzer

to

The Graduate School

in Partial Fulfillment of the

Requirements

for the Degree of

Doctor of Philosophy

in

Biomedical Engineering

Stony Brook University

December 2012

Copyright by
Gunes Uzer
2012

Stony Brook University

The Graduate School

Gunes Uzer

We, the dissertation committee for the above candidate for the

Doctor of Philosophy degree, hereby recommend

acceptance of this dissertation.

**Stefan Judex, Ph.D. –Dissertation Advisor
Professor
Biomedical Engineering**

**Mary D. Frame, Ph.D. - Chairperson of Defense
Associate Professor and Vice Chair
Biomedical Engineering**

**Clinton T. Rubin, Ph.D.
Distinguished Professor and Chair
Biomedical Engineering**

**Janet Rubin, M.D. – External Member
Professor of Medicine
Division of Endocrinology and Metabolism
University of North Carolina, Chapel Hill**

This dissertation is accepted by the Graduate School

Charles Taber
Interim Dean of the Graduate School

Abstract of the Dissertation

Role of Fluid Shear Modulation on Bone Cell Metabolism during High-Frequency Oscillatory Vibrations

by

Gunes uzer

Doctor of Philosophy

in

Biomedical Engineering

Stony Brook University

2012

Human, animal and cell studies indicate that the application of vibrations can be anabolic and/or anti-catabolic to bone. Dynamic oscillations create a complex mechanical environment which generates forces not only through accelerations but also through fluid forces. The specific mechanical signal which cells respond has not been identified, in-part because the generated fluid shear is coupled with the magnitude of the applied acceleration in most *in vivo* and *in vitro* studies. Looking at how these two mechanical parameters previously proposed to drive the cellular response to vibration – fluid shear and accelerations, act together is critical for understanding their effects on bone cell metabolism.

Overall aim of this dissertation was 1) Quantify the vibration-induced fluid shear stresses *in vitro* and test whether the separation of two mechanical parameters is possible to identify mechanical information carried by vibrations into both macro and cellular level. 2) Determine the possible interactions between vibration-induced mechanical information (acceleration, fluid shear, frequency) that would modulate cellular response to vibrations.

Our data demonstrated that peak shear stress can be effectively separated from peak acceleration by controlling specific levels of vibration frequency, acceleration, and/or fluid viscosity. Role of vibration specific mechanical components were further investigated using osteoblasts, osteocytes and mesenchymal stem cells. Fluid shear did not have a profound effect on vibration response of cells. Consistently across all the experiments, groups with lower fluid shear stress elicited higher or equal responses when compared to groups with higher fluid shear. Cellular mechanosensitivity to vibrations were specific to level of cell maturation/cytoskeletal remodeling and frequency. Level of cytoskeletal development was dependent on accelerations but not to fluid shear. When compared to accelerations, fluid shear induced smaller cellular deformations.

In conclusion, results presented in this dissertation indicated that cells can exclusively sense and respond to accelerations in the presence of fluid shear stresses. Results suggest that response of cells to vibrations induced signals converge on the forces created on the cytoskeleton, rather than independently affecting the cellular response. There exists a relationship exists between frequency, signal strength and cytoskeletal adaptation, offering that non-pharmacological potential of vibration treatment for bone loss can be directed towards cell specific populations.

Table of Contents

List of Figures	ix
List of Tables	xv
List of Symbols and Abbreviations.....	xvii
Acknowledgments.....	xix
Publications.....	xxii
Chapter 1	1
Introduction to Bone Metabolism	2
Mechanical Environment of Bone	7
Bone Cell Mechanotransduction and Cytoskeleton	9
Regulation of Bone by Mechanical Vibrations.....	16
Objectives of Hypotheses	22
Chapter 2	25
Abstract.....	26
Introduction	28
Materials and Methods.....	31
Results.....	39

Discussion.....	44
Acknowledgements.....	52
Chapter 3	61
Abstract.....	62
Introduction	64
Materials and Methods.....	67
Results.....	72
Discussion.....	77
Acknowledgements.....	83
Chapter 4	91
Abstract.....	92
Introduction	94
Materials and Methods.....	97
Results.....	105
Discussion.....	109
Acknowledgements.....	113
Chapter 5	122

Summary	123
Limitations of the <i>in vitro</i> and Computational Model	125
Vibration as a Therapeutic Agent of Bone Formation	129
Mechanosensitivity of a Bone Cells to Vibration	130
Optimization of Patient Specific Outcomes by Controlling Mechanical Signals.	134
Conclusions	136
Bibliography	137

List of Figures

Figure 2.1. Experimental and computational methods used to describe fluid motions at the well bottom. (a) Schematic of the Particle Image Velocimetry (PIV) setup. A high-speed camera recorded the motions of $1\mu\text{m}$ red fluorescent polystyrene particles vibrating within a fluid filled chamber attached to a microscope slide. Fluid shear was quantified by comparing the motion of the slide surface to the particle motions measured at $37.5\mu\text{m}$ distance intervals. (b) A fluid filled cell culture well was modeled as viscous fluid within a rigid well with the Finite Element Method (FEM). Vibration induced fluid shear at the bottom of the well was calculated by computing the relative velocity between wall and fluid assuming linear velocity gradients.

Figure 2.2. Shear rates between fluid and the well bottom as determined by PIV. PIV showed a steep non-linear increase in shear rate towards the surface of the glass slide (bottom of the well).

Figure 2.3. Motions of the well and the fluid as determined by speckle photography (a) Displacement of the well, during $1g$, 60Hz oscillatory motions. (b) Elevation of the fluid surface near the side-wall of the well

(vertical red line in inset) as a function of vibration frequency. Non-linear surface motions at frequencies around 10Hz are indicative of resonance behavior. (c) Upon completion of one full oscillatory cycle, out-of-phase fluid displacements relative to the well demonstrated sloshing behavior are visualized in the mid-sagittal plane of the well.

Figure 2.4. Fluid velocities and shear stress determined by FEM (a) Velocity profile of the rigid well (solid-red), fluid velocity (dashed-red), and fluid shear at Point B (see Figure 4b) during a 60Hz, 1g oscillatory motion. The phase difference between the well and the fluid was $\frac{\pi}{10}$ radians. (b) The velocity profile of the viscous fluid at $t=0.005s$ during the 1g, 60Hz oscillatory motion of the rigid well (in black). Shown is a mid-sagittal plane of the well. Points A, B, and C were used to compare relative fluid velocities against the linear solution depicted in Table 2.1. (c) Histogram with the distribution of fluid nodes subjected to a given level of fluid shear at $t=0.005s$. In spite of spatial non-uniformity, approximately 75% of the well surface received shear stresses within 20% of the peak shear stress magnitude.

Figure 2.5. Validation of FEM simulations by PIV. Comparison of shear rates between FEM and PIV at heights of 150, 300, 450 and 600 μm from the well

bottom. Measurements were taken in a well with a total fluid height of 5mm.

Figure 2.6. Modulation of fluid shear by vibration parameters. Peak fluid shear stress was modulated by vibration acceleration magnitude and vibration frequency, demonstrating that different combinations of frequency and acceleration can produce identical shear stress values.

Figure 2.7. Change in COX-2 expression of MC3T3-E1 cells exposed to five different frequencies under low-shear (0% dextran) and high-shear (6% dextran) conditions. Fluid shear for each frequency is represented by horizontal black bars. Shear at 10Hz could not be quantified because of resonance behavior of the fluid at this frequency. P<0.05: * against 0Hz, † against 10Hz, ‡ against 30Hz, § against 60Hz, ¥ against 100Hz.

Figure 3.1. For mRNA and mineralization (Ca^{2+}) experiments cells were plated at 18,000cell/cm² and for proliferation cells were plated at 750cells/cm². Vibration effects on early osteogenesis at day 1, proliferation at day 3, cytoskeletal remodeling at day 7 and mineralization at day 13 were assessed.

Figure 3.2. Calcification of cells were determined by alizarin red staining at day 16 after 13 days of vibration. Cells were kept in osteo-inductive medium for 14 days and were vibrated with seven different vibration parameters. $p < 0.05$: *against non-vibrated control.

Figure 3.3. Cell proliferation characterized by total cell number at day three after two days of vibration. Culture plates were not coated (a) or coated with 0.15mg/ml collagen (b). $p < 0.05$: *against non-vibrated control.

Figure 3.4. Gene expression after one day of vibration: Change in RUNX-2(a), OPG(b) and RANKL(c) expression of MC3T3-E1 cells exposed to three different mechanical signals under low-shear (Normal) and high-shear (6% dextran) and increased cell prestress (LPA) conditions. $p < 0.05$: *against non-vibrated control.

Figure 4.1. FE model of an adherent cell was constructed to predict the vibration induced nucleus motions. Vibration induced accelerations and fluid shear were evaluated in separate dynamic simulations to compare the nucleus motions induced. During fluid shear simulations contact surface was fixed and forces applied to membrane in a sinusoidal manner. During acceleration simulations contact surface was subjected to dynamic sinusoidal accelerations the horizontal plane.

Figure 4.2. MLO-Y4 cells were vibrated with four different vibration parameters.

(a) GJIC+ cells were determined via flow cytometry following 1hr of incubation at 37°C in 5%CO². (b) Vibrated MLO-Y4 cells can communicate farther as determined by microscope images. p<0.001: ***against non-vibrated control.

Figure 4.3. mRNA expression determined 1hr after cell communication. Vibration

induced increases in GJIC were accompanied by decreases in C-FOS and increases in RANKL. p<0.05: *against non-vibrated control. p<0.001: ***against non-vibrated control.

Figure 4.4. Gap junction function in both donor (MC3T3) and acceptor (MLO-Y4)

cells were blocked by 75µM of 18α-GA. Compared to non-blocked groups (Normal), groups treated with 18α-GA showed significant decreases in GJIC+ cell number. p<0.001: ***against non-vibrated control, p<0.0001: # against non-vibrated control.

Figure 4.5. mRNA and protein levels of Cx43 were determined 1hr after vibration

treatment. Following vibration treatment no changes were observed in mRNA or protein levels of Cx43.

Figure 4.6. Akt signaling was blocked in MLO-Y4 cells with siRNA two days prior

to vibration treatment. Following either (a) 30Hz-1g or (b) 100Hz-1g there

was no difference between vibrated and control siRNA groups. (c) Blocking gap junction function only in MLO-Y4 cells decreased the GJIC similarly but the difference between control and vibration samples were preserved. $p < 0.01$: **against non-vibrated control. $p < 0.001$: ***against non-vibrated control.

List of Tables

Table 2.1. Comparison between the linear and finite element solutions at different spatial locations as specified in Figure 3 during 60Hz, 1g oscillations. Results are represented as percentages of the peak well velocity of 0.027m/s.

Table 3.1. Peak fluid shear values during high frequency vibrations. Columns represent acceleration magnitudes where 'g' is earth gravitational field (9.81 m/s^2) and rows represent signal frequency and dextran concentrations.

Table 3.2. After 6d of vibration in osteogenic medium, 84 gene PCR array was used. Total of 25 genes showed a response to vibrations (>2-fold). Genes were subdivided into 9 functional categories. For both frequencies, greatest mRNA response was observed under 1g and 2g conditions. For clarity only genes showed a response bigger than 4-fold and functional groups shown in the table.

Table 4.1. Peak fluid shear values during high frequency vibrations. Columns represent acceleration magnitudes where 'g' is Earth gravitational field (9.81 m/s^2) and rows represent signal frequency.

Table 4.2. Relative nuclear motions predicted by FE model. Nuclear motions during vibrations were estimated for both acceleration magnitudes and the fluid shear stress using two different dynamic simulations. Accelerations create larger nucleus deformation when compared to fluid shear. Nucleus motions depend on frequency and cell stiffness and amplitude.

List of Symbols and Abbreviations

$\mu\epsilon$: micro strain	C-FOS: murine osteosarcoma viral oncogene homolog
18 α -glycyrrhetic acid (18 α -GA)	COX-2: cyclooxygenase-2
Akt: Rac-alpha serine/threonine-protein kinase	Cx43: connexin 43
ALP: alkaline phosphatase	DMP-1: dentin matrix protein 1
ANOVA: analysis of variance	ERK: extracellular signal-regulated kinases
AP-1: activator-protein-1	FAK: focal adhesion kinase
ARP: actin-related protein	FBS: fetal bovine Serum
BCS: bovine calf serum	FEM: Finite element modeling
BMD: bone mineral density	GFP: green fluorescent protein
BMP- bone morphogenic protein	GJIC: gap junctional intracellular communication
BSP: bone sialoprotein	GSK3: Glycogen synthase kinase 3
CDC42A: cell division control protein 42	

LPA: lysophosphatidic acid

PS: penicillin-streptomycin

LRP-6: Low-density lipoprotein
receptor-related protein 6

qPCR: quantitative real time
polymerase chain reaction

MAPK: mitogen-activated protein
kinase

RANKL: nuclear factor kappa-B ligand

mRNA: messenger ribonucleic acid

Rock: Rho-associated protein kinase

MSC: Mesenchymal stem cell

RhoA: Ras homolog gene family,
member A

N: newton

RNA: ribonucleic acid

NFAT: nuclear factor of activated T-cell

RUNX-2: runt-related transcription
factor 2

NO: nitric oxide

siRNA :small interfering RNA

OVX: ovariectomized

SOST- Sclerostin

PBS: phosphate buffered saline

WAS: Wiskott-Aldrich syndrome

PGE₂: prostaglandin E₂

PIV: particle image velocimetry

Acknowledgments

There are number of people who helped me through graduate school and without them this dissertation would never have come to pass as. I am very grateful and happy for all their help.

Dr. Stefan Judex, my advisor, guided me through this entire process. When I was getting too creative he always put my flow in the right track and all my great ideas were *somehow* started by him. I am extremely lucky to have such a great advisor and I am sure he will never stop forging me into a better scientist my whole career.

Dr. Fu-pen Chiang, my thesis advisor, I am grateful to him for teaching me how to look at things the right way and continue to support me in my work in biomedical engineering.

I would like to thank to my committee members, their input was invaluable. Dr. Clinton. T. Rubin, made me realize how important is to look into problems critically and how delightful to reveal the whole story. Your presence guided me the whole time to become a true bonehead and it will continue to do so. Dr. Mary D. Frame, since we started looking into “disco nucleus”, your expertise not only helped me figure out how the fluid shear works in small scale,

it actually made me measure it. Thanks for suffering through a long summer with lots of questions. Dr. Janet Rubin, thank you for agreeing to be in my committee and open my unsuspecting engineer eyes to the cellular world. You directly or indirectly made me realize how interconnected the mechanical and molecular mechanisms are which guided me through the whole way.

When I first arrived in Biomedical engineering the most amazing thing was the scientific environment. It was my privilege to work with so many bright scientists, who did not hesitate to help me every step of the way. Alyssa Tuthill, without her diligence, the lab would have imploded long time ago. Dr. Ete Chan, who was never shy of discussing every single detail of my experiments and results and lend me a hand at the bench whenever I needed. Dr. Sarah Manske, created wonders in setting up all that PCR groundwork, shared the burden of the osteoblast experiments and refused to believe me unless I repeat my experiments three times, for that I am grateful. Ben Adler , Sardar Zia, Danielle Green and Gabriel Pagnotti thank you for being there for great discussions whether it was, fish, politics or work related. Suphannee Pongwitkitoon, you arrived late but without your diligent help, my work would never have finished in time. Lastly, Dr. Engin Ozcivici who helped me for years from the shadows, without his support and help, I would not be in here, many thanks.

My family was extraordinary in their support, they believed in every decision I made. They were always in the background being an inspiration for me to work harder. Whenever I needed to talk with someone, I knew I can always call and talk to my brother. Thank you for being there.

Finally, my lovely wife Guniz Bas Uzer, her support was so essential that I could not have survived a single day. She was with me every step of the way, patient, supportive and loving. I am glad and honored to dedicate this dissertation to her.

Publications

List of peer-reviewed publications and conference proceedings that were produced during the course of the dissertation.

PEER REVIEWED JOURNAL PUBLICATIONS

1. **Uzer G**, Manske S, Chan ME, Chiang FP, Rubin CT, Frame MD, Judex S, Separating Fluid Shear Stress from Acceleration during Vibrations in Vitro: Identification of Mechanical Signals Modulating the Cellular Response, Cellular and Molecular Bioengineering, Vol.5(3),p.266, 2012
2. Gupta S, **Uzer G**, Surabhi P, Judex S, Multiple Multiple Exposures to Unloading Decrease Bone's Responsivity but Compound Skeletal Losses in C57BL/6 Mice, American Journal of Physiology- Regulatory, Integrative and Comparative Physiology, Vol. 303(2), p.159, 2012
3. Holguin N, **Uzer G**, Chiang FP, Rubin C, Judex S, A Brief Daily Exposure to Low Intensity Vibration Mitigates the Degradation of the Intervertebral Disc in a Frequency-specific Manner, Journal of Applied Physiology, Vol.111(6), p. 1846, 2011

CONFERENCE PROCEEDINGS AND PRESENTATIONS

1. **Uzer G**, Manske S, Qin YX, Chan ME, Rubin CT, Frame MD, Judex S, Vibration Induced Mechanical Signals that Increase Proliferation and Osteogenic Commitment of Mesenchymal Stem Cells, Journal of Bone Mineral Research 27 (Suppl 1), 2012.
2. **Uzer G**, Manske S, Qin YX, Chan ME, Rubin CT, Frame MD, Judex S, Fluid Shear Modulates COX-2 mRNA Expression but not Mineralization during Oscillatory

Motions, Journal of Bone Mineral Research 26 (Suppl 1), 2011.

3. Manske S, **Uzer G**, Judex S, Does loading direction influence the cell's response to high frequency, low magnitude vibration?, Journal of Bone Mineral Research 26 (Suppl 1), 2011
4. **Uzer G** and Judex S, Fluid induced mechanical environment of cells during high-frequency oscillations in-vitro. IEEE 37th Northeast Bioengineering Conference, April 1-3, Troy, NY, 2011
5. **Uzer G**, Fievisohn E, Chan, ME, Ferreri S, Qin YX, Judex S, Cell proliferation is modulated by oscillatory accelerations but not by differences in fluid shear, Journal of Bone Mineral Research 25 (Suppl 1), 2010
6. Gupta S, **Uzer G**, Judex S, Recovery of Abdominal Adiposity and Vertebral Bone after Multiple Exposures to Mechanical Unloading, Journal of Bone Mineral Research 25 (Suppl 1), 2010.
7. **Uzer G**, Qin YX, Rubin CT, Judex S, Fluid Forces in the Bone Marrow during High Frequency Oscillatory Vibrations, Journal of Bone Mineral Research 24 (Suppl 1), 2009.
8. Judex S, Gupta S, **Uzer G**, Bone Atrophy and Recovery upon Multiple Exposures to Mechanical Unloading, Journal of Bone Mineral Research 24 (Suppl 1), 2009.

Chapter 1

INTRODUCTION

Introduction to Bone Metabolism

Bone provides the protection and mechanical support to the whole body and creates a framework in which muscles can accomplish work. It is also an integral part of mineral homeostasis, blood and immune cell production. Bone is continuously eroded and rebuilt by a process called remodeling. Remodeling is a dynamic process where cells form new bone (osteoblast) and resorb old bone (osteoclast). The remodeling process starts with osteoclasts forming resorption lacunae, followed by osteoblasts which fill the lacunae with new bone. Remodeling is affected by many factors such as hormone levels and age, however perhaps the most important factor is the mechanical demands on the bone structure. This mechanical regulation of remodeling is likely orchestrated by resident cells in the bone tissue.

Mesenchymal Stem Cells

Mesenchymal stem cells (MSCs) originate from stem cells of the mesoderm during embryologic development, creating mesenchymal tissue including bone, cartilage, fat and muscle. MSCs are multipotent progenitor cells

that can differentiate into adipocytes,¹ osteoblast,² chondrocytes,³ and cardiomyocytes.⁴ In the bone marrow MSCs position themselves on periosteal surfaces and near vasculature.⁵ Their close contact with hematopoietic cells, the source of osteoclasts and their ability to express receptor activator of nuclear factor kappa-B ligand (RANKL) suggests that they play a regulatory role in osteoclastogenesis.⁶ In bone, MSCs are ultimately responsible for rejuvenating osteoblast and osteocyte cell populations. For example, in mice, negative impact of disuse on the population size of MSC can hinder regenerative capacity and limit bone recovery during reambulation.^{7,8} Lineage commitment of MSCs can be differentially regulated by both mechanical and biochemical factors. For example, the application of compressive forces increase expression of chondrogenic genes including aggrecan (ACAN), type II collagen (COL-2), SOX-9 and bone morphogenic protein 6 (BMP-6).^{9, 3} On the other hand forces that induce elongation such as tensile strain^{10, 11} or laminar fluid flow¹² induce the osteogenic phenotype. Early osteogenic commitment is controlled by two early osteogenic markers, Osterix (OSX) and Runt-related transcription factor 2 (RUNX-2). Both are transcription factors required for bone formation^{13, 14} and regulate commitment of undifferentiated MSCs to the osteogenic lineage. Interestingly, mechanical induction of osteogenic phenotype decreases adipogenic potential of MSCs both *in vitro*¹⁵ and *in vivo*.¹⁶ These results suggest that lineage

commitment of MSCs that ultimately determine bone homeostasis and regeneration may be strongly influenced by mechanical signals.

Osteoblasts , Osteocytes and Osteoclasts

Osteoblasts are originated from the MSC lineage in the marrow cavity. Differentiation of MSCs to the pre-osteoblast stage is predominantly mediated by RUNX-2^{17, 13} and OSX.¹⁴ During the pre-osteoblasts stage, cell has the ability to proliferate and factors related to activator-protein-1 (AP-1) such as C-FOS believed to suppress the further differentiation and accelerate proliferative capacity.¹⁸⁻²¹ Pre-osteoblasts expressing OSX are also responsible from maintaining RANKL levels in mature mice.²² As the maturation continues from the pre-osteoblast to osteoblast phenotype, production of interstitial fibronectin,^{23, 24} collagen,^{25, 26} osteocalcin,²⁷ bone sialoprotein (BSP),²⁸ and alkaline phosphatase (ALP)²⁹ are observed. The last step in osteoblast maturation is the terminally differentiated state called the osteocyte. Osteocyte differentiation starts as the osteoblast is entombed by new bone formation. E11w/gp38 is the earliest osteocyte selective protein found in differentiating osteoblasts.³⁰ Other selective osteocyte proteins include SOST and dentin matrix protein 1 (DMP-1).³¹⁻³³

Osteoblasts are mechanosensitive and they are the effector cells that regulate local bone remodeling. Osteoblasts respond to a wide variety of forces including fluid flow,³⁴⁻³⁶ substrate strain^{37, 38} and vibrations.^{39, 40} Mechanical signals positively regulate many aspects of osteoblast function including proliferation,⁴¹ mineralization⁴² and inhibition of osteoclastogenesis.³⁸ Mechanical signals also regulate β -catenin levels through Akt, Wnt, and cAMP signaling pathways.⁴³⁻⁴⁵ In turn β -catenin controls many cellular functions such as cyclooxygenase-2 (COX-2) levels. COX-2 is a mechanically inducible enzyme which is responsible for prostaglandin E₂ (PGE₂) production, COX-2 deficient mice shown greatly decreased fracture healing and reduced MSC differentiation.

Osteocyte's organized spatial distribution led to the hypothesis that they are the sensor cells that drive the responses of effector cells (osteoblast, osteoclast)⁴⁶. Osteocytes can relay local mechanical and biochemical signals to other cells through gap junctions^{47, 48} or membrane bound hemichannels.⁴⁹ For example deletion of RANKL from osteocytes mutes any osteoclastic activity and causes severe osteopetrosis.^{50, 22} It is widely accepted that pressure gradients as caused by tissue strains and intramedullar pressure creates fluid flow in and out of the lacunar-canalicular network and these flow patterns are sensed by osteocytes.^{51, 52} Interestingly, osteocytes are more sensitive to fluid shear

compared to less differentiated cells.^{53, 54} Osteocytes respond to fluid flow by increasing the length of their dendrites through expression of E11w/gp38, the earliest osteocyte selective protein.³³ Suggesting osteocyte differentiation selectively increases the cellular mechanosensitivity.

Osteoclasts are bone specific multi nucleated macrophages created by the fusion of macrophage precursors near the resorption surface. They were first found in the presence of osteoblastic cells from marrow cultures.⁵⁵ The two most critical factors for osteoclastogenesis are colony stimulating factor 1 (CSF-1)^{56, 57} and RANKL.⁵⁸ Expression of other transcription factors also required for osteoclast function, for example mice lacking the c-fos component of AP-1 protein complex develop osteopetrosis⁵⁹ which can be rescued by nuclear factor of activated T-cells (NFAT).⁶⁰ Activation of surface receptors on osteoblasts such as prostaglandin E₂ (PGE₂) , transforming growth factor β (TGF- β) and interleukin 1 (IL-1) can potentiate effects of RANKL on osteoclast function.⁶¹ Osteoprotegerin (OPG)^{62, 63} on the other hand binds to the RANK receptor thus inhibiting the RANKL-RANK interaction. Therefore the RANKL/OPG ratio is used by many researchers to determine the rate of osteoclastogenesis.^{64, 65}

Mechanical Environment of Bone

The dynamic mechanical environment is essential for healthy bone homeostasis. Bone as a tissue and at the cellular level can sense and undergo adaptation to daily loading events that induce matrix deformations,⁶⁶⁻⁷⁰ accelerations,⁷¹⁻⁷⁶ muscle activity⁷⁷⁻⁷⁹, fluid flow^{42, 80, 44, 81, 52} and changes in intramedullary pressure.⁸²⁻⁸⁴

During locomotion, the bone matrix encounters strains ranging from 2000 to 3500 $\mu\epsilon$.⁸⁵ These matrix strains can directly be sensed by entombed osteocytes, or osteoblasts and osteoclasts on bone surfaces⁸⁶⁻⁸⁸. Within the bone marrow compartment, endothelial surfaces share a mechanical connection with the bone marrow and therefore, it is likely that matrix strains not only sensed by cells on bone surfaces but also by osteoprogenitor cells residing within one to three cell layers distance⁸⁹ through cellular and vascular connections.

Secondary mechanical signals are also triggered by dynamic strains in the bone. Due to bone's porous structure, local strain concentrations create pressure gradients and induce local fluid flow in and out of bone. Fluid flow maybe an important regulator during development^{90, 91} and potent stimulus for

many cell types including endothelial cells,^{92, 93} neurons,⁹⁴ osteoblasts,^{41, 95, 96} osteoclasts⁹⁷ and osteocytes.⁹⁸ Relatively low strains (400 $\mu\epsilon$) are capable of producing fluid flow within the lacunar-canalicular network as high as 5Pa *in vivo*.⁹⁹ Osteocytes were implicated as the most sensitive bone cells because of their osteocyte processes within lacunar-canalicular network which may enhance fluid shear sensitivity.^{100, 99} However, as evidenced *in vitro*,^{101, 102, 97, 44} other cell types that reside on or in proximity of bone surfaces such as osteoblasts, osteoclasts, progenitor cells and cells from the hematopoietic origin can also sense the strain derived fluid flows.

Bone compartments that trabecular bone resides in are filled with bone marrow. Within the bone marrow, small motions at the interface between marrow and bone can generate a fluid shear that is essentially independent from strain derived fluid flow.¹⁰³ It is likely that the barrage of extremely small strains encountered during daily activities¹⁰⁴ will cause shear stresses at the bone marrow interfaces^{103, 105} but will not cause large pressure gradients for interstitial fluid flow. Bone marrow is an important source of hematopoietic cells and also contains mesenchymal stem cells.^{106, 107} Hematopoietic red bone marrow coexists with fatty yellow bone marrow. The viscosity for red marrow was found to be much higher (400cP) than fatty marrow (40cP).¹⁰⁸ Implying that fluid shear at the bone-marrow interface can change dramatically because of

viscosity.¹⁰⁹ Red and fatty bone marrow can replace one another¹¹⁰ and conditions such as aging and osteoporosis have shown to increase fat tissue volume in the marrow, while depleting the bone.¹¹¹ Aside from a negative indicator bone of health, a decrease in the bone marrow viscosity due to increased fat infiltration will also decrease the overall fluid shear stress, further contributing to the pathological conditions by decreasing the potency of daily mechanical input.

Bone Cell Mechanotransduction and Cytoskeleton

Mechanotransduction refers to the mechanisms by which cells convert external stimuli into intracellular signals. Many cell types are mechanosensitive including but not limited to endothelial cells,¹¹²⁻¹¹⁴ myocytes,^{115, 116} chondrocytes,^{117, 118} fibroblasts,¹¹⁹ mesengial cells¹²⁰ and lung cells.¹²¹ Cells can respond to forces such as, fluid shear, pressure, matrix deformation, substrate stiffness and activate redundant intracellular pathways such as mitogen activated protein kinases (MAPK), G proteins or β -catenin signaling.

By attachments attachment to the outside world many cells to sense their mechanical environment which constitutes an integral and first step of the mechanotransduction process. Integrins are integral membrane proteins that connect the extracellular matrix to the cytoskeleton.¹²² Structure of integrin consists of non-covalently bound α and β heterodimer subunits. Extracellular domain is composed of a ligand binding head that is connected to two legs that tether into the intracellular domain. A total of 18 α and 8 β subunits were identified giving rise to 24 unique integrins.¹²³ In osteoblasts, the β_1 subunit appears to be dominant while the α subunit can be found from α_1 to α_5 and α_v .¹²⁴ The extra cellular domain heads of integrins can bind to ECM components including collagen, fibronectin, laminin and vitronectin.¹²³ Integrins play a role in stabilizing tissue architecture¹²⁵, attachment^{126, 127} and differentiation.²⁴ In calvarial osteoblasts $\alpha\beta_3$ mediate interactions with fibronectin, critical for both morphogenesis and differentiation.²⁴ Integrins sense the stiffness of the ECM by changing their binding affinity¹²⁸ and change the linked cytoskeleton.¹²⁹ Fluid flow also increased the β_1 integrin expression⁴¹ and activated $\alpha\beta_3$, which co-localized with Src,¹³⁰ implying that integrins can play an active role in cellular mechanotransduction.

Integrins connect the ECM to a bundle of actin fibers called stress fibers, and the points of contacts are called focal adhesions.¹³¹ At the focal adhesion

sites number of proteins have been identified that facilitate structural and biochemical roles. These proteins include including focal adhesion kinase (FAK)^{132, 133}, paxilin¹³⁴ and talin.¹³² Most of these proteins are involved in, “outside-in”, signaling that convert mechanical cues coming from integrin attachment sites into biochemical signals that will initiate the mechanotransduction cascade. FAK, vinculin and paxilin knockout mice are embryonic lethal.¹³⁵⁻¹³⁸ Furthermore, paxilin deficient fibroblasts show abnormal focal adhesions and are defective in lamellipodium formation.¹³⁶ In both cardiomyocytes¹¹⁵ and osteoblasts¹³⁹ mechanical stretch activates MAPK through autophosphorylation of tyrosine 397 by FAK. Once activated FAK interacts with src and ras family proteins.

Ultimately all integrins share a mechanical connection through the cytoskeleton. The cytoskeleton forms a physically and biochemically connected network within the cell. This dynamic network functions as an organizing structure and generates forces to guide cell movement, shape and differentiation. The cytoskeleton is composed of three main components intermediate filaments, microtubules and actin fibers.

Intermediate filaments acts as stabilizers of the cytoskeleton, they play a role in resisting shear stress¹⁴⁰ and provide stiffness to the cell nucleus¹²⁵. Microtubules are the stiffest of the three building blocks of the cytoskeleton and can form long tracks that span the length the cell. During mitosis, these long and

stiff networks assemble into radial arrays that function as central hubs and facilitate intracellular transport. It is not entirely clear if microtubules are directly involved in mechanosensory functions. However, microtubules are known to buckle under compressive loads in cells¹⁴¹ and these compressive loads can increase the overall curvature and create fractures in microtubules. The relationship between microtubule fracture and intracellular forces suggests a regulatory mechanism.¹⁴² Additionally, microtubules act to stabilize the cytoplasm and nucleus.¹⁴³ When endothelial cells were stretched by pulling actin filaments, removal of functional microtubules resulted in the release of normal restriction of nuclear movement,¹²⁵ suggesting that microtubules may indirectly be involved in mechanosensory functions by protecting nucleus from extreme deformations. Experimental evidence regarding the regulatory function of microtubule integrity on mechanosensing is not clear. For example, when microtubules were disrupted by colchicine, fluid flow increased cell sensitivity to further by increasing PGE₂ release in osteoblast cells.¹⁴⁴ A different study, however, showed muting of the PGE₂ response.¹⁴⁵ Showing that microtubules play a role in mechanotransduction but the mechanism by which the regulation is controlled is unknown.

Through focal adhesions, the actin cytoskeleton maintains a constant contact with the ECM.¹³¹ Dynamic interaction between integrins and actin stress

fiber formation bestows the actin network a unique sensitivity to mechanical signals.¹⁴⁶ Actin cytoskeleton driven cell spreading, shape and tension are important for cell mechanotransduction¹⁴⁷⁻¹⁴⁹ and may play a critical role in the osteogenic commitment of MSCs.¹⁵⁰ Mechanically or biochemically driven GTPase activity has been shown to regulate actin polymerization and contractility.^{151, 148} Polymerization of new actin filaments is largely modulated by actin related protein (Arp) 2/3 complex which acts as a nucleation core.¹⁵² Function of Arp2/3 complex is tightly regulated by the Wiskott-Aldrich syndrome (WAS) family of proteins (WASP, N-WASP and SCAR) which enable rapid polymerization.¹⁵²⁻¹⁵⁴ Arp/23 complex and WAS family proteins also play a role in binding newly formed actin filaments to the existing actin network.^{155, 156} Aside from creating a new formation of actin cytoskeleton, Rho GTPases such as RhoA, Ras and CDC42A are important regulators of cell tension and may therefore be a powerful agents of mechanotransduction.¹⁵⁷ RhoA activity increases the cell tension through its effector protein Rock, activating myosin light chain kinase, which in turn, activates the dimerized motor protein myosin II.¹⁵⁸ These findings are significant because mechanical cues such as fluid flow and strain and even ECM compliance have been shown to consistently regulate RhoA activity and stress fiber formation.^{151, 159, 160}

Early experiments with bone cells showed that stress fiber formation is a common response to laminar fluid flow.¹⁶¹ However, laminar fluid flow regimes do not reflect physiological loading scenarios. Not surprisingly, physiologically more relevant loading cases such as oscillating fluid flow does not create prominent stress fibers.¹⁵¹ Both laminar and oscillating flows support a similar phenotype.¹⁶² Perhaps the more interesting function of RhoA mediated stress fiber formation lies in its function of mechanosensing. In airway smooth muscle cells, integrin bound surface deformation of 0.4 μ m (peak) deformed the nucleus and stress propagation within the cell was controlled by intracellular stress levels.¹⁶³ These results suggest that mechanical forces not only increase intracellular stress favoring osteogenesis,¹⁵⁰ but also intracellular stress amplifies the efficiency of the force transfer within the cells. Very interestingly, RhoA and focal adhesion activity increases the effectiveness of the mechanical stimuli.¹⁶⁰

Even small local deformations to the cytoskeleton can have global implications to the cells. The cytoskeleton is a tensegrity structure meaning it is under constant tension/compression balance. Thus even small changes in force balance should be compensated by the whole structure. Consistent with the hypothesis, fluid flow induced deformations in a single cell were weakly correlated with direction of the flow.¹⁶⁴ The tensegrity model also predicts

instantaneous and non-linear cell stiffening under magnetically induced membrane deformations.^{165, 166} These key studies open up a new perspective where mechanical signals are the first signals that propagate through the whole cell body even earlier than biochemical signals. These forces may use a pre-stressed cytoskeleton as a conduit since the force will choose the path of least resistance. This suggests that, irrespective of the mechanical input a cell receives, it converts the input to stress throughout the whole cytoskeleton.

The nucleus is positioned in the middle of all the cell activity and mechanical signals transferred by the cytoskeleton ultimately reach to the nucleus as the cytoskeleton mechanically couples the chromosome and the cell membrane.¹⁶⁷ The nuclear envelope is connected to the interior of nucleus by lamina.¹⁶⁷ Forces are transmitted via the cytoskeletal network to the nuclear envelope and from there via lamin network to chromatin.¹⁶⁸ Sun proteins in the inner nuclear membrane extend through the lipid bilayer and connect with Nesprin-1 and Nesprin-2 to F-actin at the outer nuclear membrane.¹⁶⁹ Nesprins maintain the connection between cytoskeleton and inner nucleus. Cells with impaired Nesprin 1, Nesprin 2 or Nesprin 3 functionality exhibit decreased mechanical stiffness.¹⁷⁰ Nuclei in HeLa cells under shear stress show upregulation and redistribution of A-type lamins to the nuclear periphery, which in-part are responsible from common cell stiffening.¹⁷¹ The ability of instantaneous

mechanical transfer of forces into the nucleus was found to be specific to integrins and the actin cytoskeleton.^{143, 125, 166} These findings suggest that, similar to integrin related proteins, the proteins connecting the cytoskeleton to the nucleus are also mechanically sensitive and should be considered as a mechanosensory site.

Regulation of Bone by Mechanical Vibrations

During daily activity measurements of peak strain amplitudes on the load bearing bones across different species (horse, dog, pig, fish, sheep, lizard and others), the bones encountered similar strain levels, ranging from 2000 to 3500 $\mu\epsilon$.^{172, 173} This well defined strain range suggests that bone cells are adapted to sense a certain range of mechanical signals. High resolution measurements of strains in dog, sheep and turkey¹⁰⁴ revealed that in addition to rare high magnitude strains, lower magnitude strains have a much larger and continuous presence throughout the day. It is likely that these very small vibrations (<10 $\mu\epsilon$) encountered daily are a result of muscle activity.⁷⁷ The negative relationship between muscle activity and age¹⁷⁴ bears the question do the continuous presence of small vibrations in-part contributes to the homeostasis and

mechanosensitivity of the bone? For example, although not directly answering the question, differences between the effectiveness of exercise regimes in younger¹⁷⁵ and older⁷⁹ adults points to a possible interplay between daily presence of small vibrations and mechanoregulation of bone. Consistent with the hypothesis that low level vibrations can modulate mechanoregulation of bone, the application of broad frequency (0-50Hz) mechanical vibration with a maximum peak of 300 $\mu\epsilon$ were shown to potentiate the effectiveness of low frequency (3Hz) strains of 3000 $\mu\epsilon$ *in vitro*.⁷⁵ Additionally, the application of small broad frequency signals alone were more efficacious in increasing ALP activity and osteocalcin expression of osteoblasts when compared to much larger low frequency strains, demonstrating that low magnitude vibrations are an essential part of bone metabolism.

Recent evidence from preliminary clinical studies reveals that the application of low magnitude high frequency vibrations can be anabolic or anti-catabolic to bone. In healthy women with low BMD, the application of vibrations of 0.3g at 30Hz increased the trabecular bone in the lumbar vertebrae (2.1%) and cortical bone in the femoral midshaft (3.4%) compared to non-vibrated controls.¹⁷⁶ Similarly in an another study conducted with postmenopausal women, vibrations of 0.2g at 30Hz for 10min/day showed a benefit of 2.13% in the femoral neck, 1.5% in spine and 3.5 % in overall BMD when compared to

non-vibrated subjects.¹⁷⁷ Vibrations of 0.3g and 90Hz showed strengthen the cortical bone structure in children with cerebral Palsy.⁷⁶ Additionally following 6 weeks of bed rest, vibrations were able to halt the deterioration of postural control and partially retain flexion strength by 46.2% compared to non-vibrated controls.¹⁷⁸ While the observed anabolic outcomes of low magnitude vibrations in human subjects are important to underline its non-pharmacological applications for the intervention of bone loss, there exists a gap of information that's has to be addressed by animal and cell studies regarding the mechanism(s) of action activated by the vibrations.

Resident cell populations are ultimately responsible for the fate of the bone structure, whether it is a pathological or an anabolic outcome. A disuse rat model, one month hind limb suspension decreased the bone formation rate in the proximal tibia by 92% compared to the age match group. The application of 0.25g, 90Hz vibrations restored the bone formation rate to control levels.¹⁷⁹ A subsequent murine study of limb disuse, three weeks of hind limb unloading caused 51% bone loss in the proximal tibia. During disuse, bone loss was facilitated by both a decrease in osteoblast and an increase in osteoclast numbers on the bone surfaces. Disuse induced decreases were partially rescued by vibrations of 0.2g, 90Hz. Interestingly, vibrations also retained the resident bone marrow stem cell population during disuse. Receiving vibrations only in the

first three weeks was more beneficial compared to receiving vibrations only during the three week reambulation period,⁷ suggesting that vibrations may retain rejuvenative capacity of stem cells and mitigate disuse induced bone loss.

Vibrations also play an important role in progenitor cell fate and are capable of biasing fat and bone metabolism. For instance, mice fed by high fat diet show a marked increase in fat accumulation and bone loss.¹⁸⁰ During a high fat diet, the application of 0.2g, 90Hz signals increased the MSC population by 46%, which was accompanied by a 72% increase in total RUNX-2 levels in the bone marrow and 27% decrease in PPAR γ levels. This biasing towards osteogenesis was able to suppress visceral adipose tissue formation by 28%, and increase trabecular bone volume fraction in the tibia by 11%.¹⁶ Similar biasing towards osteogenesis in the expense of adipogenesis was also evident on MSCs directly subjected to 0.7g, 90Hz vibrations *in vitro*.¹⁸¹

Most if not all resident cell types of bone have been shown to directly sense and respond to vibrations including osteoblasts,^{182, 183, 39, 184, 185, 40, 75,} osteocytes¹⁸⁶ and MSCs.^{181, 187, 188} Available evidence reveals that vibrations may indirectly affect the function of other cells. Excitation of osteocytes using vibrations of 0.15g acceleration with varying frequencies of 30, 60 and 90Hz modulate the RANKL expression. Conditioned medium taken from osteocytes were able to inhibit bone resorption of osteoclasts.¹⁸⁶ Another study showed the

matrix produced by osteoblasts under the vibration treatment was much more beneficial for the osteogenic commitment of MSCs when compared to non-vibrated controls.¹⁸³ However, during application of vibrations, the degree of interaction between different cell compartments is poorly understood. For example an *in vivo* study showed using GFP labeled MSCs that, applications of 0.2g, 90hz signals decreased the adipogenesis of MSCs by 17%.¹⁸⁹ However, it is not possible to infer from the results if the MSCs directly respond to vibrations and limit adipogenesis or mechanosensitive osteoblasts created a bone surface that is more favorable for osteogenesis to bias the available MSC pool.

Cell Mechanosensitivity to Vibrations

Perhaps, one of the ways to predict the vibration induced interaction cascades within bone is to start with the identification of the mechanical information created by the vibrations and the sensitivity of different cells to varying mechanical information. This mechanical mapping could provide a first approximation for the origin of mechanical regulation and interactions within the bone. For example proliferating osteoblasts were more sensitive to 20Hz vibrations while differentiating osteoblasts favored 60Hz.⁴⁰ Similarly *in vivo* studies showed that 90Hz signals that increase osteoblast driven bone formation

rates¹⁷⁹ were much more efficient compared to 45Hz signals.¹⁹⁰ Suggesting that, it is unlikely that strains are responsible for the vibration bound responses. Consistent with the hypothesis, in the absence of functional load bearing, applying vibrations results in strain magnitudes as low as 2 $\mu\epsilon$ and still retains their efficacy.¹⁹¹ It has been suggested that other internal mechanisms such as nucleus motion can be sensed by the cells.^{182, 71, 192} Since the nucleus is directly connected with the cell's cytoskeleton, it can readily transfer the forces within the cell. It can be expected that the forces originating from nucleus motion can easily transfer to the other mechanosensitive sites within the cell. This approach could explain why different cells favor different vibration frequencies since efficiency of force transfer and harmonic oscillation properties of cells depends directly on the mechanical properties of the cytoskeleton and nucleus which, in turn, depend on cooperative interactions between microfilaments, intermediate filaments and microtubules¹⁴³. Additionally, without a functional cytoskeleton, vibrations fail to elicit any cellular response to mechanical signals.¹⁸⁵

Another major player in the mechanical information shared by bone cells is the fluid shear. Computational studies reveal that the bone surfaces in contact with the bone marrow will be subject to significant fluid shear stresses (0.5-5Pa) even during vibrations as small as 0.1g.^{103, 105} Based on the geometry and the composition of the bone marrow these fluid shear forces may possess an ability

to alter the mechanical environment of bone marrow. In a clinical study conducted in healthy men, following 60 days of bed rest, high magnitude vibrations were able to protect the vertebral bone marrow from the fatty infiltration.¹⁹³ Since red bone marrow possesses higher viscosity compared to fatty marrow,¹⁰⁸ these results suggest an indirect protection of mechanical signals within the bone marrow through viscosity.

Overall, the studies listed above suggest that vibrations deliver complex mechanical information to the cells. However, only a few studies either analyzed^{109, 194, 195} or simplified^{182, 186, 196} the complex mechanical environment created by the vibrations while majority of the literature neglected the role of different forces at the cellular level. In this dissertation we examined the mechanical information carried by vibrations at the cellular level and studied the cellular mechanosensitivity to those various mechanical signals across different bone cells.

Objectives of Hypotheses

The main objective of this study is to identify the mechanical information carried into the cells by vibrations and interaction between vibration induced forces in

regulating bone cell function. This objective was addressed using following hypothesis and research questions.

Hypothesis 1. (a) *In vitro* vibrations will exert fluid shear stress on monolayer of cells.

(b) Both vibration frequency and vibration induced fluid shear can in-part modulate cellular response.

Research Questions

(1) Does the vibration induced fluid shear be controlled by fluid viscosity and vibration parameters in an *in vitro* system?

(2) Does fluid shear generated by vibrations alter transcriptional levels of cyclooxygenase-2 (COX-2), a gene implicated in regulating mechanically induced bone formation?

Hypothesis 2. (a) Vibration induced fluid shear is not necessary to enhance mesenchymal stem cell (MSC) differentiation and cytoskeletal remodeling

(b) Cell sensitivity to vibrations can be promoted via actin stress fiber formation.

Research Questions

(1) Does vibration modulate the MSC proliferation, mineralization and early osteogenic commitment during application of vibrations?

(2) Does stronger cell attachment and cytoskeletal remodeling potentiate the cell responsiveness to vibrations?

Hypothesis 3. (a) Application of high frequency accelerations induce larger relative nucleus motions compared to fluid shear.

(b) Vibrations will increase the gap junctional intracellular communication (GJIC) independent of fluid shear through Akt dependent pathway.

Research Questions

(1) Do vibrations create nucleus motions similar to the fluid shear?

(2) Does fluid shear modulate the GJIC in osteocytes during vibrations?

(3) Does the communication can be blocked by blocking the function of gap junctions or Akt pathway?

(4) Does the cellular prestress characterized by overall cell stiffness modulate the cell response to vibrations or fluid shear?

Chapter 2

*SEPARATING FLUID SHEAR STRESS FROM
ACCELERATION DURING VIBRATIONS IN VITRO:
IDENTIFICATION OF MECHANICAL SIGNALS
MODULATING THE CELLULAR RESPONSE*

Abstract

The identification of the physical mechanism(s) by which cells can sense vibrations requires the determination of the cellular mechanical environment. Here, we quantified vibration-induced fluid shear stresses *in vitro* and tested whether this system allows for the separation of two mechanical parameters previously proposed to drive the cellular response to vibration – fluid shear and peak accelerations. When peak accelerations of the oscillatory horizontal motions were set at 1g and 60Hz, peak fluid shear stresses acting on the cell layer reached 0.5Pa. A 3.5-fold increase in fluid viscosity increased peak fluid shear stresses 2.6-fold while doubling fluid volume in the well caused a 2-fold decrease in fluid shear. Fluid shear was positively related to peak acceleration magnitude and inversely related to vibration frequency. These data demonstrated that peak shear stress can be effectively separated from peak acceleration by controlling specific levels of vibration frequency, acceleration, and/or fluid viscosity. As an example for exploiting these relations, we tested the relevance of shear stress in promoting COX-2 expression in osteoblast like cells. Across different vibration frequencies and fluid viscosities, neither the level of generated fluid shear nor the frequency of the signal were able to consistently account for differences in the relative increase in COX-2 expression between groups, emphasizing that the eventual identification of the physical

mechanism(s) requires a detailed quantification of the cellular mechanical environment.

Introduction

Exposure to vibrations is ubiquitous during daily activities and includes externally generated signals such as road noise during car rides¹⁹⁷ or internal signals such as muscular vibrations generated during postural activities.¹⁷⁴ Because of the physiologic nature of the signal, it may not be surprising that a large number of tissues and cell types are capable of responding to vibrations. Exploiting this cellular mechano-sensitivity at high-frequencies, benefits of vibrations have been suggested for a wide range of applications – from athletic training¹⁹⁸ to the treatment of Parkinson's¹⁹⁹ or cardiovascular diseases.²⁰⁰ The potential anabolic and anti-catabolic effects of vibrations on the musculoskeletal system to maintain and enhance tissue quality and quantity have received particular attention,^{201, 190, 202} facilitated by the high level of transmissibility of the oscillatory signal (20 to 90Hz) through the lower and axial skeleton (> 90% transmissibility at ankle and knee).²⁰³

The physical mechanisms by which cells can perceive and respond to low-intensity vibrations are largely unknown. In bone, accelerations of up to 0.5g induce matrix deformations of less than 10 $\mu\epsilon$, at least two orders of magnitude below those strains that are typically considered osteogenic when the frequency

of the mechanical signal is less than 10Hz.²⁰⁴ Emphasizing that matrix deformations are unlikely required in the mechanotransduction of vibrations, low-intensity vibrations applied as simple oscillatory motions to freely moving limbs (“shaking”), rather than induced by whole-body vibrations against the gravitational force of the body, result in matrix strain magnitudes of less than $1\mu\epsilon$.⁷¹ That vibrations can engender a biologic response even at these extremely small deformation magnitudes¹⁹² suggests that the deformation-response relation proposed for lower frequency mechanical signals²⁰⁵ does not apply to high-frequency mechanical signals.⁷⁷

While the extremely small deformations associated with low-level vibrations are insufficient to create pressure gradients large enough to cause local fluid flow in the matrix or canalicular system,⁵² oscillatory accelerations will generate relative motions between cells and the surrounding fluid because of density differences. Thus, cells residing in most tissues and cavities will be subjected not only to accelerations transmitted from the vibrating device but also to fluid shear. As both fluid shear and direct forces acting on the cell have been suggested as modulators of mechanotransduction, it becomes necessary to decouple them for identifying their respective roles in driving the biologic response to vibrations.

Exploiting the opportunities of cell culture systems to investigate the underlying mechanisms, distinct cell types including osteoblasts,¹⁸² osteocytes,¹⁸⁶ myoblasts,²⁰⁶ chondrocytes,²⁰⁷ or progenitor cells¹⁸¹ have been shown to respond to vibrations *in vitro*. While providing important data on the biologic response of cells to vibrations, the identification of the specific component(s) of the vibratory signal that modulates the response requires the quantification of the cellular mechanical environment. Here, we mechanically characterize an *in vitro* model of vibrations in which, similar to *in vivo* vibrations, cells are exposed to both accelerations and fluid shear forces. As an example of using this model, we collected data from osteoblast like MC3T3-E1 cells to test whether fluid shear generated by high-frequency oscillations may alter transcriptional levels of cyclooxygenase-2 (COX-2), a gene implicated in regulating mechanically induced bone formation.^{208, 209}

Materials and Methods

Experimental design

To generate *in vitro* fluid shear magnitudes similar to those estimated *in vivo*,¹⁰⁵ cell culture plates were oscillated in the horizontal, rather than vertical, direction. Horizontal oscillations may engender fluid shear by sloshing, similar to recently analyzed fluid filled structures such as road tankers²¹⁰ or nuclear reactor design.²¹¹ The mechanical environment of cells during *in vitro* vibrations, including fluid motions and fluid shear, was measured with particle image velocimetry (PIV) and modeled with the finite element method (FEM). Speckle photography, an analytical sloshing model, and PIV were used to validate the FEM. Fluid shear within an oscillating cell culture well was determined as a function of vibration magnitude, frequency, fluid viscosity, and total fluid volume in the well. Fluid viscosity was altered by the addition of dextran to the culture medium⁴⁴ and measured by a viscometer (ASTM D455). All data were quantified in a sagittal plane through the center of the well that was positioned in the direction of the imposed oscillatory motion. Shear was reported primarily in the horizontal direction because of the horizontal alignment of the cell layer and the much smaller values for vertical shear.

Vibrating stage

A stage was constructed capable of transmitting the sinusoidal oscillations from the actuator at frequencies between 10-400Hz and peak accelerations up to 1.8g (400Hz) or 3g (10Hz). However, frequencies above 250Hz created secondary vibrations of the whole system which were eliminated by selecting 100Hz as the maximal frequency. A linear actuator (NCM15, H2W Technologies Inc., CA) controlled by a signal generator was attached to a platform mounted onto a linear frictionless slide (NK2-110B, Schneeberger GmbH, Germany) which horizontally constrained the motion. An accelerometer (CXL10, Moog Crossbow Inc., CA) attached to the oscillating platform recorded accelerations in three orthogonal directions in real-time. Up to three 24-well cell culture plates (CLS3527, Corning, NY) were firmly secured to the platform to avoid any secondary vibrations.

Particle image velocimetry (PIV)

PIV was used to experimentally measure vibration induced fluid velocity gradients and the resultant shear rates in the close vicinity of the cell layer at 37.5, 75, 112.5, and 150 μ m from the well bottom for a well filled with 2.5mm of

fluid. A well filled up to 5mm fluid was used to validate shear rates calculated by FEM at 150, 300, 450 and 600 μm from the well bottom. A glass fluid chamber was fixed on a single glass slide, attached to the actuator and mounted under a fluorescent microscope. One-micron fluorescent polystyrene microspheres (Fluorospheres-580/605, Invitrogen, CA) served as markers for tracking motions during 60Hz vibrations. Microspheres were uniformly distributed at the bottom of the fluid chamber at a concentration of $37 \times 10^6 / \text{cm}^2$ to establish a reference coordinate system on the bottom of the well. In the absence of fluid in the well, the vibration (60Hz) induced motion of the slide was visualized and recorded (250fps) with a high-speed camera (Motion-scope, Redlake Digital Imaging Systems, FL) using a 20X objective (Fig. 2.1a). The absence of fluid increased the fluorescent signal intensity of the polystyrene beads, enabling the verification of the sampling rate by comparing it to 500fps. Motions recorded at 250fps were not different from those recorded at 500fps. Fluid containing 40,000 spheres/ml to reach fill heights of either 5mm (1000 μl fluid) or 2.5mm (500 μl fluid) was then added and particle motions were tracked at the horizontal planes specified above (250fps). Acceleration was varied through the output voltage of the function generator. Above 0.6V, our ability to accurately track particles decreased considerably due to total particle travel being larger than field of

view. Thus, 0.6V was used as the maximal voltage, corresponding to 0.86g at a vibration frequency of 60Hz.

Finite element modeling (FEM)

FEM (Abaqus 6.9.1, Simula, RI) was used to determine the 3D fluid flow field within the modeled cell culture well and to investigate how changes in vibration frequency, acceleration magnitude, fluid viscosity and fluid volume alter flow patterns (Fig. 2.1b). To accommodate the computational resources, the distance between fluid nodes was set to 150 μ m, creating 861,888 fluid nodes. Fluid shear acting on the bottom of the well was calculated through the relative velocity magnitude between the bottom and the adjacent fluid layer. To maintain continuity of velocity between the bulk motion of the fluid and the bottom (Fig. 2.1b), a linear velocity gradient between the wall and the first fluid layer was assumed similar to Couette flow,²¹²

$$\tau(y) = \frac{\mu(V_w - V_f)}{h}, \quad (1)$$

where $\tau(y)$ = fluid shear, μ = viscosity, V_w = velocity of well bottom, V_f = fluid velocity, and h = distance between fluid layer and the well bottom. Results were obtained for vibration frequencies of 30, 60, 75, and 100Hz, acceleration magnitudes of 0.01, 0.1, 0.5, and 1.0g, and normal (0% dextran) and viscous

mediums (6% dextran). Data acquired at a level of 150 μm from the well bottom were extrapolated to the cell vicinity of 37.5 μm from the bottom through the PIV defined spatial gradient pattern (Fig.2.2).

The model was validated by comparing shear rates between FEM and PIV at 150, 300, 450 and 600 μm from the well bottom. Further validation of FEM was performed by comparing bulk motions of the fluid to speckle photography and an analytical sloshing model.

Speckle photography

Speckle photography²¹³⁻²¹⁵ was performed to quantify the motion of the well and the relative motion of the fluid within the well during high-frequency oscillations. An acrylic well was casted (18mm wide and 2mm deep), filled with culture medium (α -MEM, Invitrogen, CA) to reach 5mm in height and attached to a horizontally vibrating plate. Mixtures of silicon carbide (SiC) and talc speckles ranging in size from 3 to 20 μm were suspended in the medium to facilitate the tracking of fluid motions throughout the well. The well was vibrated at 60Hz and 1g acceleration. A high-speed camera (Motion-scope, Redlake Digital Imaging Systems, FL) recorded motions of the vibrating well section and its fluid at 250fps. During the analysis, two consecutive frames (720x630pixels) were

extracted and segmented into sets of 16x16 pixel sub-images. The displacement vectors for the speckles within the sub-image were determined with a two-step fast Fourier transform algorithm.²¹⁵

Linear sloshing analytical model

A linear wave theory solution was used to analytically describe the fluid motions caused by the horizontal oscillations.²¹⁶ Briefly, we assumed that the fluid will have a relative velocity $u = \nabla\phi$ with respect to the well during oscillations. The relative velocity potential of a fluid $\phi(x, y; t)$ with a depth (H) in a rectangular container with a width of 2a that is vibrating horizontally at an acceleration of $\ddot{G}_x(t)$ is,

$$\phi(x, y; t) = \sum_{n=0}^{\infty} \dot{C}_n(t) \sin(\alpha_n x) \cosh(\alpha_n (y + H)) \tag{1}$$

where C_n can be determined by the following differential equation.

$$\ddot{C}_n + 2\zeta_n \omega_n \dot{C}_n + \omega_n^2 C_n = \frac{(-1)^{n+1} 2}{\alpha_n^2 a \cosh(\alpha_n H)} \ddot{G} \quad (n = 1, 2, \dots) \tag{2}$$

Here, $\alpha_n = (2n-1)\pi/2a$ and $\omega_n = \alpha_n g \tanh(\alpha_n H)$ are the n^{th} wave number and natural frequency, respectively. ζ_n is a damping ratio to simulate the viscosity of the fluid. Taking the partial derivative of the velocity potential

$\varphi(x, y; t)$ with respect to x and y yielded the relative velocity of the fluid in the well at any given time t . Input parameters were: $H=5\text{mm}$, $a=7\text{mm}$, $\zeta_n=1$, $G=9.81\text{m/s}^2$ and $w=367.99\text{ rad/s}$ (60Hz). At $n>3$, the higher-order terms did not significantly contribute to the solution and, therefore, $n=3$ was used.

In vitro COX-2 experiments

As an application of the model developed above, we tested whether increasing fluid shear, independent of the peak acceleration that the cell receives, increases COX-2 gene expression levels in osteoblast like MC3T3-E1 cells. COX-2 is an enzyme that directly produces PGE_2 and thereby plays a key role in mechanically induced bone formation.^{208, 209} Inhibition of COX-2 and PGE_2 blocks new bone formation by mechanical signals *in vivo*.²¹⁷ Cells were subjected to vibrations for 30min at frequencies of either 10, 30, 60 or 100Hz in standard or viscous medium that contained 6% dextran ($n=9$ / group). The peak acceleration of the sinusoidal oscillatory signal was selected as 1g because data from our model indicated that this acceleration level can generate fluid shear stresses that are similar to those generating a MC3T3-E1 response in previous fluid shear investigations.^{151, 35} Experiments were performed at a fluid height of 2.5mm within each well to maintain optimal oxygen diffusion (Corning Inc.). Cells in the

control groups were subjected to identical procedures as those in the vibration groups but the oscillating stage was not turned on.

MC3T3-E1 cells (CRL-2593, ATCC, Manassas, VA) were cultured in culture dishes (100mm, Corning Inc., NY) using α -MEM supplemented with 10% fetal bovine serum (FBS, Gibco, CA) and 1% Penicillin-Streptomycin (PS, Gibco, CA) and incubated at 37°C, 5% CO₂. Medium was changed every 48h. Cells were sub-cultured prior to reaching confluence. Cells were then seeded in 24-well plates (CLS3527, Corning Inc.) using 0.5ml of culture medium at a density of 140,000 cell/ml. Cells were then incubated at 37°C and 5% CO₂ for 24h to facilitate attachment. Prior to exposure to the mechanical signal (1g peak acceleration at 10, 30, 60, or 100Hz), the fluid in each well was aspirated out and cells were supplied with new culture medium containing 2% FBS and 1%PS. Fluid shear was modulated by increasing the viscosity of the culture medium via the addition of 6% (w/v) dextran (Molecular Weight ~70,000, Sigma, Lot#0001352455). Upon vibrating the cell culture dishes for 30 minutes, all fluid was aspirated from the wells and cells were supplemented with a culture medium without dextran containing 2% FBS and 1% PS. In an preliminary experiment to evaluate temporal response, COX-2 shown to peak within one hour and return back to control levels after three hours. To add up the total time after vibrations to one hour, cells were returned to incubator for 30 minutes.

Following a 30min incubation period at 37°C and 5% CO₂, cells were treated with 600ml of TRIzol (Ambion, TX) and stored at -80°C. Total RNA was isolated (RNeasy Mini Kit, Qiagen, CA) and its quality and concentration were determined (NanodropND-1000, Thermo Scientific, NY). Upon reverse transcription (High Capacity RNA to cDNA kit, Applied Biosystems, CA), qPCR was performed (Step-One Plus, Applied Biosystems, CA) using Taqman primer probes (Applied Biosystems, CA) for COX-2 (Mm_00478374_m1_Ptgs2) and 18S (Mm_03928990_g1_Rn18s) that served as referent. Expression levels were quantified with the delta-delta CT method.²¹⁸ Experiments were repeated three times with n=3 each. Results were presented as mean ± SEM. Differences between groups were identified by one-way analysis of variance (ANOVA) followed by Newman-Keuls post-hoc tests. P-values of less than 0.05 were considered significant.

Results

Mechanical signals in the immediate vicinity of the cell layer

Particle image velocimetry (PIV) allowed the quantification of fluid velocities in close proximity of the well bottom. In wells filled up to 2.5mm, the shear rate between layers at 37.5, 75, 112.5 and 150µm from the bottom of the well was

non-linear ($R^2=0.99$ for 2nd degree polynomial fit, Fig.2.2), reaching peak shear stresses of up to 0.47Pa at 37.5 μm and 0.15Pa at 150 μm . Increasing fluid fill height from 2.5mm to 5mm decreased the shear rate almost 2-fold as a result of decreased relative fluid velocity, from 163 to 79 $\text{sec}^{-1} \cdot \text{g}^{-1}$.

Bulk motion of the fluid within the well

Data from the accelerometer and speckle photography confirmed that the horizontal oscillation of the well was sinusoidal with an amplitude of $152 \pm 8.2 \mu\text{m}$ (Fig. 2.3a). By step-wise decreasing the oscillation frequency from 60 Hz to 10Hz and measuring the free surface elevation near the side wall of the well, the resonance frequency was determined to be equal or smaller than 10Hz (Fig. 2.3b). Thus, frequencies at 30Hz or above did not induce large nonlinear motions typically observed at resonance.²¹⁹⁻²²² Speckle photography also quantified the oscillation-induced relative motion of the fluid within the well. The relative displacement of fluid within the well was $7.1 \mu\text{m} \pm 1.3 \mu\text{m}$ on average, corresponding to a phase shift of $\frac{\pi}{10.5}$ radians over a 60Hz, 1g cycle (2π) (Fig. 2.3c). This phase shift matched the results from the FEM that was $\frac{\pi}{10}$ radians (Fig. 2.4a), corresponding to 7.5 μm of fluid displacement. As visualized by speckle photography, the oscillatory motion caused the direction of the fluid

displacement vectors to shift to a vertical direction near the side wall, justifying the selection of a previously described two-dimensional linear model of fluid sloshing in a horizontally oscillating well.²¹⁶

Bulk fluid motion was compared between the analytical closed-form solution and the FEM to test for potential discrepancies. Relative fluid velocities quantified at three random points within the well (Fig. 2.4b) were in good agreement between the two methods even though the analytical model was 2D and not 3D (Table 2.1). Similar to speckle photography (Fig. 2.3c), horizontal components of the relative fluid velocities determined by FEM decreased in the vicinity of the walls (Fig. 2.4b). The inhomogeneity of the flow field was reflected in the histogram of fluid shear stress magnitudes in a plane 150 μ m from the well bottom wall at $t=0.005\text{sec}$ ($\pi/4$). 70% of the fluid nodes in a vertical plane experienced fluid shear between 0.10 and 0.08Pa with shear at the remaining fluid nodes decreasing to 0.01Pa at the side wall (Fig. 2.4c). The central region of the well was subjected to maximal fluid shear values. At 150 μ m from the well bottom, peak fluid shear stresses in the center reached up to 0.13Pa during a 60Hz, 1g vibration cycle (Fig. 2.4a). There were also vertical motions of the fluid surface due to sloshing. However, the vertical motions of the fluid surface did not propagate to layers in the proximity of the cells (well bottom) and peak

vertical fluid shear was at least two orders of magnitude smaller than peak horizontal fluid shear.

Modulation of fluid shear stress via viscosity, acceleration and frequency

FEM defined how changes in vibration frequency, acceleration magnitude, fluid viscosity and fluid volume modulated fluid shear in the vicinity of the cell layer. For a fill height of 5mm, shear rates showed an excellent agreement between FEM and PIV at distances up to 600 μ m from the bottom (Fig. 2.5). Similar agreement was observed at 2.5mm fluid fill height. For instance at 150mm from bottom wall, FEM showed a shear rate of 150 $\text{sec}^{-1}.\text{g}^{-1}$, compared to the experimental shear rate of 163 $\text{sec}^{-1}.\text{g}^{-1}$.

To increase fluid shear without altering any variable defining the vibratory signal, fluid viscosity of the medium was increased. The addition of every 3% (v/w) dextran approximately doubled the fluid viscosity from 1.05cP at 0%, to 2.12cP at 3% and 3.58cP at 6% dextran. Independent of the applied frequency and acceleration, the greater viscosity of the fluid slightly decreased fluid shear rates because of greater fluid density. However, the modest decrease in shear rates was over-compensated by the large increase in fluid shear resulting from the greater fluid viscosity. For example, the resulting peak fluid

shear stresses measured at 150 μ m from the well bottom increased from at 0.13Pa at 0%, to 0.22Pa at 3%, and 0.33Pa at 6% dextran during 60Hz, 1g oscillations.

Increasing vibration frequency nonlinearly increased fluid shear. At an acceleration magnitude of 1g, fluid shear stress at 30Hz (0.94Pa) decreased by 70% when raising signal frequency to 100Hz. Increasing acceleration magnitude linearly increased fluid shear. At a vibration frequency of 60Hz, the fluid shear stress increased an order of magnitude from 0.047Pa to 0.47Pa when the acceleration magnitude was increased from 0.1g to 1g (Fig. 2.6).

Modulation of COX-2 mRNA levels by vibration frequency, acceleration and fluid viscosity

COX-2 mRNA expression was determined after a 30min exposure to a signals of 1g peak acceleration at four different frequencies (10, 30, 60 and 100Hz). Cells were oscillated in fluid viscosities of 1 or 3.5cP, corresponding to 0 and 6% dextran solutions. Cells did not lift off the well bottom during vibrations in either medium. Compared to controls, all frequencies significantly increased COX-2 gene expression except the 60Hz, 6% dextran group (Fig. 2.7). In standard culture medium viscosity, COX-2 transcriptional level were the highest in the 100Hz

group ($p < 0.01$). This difference in COX-2 could not be attributed to an increase in fluid shear since fluid shear stress was the smallest at 100Hz (0.28Pa). Increasing the viscosity from 1cP to 3.5cP via the addition of dextran greatly increased fluid shear stress; at an oscillation frequency of 30Hz, peak fluid shear at the well bottom increased from 0.94Pa to 2.6Pa. While control COX-2 levels were not significantly different between the 0% and 6% dextran groups, COX-2 levels increased less with vibrations in the more viscous medium. In contrast to the relatively similar COX-2 levels across the frequency spectrum in normal culture medium, there was a trend towards lower COX-2 expression in the higher frequency groups in the 6% medium; COX-2 expression in the 10Hz and 30Hz groups was significantly greater ($p < 0.001$) than in the 60Hz and 100Hz groups (Fig. 7).

Discussion

Particle image velocimetry and finite element modeling were used to characterize mechanical signals, in particular fluid shear, that the cell layer in a culture well experiences during high-frequency vibrations. FEM, speckle photography, and an analytical sloshing model characterized the motion of the bulk flow. Cellular fluid shear stress was modulated by fluid viscosity, fluid

volume, vibration frequency and acceleration. At 30Hz and 1g, shear stresses reached up to 1Pa. Tripling vibration frequency decreased shear more than 2-fold while decreasing acceleration magnitude to 0.1g reduced shear by an order of magnitude. To highlight potential applications of this model, we tested whether vibration induced fluid shear in pre-osteoblasts drives the expression of a gene known to be responsive to low-frequency fluid shear. In regular culture medium, the group that experienced the smallest amount of fluid shear (100Hz) showed the greatest increase in COX-2 expression. Increasing fluid viscosity and fluid shear muted, rather than increased, COX-2's response to vibrations. Within this high fluid shear (viscosity) group, shear stress was negatively associated with vibration frequency and there was a trend towards greater COX-2 transcriptional levels with greater shear stresses. The absence of consistent associations between COX-2 and the mechanical variables considered here indicates that the physical mechanism by which pre-osteoblasts sense and respond to high-frequency mechanical signals *in vitro* is not defined by fluid shear or signal frequency.

Several limitations should be considered when interpreting our findings. The full-field velocity solutions for the well showed that shear stress is distributed spatially non-uniform with the greatest stresses at the center. While this heterogeneity precludes determination of the precise level of any given

mechanical parameter that cells responded to during vibrations, it allows conclusions regarding the *change* in the cellular response when altering vibration parameters. Micron-sized surface features of the cell may alter local fluid shear gradients²²³ but the resolution of PIV was not sufficient to capture these local variations. Thus, shear stresses quantified here via linear assumptions may slightly underestimate the true shear magnitudes experienced by cells. Lastly, the 10Hz vibration group was included in the cell culture experiments but the non-linear fluid sloshing effects at this frequency did not permit an accurate assessment of fluid shear. Thus, cells subjected to 10Hz oscillations in either the normal or dextran medium experienced much greater shear levels than the higher-frequency groups and may give an indication of the cellular response to the maximal level of fluid shear that our *in vitro* system can generate at a given acceleration magnitude.

Cell culture studies using vibrations as mechanical input for regulating cell activity are becoming increasingly popular.^{224, 186, 196, 184, 207, 206} While these studies have been defining the biochemical response of the cell, the physical mechanism by which the signal is sensed and transduced is typically neglected. Primarily based on *in vivo* investigations, direct and indirect mechanisms have been suggested including out-of-phase acceleration of the cell nucleus¹⁹² or fluid shear.⁵² Unlike *in vivo* experiments in which these variables are difficult to

separate, the mechanical characterization of our horizontally oscillating cell culture system demonstrates that this can be readily achieved *in vitro*. Vibrating the cells horizontally represents a physiologically more relevant model by creating substantial amounts of fluid shear compared to vertical vibration which primarily generates fluid shear by straining the well wall but not by vertical motions.²²⁵ A model capable not only of generating but also of precisely controlling fluid shear is critical for studying many cell types/tissues including bone in which the high viscosity of the bone marrow and the geometry of the surrounding trabecular bone can give rise to significant fluid shear during vibrations *in vivo*.¹⁰⁵

In contrast to the frequently used parallel plate assumption,³⁵ experimental data showed that fluid shear stress magnitude spatially increased nonlinearly towards the cell layer, perhaps a consequence of the high frequency of the fluid motion which behaved like a harmonic oscillator.²¹⁶ Because the bone marrow cavity is entirely filled with fluid, the sloshing motion created by *in vitro* oscillations is different from fluid motions *in vivo*. The fluid within the bone marrow, however, is 40 to 400 times more viscous than water,²²⁶ linearly raising fluid shear caused by fluid motions. Thus, even though the space in the marrow cavity is fully filled and fluid motions induced by vibrations are much smaller than generated here, the resulting fluid shear stresses are significant.¹⁰⁵ In

contrast, vibrations produce only negligible fluid shear in a fully filled cell culture well,^{182, 186, 196} precluding comparisons to the *in vivo* mechanical environment. While increasing the *in vitro* viscosity of the fluid will increase shear, the viscosity of bone marrow cannot be modeled by the addition of dextran because of cell death at high dextran concentrations.²²⁷ Thus, the large difference between *in vitro* and *in vivo* fluid viscosities necessitates an *in vitro* model that raises fluid motions in an open well to generate levels of fluid shear similar to those encountered *in vivo*.

The most comprehensive analysis of vibration induced fluid shear stress *in vivo* was performed with a computational model based on mixture theory.¹⁰⁵ In this model, accelerations applied to a bone induce strain in the bone matrix which, in turn, leads to fluid shear. In this study, fluid shear was positively correlated with both viscosity and vibration frequency. In our study, fluid shear was also positively correlated with viscosity but in contrast, a negative correlation was observed between fluid shear and vibration frequency. This discrepancy is likely accounted for by differences in how confounding variables were treated. In our model, we kept acceleration magnitude constant when increasing vibration frequency, causing a decrease in peak fluid velocity and resulting fluid shear. In the previous study, however, matrix strain was kept constant when frequency was increased. As the *conservation of momentum*

dictates that all inertial forces have to be balanced with strains, increasing the frequency decreases peak velocity (*i.e.*, linear momentum). Thus, matrix strains can only remain constant if linear momentum is increased, implying that acceleration magnitudes increased concomitantly with frequency in their model. Our model however separated the role of *accelerations* from *frequency* and derived fluid shear stresses from relative motions of the fluid rather than from relying on very small matrix deformations.

Our COX-2 expression data from cells subjected to relatively low-shear in normal culture medium showed that shear stress was unrelated to vibration induced differences in transcriptional activity. These results are similar to those from *in vivo* low-intensity vibration studies, demonstrating that bone has the ability to sense vibrations over a wide range of frequencies⁷⁶ and that higher-frequency vibrations generating less fluid shear, rather than more, can be more effective in initiating new bone for a given peak acceleration.¹⁹⁰ Increasing the viscosity of the medium by adding dextran significantly increased shear stress at all frequencies. For these high-shear conditions and in contrast to the low-shear conditions, the vibration induced increase in COX-2 expression was moderately associated with the level of shear generated, consistent with an *in vivo* study in which the application of large-magnitude vibrations produced a skeletal

response that was dependent on shear stress (i.e., acceleration magnitude) to which the cells were exposed.⁷²

Previous studies that demonstrated a frequency-dependency of COX-2 expression in bone cells used completely filled and sealed containers, largely eliminating fluid shear.^{182, 186} Here, using an *in vitro* system that allowed us to generate fluid shear magnitudes similar to those experienced *in vivo* (~0.1-2Pa),¹⁰⁵ we showed that amplifying fluid shear 2.6-fold via dextran decreased and not increased, COX-2 transcriptional levels. The differential response between the two distinct viscosity groups was independent of differences in osmolarity as COX-2 levels in the two control groups were identical. Ostensibly, the lower responsiveness in the higher viscosity group could be attributed to decreased chemotransport.²²⁸ In low-frequency fluid shear studies, 0.5-1Pa are required to elicit a biologic response in osteoblast like cells *in vitro*,²²⁹ but the typically used pulsating or continuous flow profiles may provide a more potent stimulus to cells than oscillating flow generated here.³⁵ Further, a cell's responsiveness to flow may decrease at high frequencies.²³⁰ As peak shear generated at 30Hz in normal medium was at least 0.94Pa and no influence of shear on COX-2 was observed, our data suggest that fluid shear must reach levels of at least 1Pa for fluid shear to play a significant role in defining the cellular response to vibrations.

The only group in which vibrations did not increase transcriptional levels of COX-2 was the 60Hz, 6% dextran group. In the 0% dextran 60Hz group, the COX-2 response was not abolished but merely lower than for the other frequencies and, therefore, cells clearly have the ability to respond to this specific frequency. It is entirely possible that the (unknown) mechanism which senses and orchestrates the cellular response to vibrations is less sensitive to a 60Hz frequency. Considering that the COX-2 response was greater at 100Hz than at 60Hz at both dextran concentrations, it is also possible that this cellular mechanism is particularly sensitive to 100Hz vibrations (e.g., cytoskeletal resonance²³¹), and that the lack of a response in the 60Hz group, 6% dextran group merely follows the downward trend in cellular responsivity defined by the 10Hz and 30Hz signals. Previous studies indicated that the cellular responsiveness to mechanical signals can be increased by incorporating rest periods, independent of signal frequency.^{67, 181} Whether the addition of rest period could normalize the COX-2 response in the 60Hz, 6% dextran group remains to be determined.

In summary, we characterized the mechanical environment of cells *in vitro* during horizontal vibrations that exposed cells not only to oscillatory accelerations but also to oscillatory fluid shear. In this system, fluid shear can be controlled precisely and independently by acceleration magnitude, vibration

frequency, fluid viscosity and fluid volume and may allow for the potential identification of the specific mechanical parameter(s) that cells respond to during the exposure to vibrations. As an example of an application of this system, we subjected an osteoblast-like cell line to four different frequencies under two distinct fluid viscosities. Under low viscosity conditions, fluid shear was a poor predictor of the molecular response. Under high fluid shear conditions, shear stress emerged as a variable that may have played at least a role in modulating COX-2 expression levels. These data suggest that other mechanical factors such as the out-of-phase acceleration of the cell nucleus^{182, 71} may need to be considered for investigating oscillatory mechano-transduction in cells. The identification of these mechanical factor(s) and their effects and interactions under different vibration conditions will be critical to advance our understanding of the mechanisms by which cells in different tissues respond to high-frequency mechanical signals.

Acknowledgements

Funding by the National Institutes of Health (NIAMS) is gratefully acknowledged. Technical expertise from Dr. Michael Hadjiargyrou and Lester Orlick was greatly appreciated.

Tables

Table 2.1. Comparison between the linear and finite element solutions at different spatial locations as specified in Figure 3 during 60Hz, 1g oscillations. Results are represented as percentages of the peak well velocity of 0.027m/s.

	Point A	Point B	Point C
Linear Solution	98.6%	72.6%	20.7%
Finite Element	88.5%	70.4%	15%

Figures

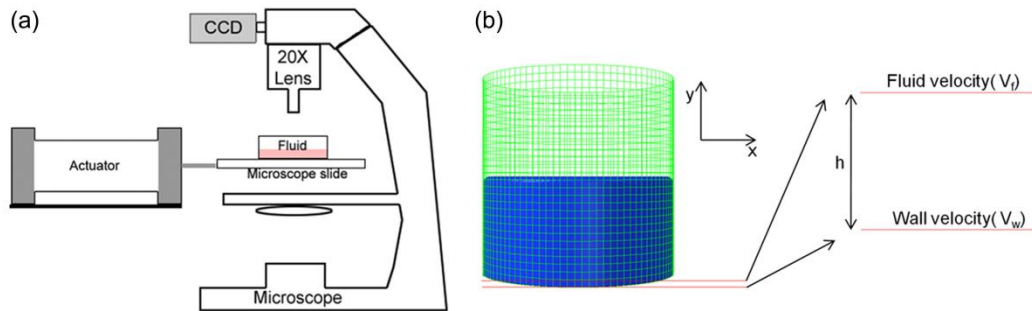


Figure 2.1. Experimental and computational methods used to describe fluid motions at the well bottom. (a) Schematic of the Particle Image Velocimetry (PIV) setup. A high-speed camera recorded the motions of $1\mu\text{m}$ red fluorescent polystyrene particles vibrating within a fluid filled chamber attached to a microscope slide. Fluid shear was quantified by comparing the motion of the slide surface to the particle motions measured at $37.5\mu\text{m}$ distance intervals. (b) A fluid filled cell culture well was modeled as viscous fluid within a rigid well with the Finite Element Method (FEM). Vibration induced fluid shear at the bottom of the well was calculated by computing the relative velocity between wall and fluid assuming linear velocity gradients.

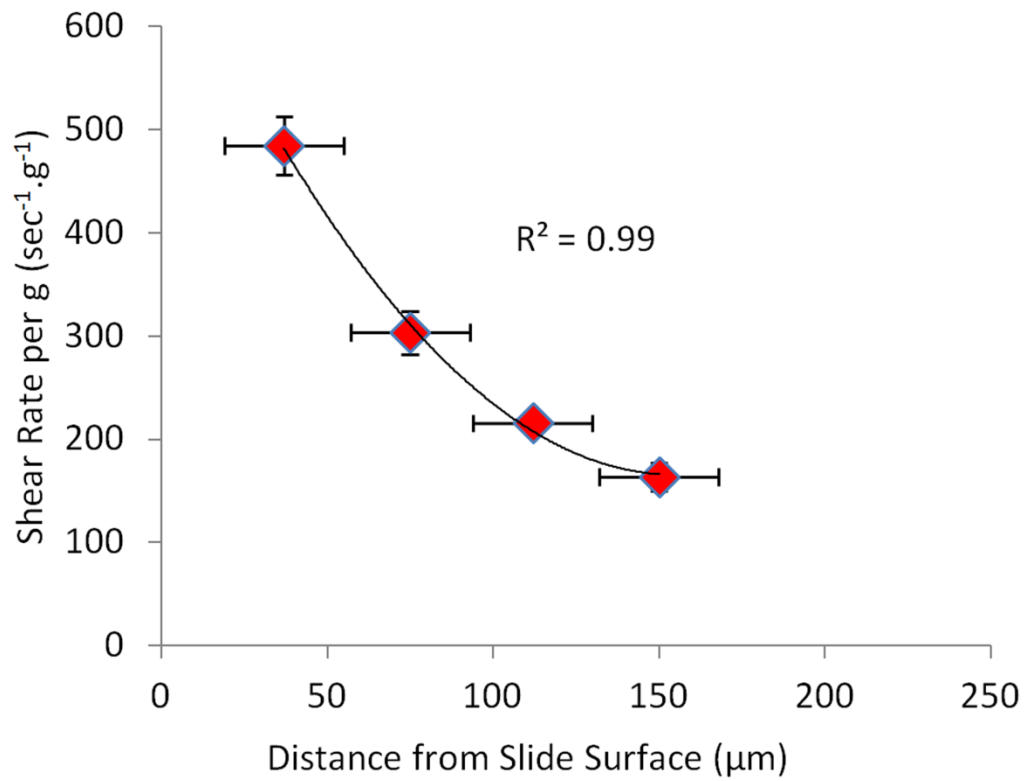


Figure 2.2. Shear rates between fluid and the well bottom as determined by PIV. PIV showed a steep non-linear increase in shear rate towards the surface of the glass slide (bottom of the well).

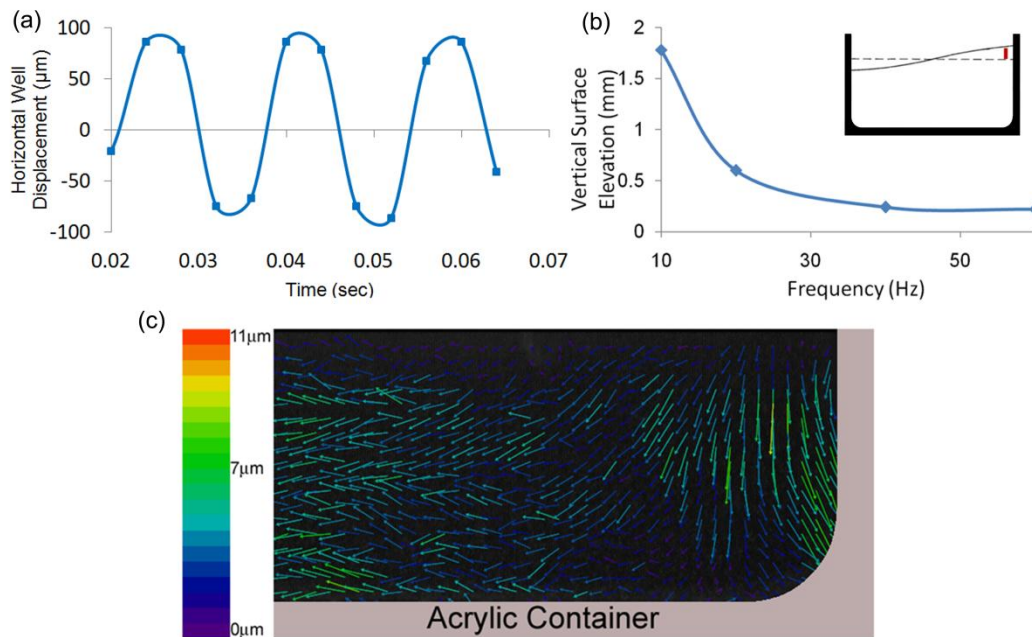


Figure 2.3. Motions of the well and the fluid as determined by speckle photography (a) Displacement of the well, during 1g, 60Hz oscillatory motions. (b) Elevation of the fluid surface near the side-wall of the well (vertical red line in inset) as a function of vibration frequency. Non-linear surface motions at frequencies around 10Hz are indicative of resonance behavior. (c) Upon completion of one full oscillatory cycle, out-of-phase fluid displacements relative to the well demonstrated sloshing behavior are visualized in the mid-sagittal plane of the well.

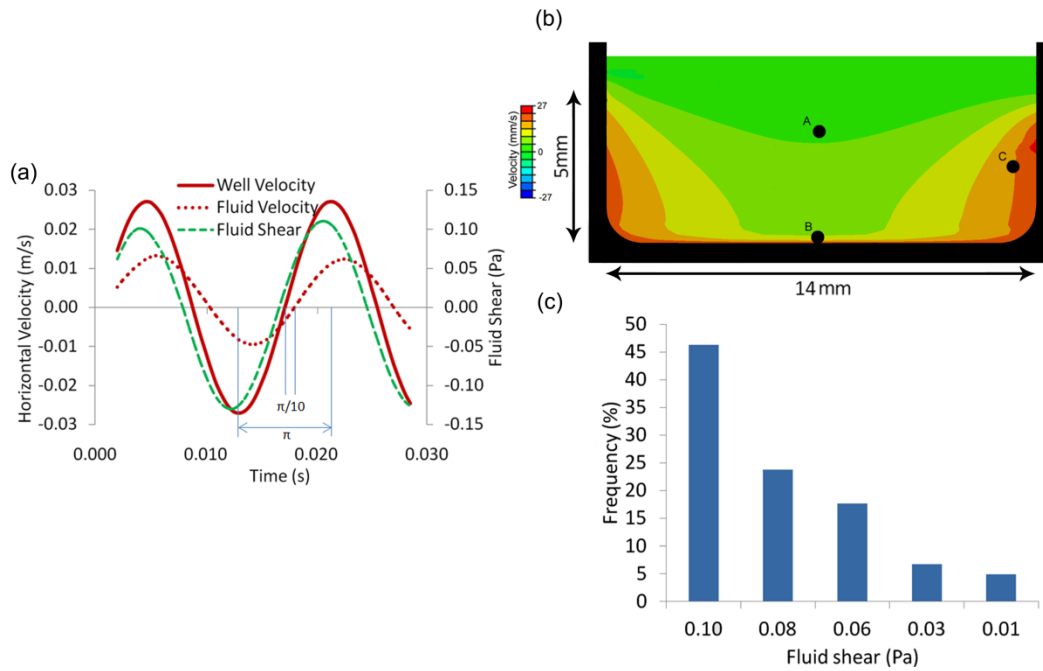


Figure 2.4. Fluid velocities and shear stress determined by FEM (a) Velocity profile of the rigid well (solid-red), fluid velocity (dashed-red), and fluid shear at Point B (see Figure 4b) during a 60Hz, 1g oscillatory motion. The phase difference between the well and the fluid was $\frac{\pi}{10}$ radians. (b) The velocity profile of the viscous fluid at $t=0.005s$ during the 1g, 60Hz oscillatory motion of the rigid well (in black). Shown is a mid-sagittal plane of the well. Points A, B, and C were used to compare relative fluid velocities against the linear solution depicted in Table 2.1. (c) Histogram with the distribution of fluid nodes subjected to a given level of fluid shear at $t=0.005s$. In spite of spatial non-uniformity, approximately 75% of the well surface received shear stresses within 20% of the peak shear stress magnitude.

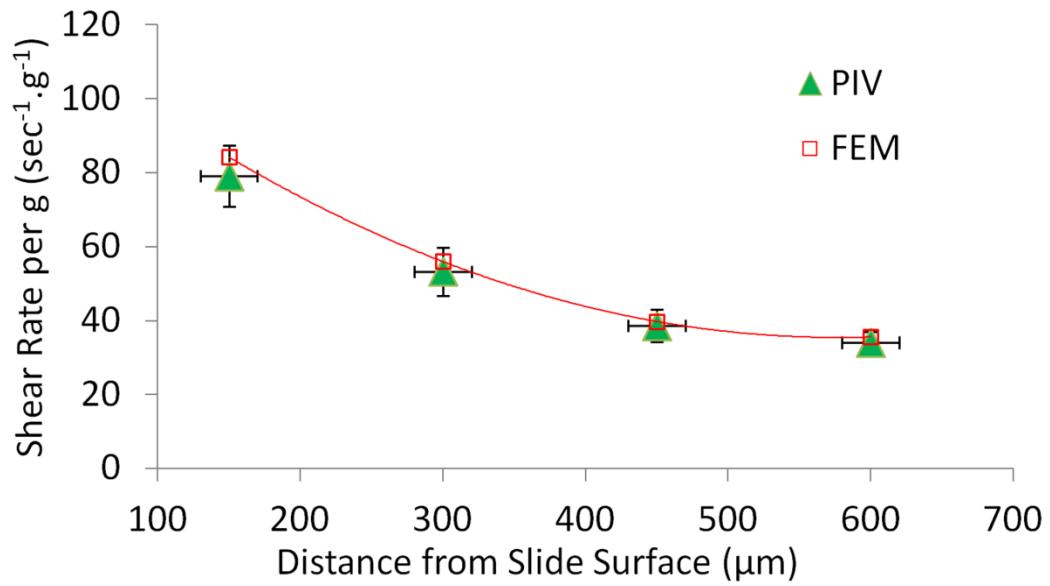


Figure 2.5. Validation of FEM simulations by PIV. Comparison of shear rates between FEM and PIV at heights of 150, 300, 450 and 600 μm from the well bottom. Measurements were taken in a well with a total fluid height of 5mm.

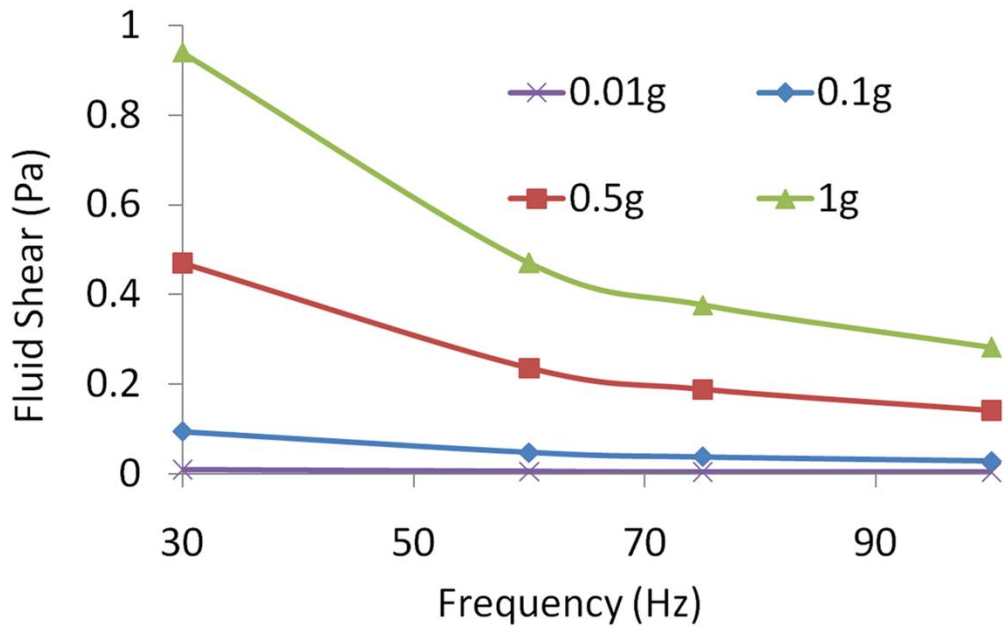


Figure 2.6. Modulation of fluid shear by vibration parameters. Peak fluid shear stress was modulated by vibration acceleration magnitude and vibration frequency, demonstrating that different combinations of frequency and acceleration can produce identical shear stress values.

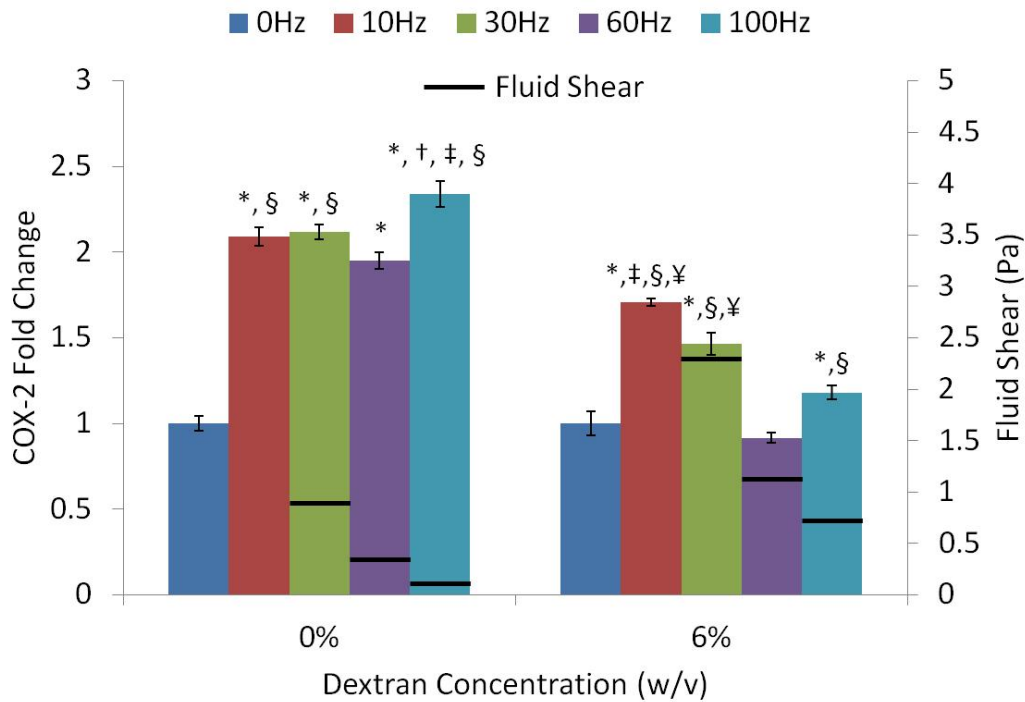


Figure 2.7. Change in COX-2 expression of MC3T3-E1 cells exposed to five different frequencies under low-shear (0% dextran) and high-shear (6% dextran) conditions. Fluid shear for each frequency is represented by horizontal black bars. Shear at 10Hz could not be quantified because of resonance behavior of the fluid at this frequency. $P < 0.05$: * against 0Hz, † against 10Hz, ‡ against 30Hz, § against 60Hz, ¥ against 100Hz.

Chapter 3

*VIBRATIONS MODULATE PROLIFERATION AND
OSTEOGENIC COMMITMENT OF MESENCHYMAL
STEM CELLS IN THE PRESENCE OF PRESTRESS*

Abstract

Consistent across studies in humans, animals and cells, the application of vibrations can be anabolic and/or anti-catabolic to bone. The physical mechanism that modulates the vibration-induced response has not been identified, in part because putative mechanisms including fluid shear and acceleration are difficult to separate *in vivo*. Recently, we developed an *in vitro* model in which acceleration magnitude and fluid shear can be controlled independently during vibrations. We hypothesized that, vibration induced fluid shear is not necessary to enhance mesenchymal stem cell (MSC) differentiation and cytoskeletal remodeling and that cell sensitivity to vibrations can be promoted via actin stress fiber formation. Adipose derived human MSCs were subjected to vibration frequencies and acceleration magnitudes that induced fluid shear stress ranging from 0.04Pa to 5Pa. Vibrations applied at 0.15g to 2g accelerations at both 100Hz and 30Hz. After 13 days, mineralization was greater in stimulated groups than in controls. The enhanced mineralization was not correlated with fluid shear in 100Hz vibration groups where fluid shear levels were low (< 1 Pa). At 30Hz, there was a trend towards a increase in mineralization with increasing acceleration and fluid shear. Early gene expression data showed that in the absence of actin stress fiber formation, mechanical

vibrations were not sufficient to induce osteogenesis. However, increasing cell tension with lysophosphatidic acid enabled mechanical vibrations to upregulate RUNX-2 mRNA levels. Mechanically induced remodeling of the actin cytoskeleton correlated with increasing acceleration magnitude at mRNA level. These results showed that fluid shear was not necessary in vibration induced osteogenesis and accelerations alone increase cytoskeletal remodeling which may play a role in cellular mechanosensitivity.

Introduction

Low-level vibrations have been recognized as a mechanical signal than can be anabolic and/or anti catabolic to calcified tissue both *in vivo and in vitro*.^{7, 39}

Studies show that the vibrations can modulate mechanical adaptation of bone in a frequency specific¹⁹⁰ or a dose dependent¹⁸¹ manner. Because of the stiffer skeleton, vibrations can be readily transmitted through calcified tissue from the site of induction over long distances²⁰³ as shown by the responses on load bearing sites including spine,²³² femur and tibia.⁷² Interestingly, vibrations found to be more specific to the trabecular bone compared to cortical regions.⁷⁴

However, the mechanical environment that a cell within the matrix or within the bone marrow perceives and responds to is unknown, precluding the interpretation of site specific signal-response data on vibration induced regulation of bone metabolism.

Strains induced by low-level vibrations²³³ are at least two orders of magnitude smaller than those required to elicit a response when the signal frequency is much lower.⁸⁸ Considering that vibrations applied during non-weight bearing retain their efficacy in the presence of extremely small deformations ($\sim 1\mu\epsilon$),⁷¹ it is unlikely that matrix deformations are critical for cells sensing the mechanical signal. However, drag forces resulting from dynamic accelerations may produce

physiologically relevant levels of fluid shear on bone/fluid interfaces.^{103, 105} Inside the bone marrow cavity and in trabecular regions, the level of shear is highly dependent on marrow viscosity which can change dramatically during aging and osteoporosis, fatty bone marrow replaces red marrow that has a 10-fold smaller viscosity.^{108, 110, 111} Changes in the magnitude of fluid shear during vibrations could modulate the function of resident bone cells and ultimately influence the mechanical adaptation of bone. For example using osteoblasts, we previously showed that during vibrations, increasing the fluid shear over 1Pa by changing the viscosity could reverse the frequency response of mRNA levels of COX-2,²³⁴ a mechanically inducible enzyme which is responsible for PGE₂ mediated bone repair and MSC differentiation.²³⁵

Cells have specialized elements to sense mechanical stimuli, such as primary cilia for sensing fluid shear.²³⁶ However it is entirely possible that cells can generally sense mechanical signals through a common element. As a continuous structure between chromosome and cell membrane, the cytoskeleton is a likely candidate for transmitting mechanical cues within a cell.¹⁶⁷ Instantaneous mechanical coupling between cell membrane and cytoskeleton was demonstrated by magnetically twisting integrin bound beads.¹⁶⁶ Cytoskeleton elements can distribute the local deformations to create global deformations²³⁷ not necessarily limiting the propagation of mechanical

information to “outside-in”.^{238, 168} Ostensibly, vibrations that cause out-of-phase movement of the denser and stiffer nucleus may be capable of initiating similar mechanotransduction cascades through cytoskeleton when compared to fluid flow. From this mechanistic viewpoint, the efficacy of different mechanical inputs directly depends on the efficiency of force transfer through the cytoskeleton. Interestingly, cytoskeleton can act as a mechanosensory site and directly modulate the force transfer by changing the prestress state of the cell based on mechanical environment¹⁶³ including fluid flow,¹⁵¹ matrix deformation¹⁶⁰ or substrate stiffness.²³⁹

To understand the contribution of the fluid shear to the effects of vibrations on the osteogenic differentiation of MSCs, we used a previously developed *in vitro* method that can control the fluid shear cells subjected to during high frequency vibrations. We hypothesized that, vibration induced fluid shear is not necessary to enhance mesenchymal stem cell (MSC) differentiation and cytoskeletal remodeling and that cell sensitivity to vibrations can be promoted via actin stress fiber formation.

Materials and Methods

Experimental design

Throughout the manuscript we divide the mechanical forces created by application of vibrations to two different main components, accelerations and vibration induced fluid shear stress. While accelerations is a direct measure of vibration magnitude, as shown previously, vibration induced fluid shear stress is a function of vibration frequency, acceleration and fluid viscosity²³⁴. For simplicity we refer vibration induced fluid shear stress as fluid shear. To investigate whether fluid shear contributes to the response of MSCs exposed to vibrations, parameters that generate a broad range of fluid shear values were selected. Three different accelerations, 0.15g, 1g, and 2g were applied at two different frequencies (30Hz and 100Hz) to create similar fluid shear conditions at different vibration magnitudes. Furthermore, we incorporated 6% (v/w) dextran into cell culture media to increase in fluid shear independent of vibration parameters (Table 3.1). At day 1 mechanosensitivity of early RUNX-2, RANKL and OPG mRNA expressions to increasing fluid shear or accelerations were assessed with or without actin stress fiber formation. Additionally the effects of vibration on cytoskeletal remodeling were profiled using a PCR array at day 7.

Mechanically-induced cell proliferation and mineralization were assessed at days 3 and 16, respectively (Fig. 3.1).

Cell culture

The commercially available adipose derived MSCs (18yr old female, Lifeline Technologies, Walkersville, MD) were cultured in standard flasks (75cm², Corning Inc., NY) at a density of 5,000 cell/ cm² using Stemlife basal medium (Lifeline Technologies) supplemented with penicillin-streptomycin (PS, Gibco, CA) and incubated at 37°C, 5% CO₂. Medium was changed every 48h. Cells were sub-cultured prior to reaching 70% confluence. For all experiments, only cells of passage four or less were included.

For the experiments utilizing osteogenic differentiation, osteogenic medium (Osteolife complete osteogenic medium, Lifeline technologies). All the other experiments used Stemlife basal medium (Lifeline Technologies) unless stated otherwise, which we refer to as normal medium.

Application of vibrations and determination of fluid shear

The vibration system that horizontally oscillated the cells is described in detail elsewhere²⁴⁰. Briefly, an actuator (NCM15, H2W Technologies Inc., CA) capable of producing frequencies between 10-100Hz and peak accelerations of up to 2g

was attached to a stainless steel plate mounted on a linear frictionless slide (NK2-110B, Schneeberger GmbH, Germany). Up to three 24 or 96-well cell culture plates can be vibrated simultaneously with this system. Vibration treatment was applied for 30 minutes at 0.15, 1, or 2g peak vibration magnitudes using 30 and/or 100Hz signals across all experiments. Vibrations were applied at room temperature. Control samples were handled exactly the same except vibration was not applied. Out-of-phase sloshing of cell culture medium during vibrations was calculated using previously constructed and experimentally validated finite element model.²³⁴ Using full-field velocity distribution within cell culture well fluid shear was calculated. Level of generated fluid shear correlates positively with vibration magnitude (acceleration) and negatively with vibration frequency.

Calcification assay

Forty-eight hours prior to commencing an experiment, cells were seeded at a density of 18,000 cells/cm² in 24-well plates. Osteogenic factors were introduced after 48 hours. Vibration treatment was applied using both 30 and 100Hz signals for a total of seven groups (n=5 / group). After 13 days of vibration cells were fixed with 70% ethanol for 1 hour and stained with 40mM alizarin red S (Sigma-

Aldrich, St Louis, MO). Cells were de-stained with Cetylpyridinium chloride (Sigma) and the concentration of total dye was quantified using spectrophotometer at 590nm.

Cell proliferation assay

Cells were seeded on 24 well plates with or without 0.15mg/ml rat tail Collagen I (Cell Applications Inc., CA) at a density of 750 cells/cm². Collagen was implemented to create stronger integrin attachment²⁴¹ which might enhance cell responsiveness.¹⁶⁰ After allowing attachment for 24 hours, vibration treatment was applied using both 30 and 100Hz signals (n=4 / group). Cell number was determined with a XTT cell proliferation assay (ATCC, VA) 24 hours after two days of vibration treatment.

Gene profiling assay

In the first set of mRNA experiments, we investigated the immediate effects of large changes in fluid shear and increased cell pre-stress after one time application of vibrations on mRNA levels and cell viability. Fluid shear was controlled by vibration magnitude or by changing fluid viscosity via dextran (Molecular Weight ~70,000, Sigma) which facilitated acceleration independent

increase of fluid shear. LPA (lysophosphatidic acid, Cayman chemical, MI) was used to create rapid actin stress fiber formation within two hours. Cells were plated at 18,000 cell/ cm². After 46 hours, the medium from each well was aspirated and replaced with mediums containing either normal medium, normal medium + 6% (w/v) dextran or normal medium + 125uM LPA. Dishes were then incubated at 37°C and 5% CO₂. After two hours, cells were exposed to vibrations once for 30min at 0.15, 1, or 2g peak acceleration magnitudes at 30Hz (n=6 / group). mRNA levels of RUNX-2, RANKL and OPG were determined immediately after vibration treatment.

In the second set of mRNA experiments we investigated the longer term relation between cytoskeletal remodeling and fluid shear. Cells were vibrated for 6 days (n=3/group). Since only cells that undergoing cytoskeletal remodeling (normal medium + 125uM LPA) was responsive to vibrations, long term remodeling of cytoskeleton was facilitated by culturing the groups in osteogenic medium. 24h after last vibration treatment, samples within each group were pooled and mRNA levels for 84 genes controlling cytoskeletal remodeling were profiled using commercially available PCR array (Human cytoskeleton regulators, Qiagen, CA)

RNA extraction and qPCR

Cells were lysed with 600µl of TRIzol (Ambion, TX) and stored at -80°C. Total RNA was isolated (RNeasy Mini Kit, Qiagen, CA) and its quality and concentration were determined (NanodropND-1000, Thermo Scientific, NY). Upon reverse transcription (High Capacity RNA to cDNA kit, Applied Biosystems, CA), RT-PCR was performed (Step-One Plus, Applied Biosystems, CA) using Taqman primer probes (Applied Biosystems, CA) for RUNX-2, RANKL, OPG and GAPDH that served as referent. Expression levels were quantified with the delta-delta CT method²¹⁸ and results were reported relative to non-vibrated control.

Statistical analysis

Data were presented as mean±SEM. Differences between groups were identified by one-way analysis of variance (ANOVA) followed by Student-Newman-Keul (SNK) post-hoc tests. P-values of less than 0.05 were considered significant.

Results

Fluid shear is not necessary for the vibration induced osteogenesis

Measuring total mineralization allowed us to compare level of osteogenic differentiation induced by different combinations of mechanical signals (Fig. 3.2). The range of fluid shear generated by out-of-phase motion of the cell culture medium and the vibrating cell culture well during vibrations was between 0.04 and 1.88 Pa. Many studies use 1 Pa fluid shear stress for mechanical stimulation *in vitro*, and thus fluid shear magnitudes smaller than 1 Pa were considered low. At day 16, low fluid shear groups at 100 Hz (0.15g, 1g, and 2g) showed significantly higher mineralization compared to the non-vibrated control ($p < 0.001$). No dependence of mineralization on acceleration was observed between 2g and 0.15g groups. At 30 Hz, increasing acceleration from 0.15g to 1g and to 2g elicited larger increases in fluid shear (0.14, 0.98 and 1.88 Pa, respectively) compared to the same acceleration increases at 100 Hz. 0.15g (0.14 Pa) and 1g (0.98 Pa) groups showed a trend of higher mineralization but were not significantly different than non-vibrated control. 2g (1.88 Pa) showed the highest mineralization and was significantly higher than the control, 0.15g and 1g groups. Interestingly, even though there was a large fluid shear difference between 100 Hz-0.15g (0.14 Pa) and 30 Hz-2g (1.88 Pa) groups, no difference in mineralization was observed.

Sensitivity of cell proliferative response to acceleration is reduced with stronger cell attachments

The total cell numbers were measured at day three after two days of vibration treatment at 100Hz and 30Hz using 0.15g, 1g, and 2g accelerations. Inspection of cells under a microscope did not show any detachment or dead cells. Both 100 Hz and 30Hz groups showed a significant decrease in proliferation with increasing acceleration (Fig. 3.3a). The total cell number difference between 0.15g and 2g groups was 43% ($p < 0.001$) and 54% ($p < 0.001$) in 100Hz and 30Hz groups, respectively. The same experiments were repeated using collagen-coated plates (type I) to test whether the stronger cell attachments would change the cell proliferation response or not. With the addition of collagen, the total number of cells decreased 20% ($p < 0.05$), in the control group possibly due to decreased mobility via better cell attachment (Fig. 3.3b). Groups vibrated at 100Hz remained significantly different compared to non-vibrated control. Collagen coating reduced the cell's sensitivity to acceleration, reducing the gap between 0.15g and 2g groups by half, down to 24% ($p < 0.05$), which was the only significant difference within 100Hz treatment groups. In 30Hz, differences between 0.15g and 2g groups was 53% ($p < 0.001$), essentially retaining those results observed without collagen coating.

Osteogenic mRNA levels increased by mechanical signals in the presence of increased cell tension

To investigate the immediate mRNA regulation of MSCs we looked at immediate gene expression patterns between different fluid shear values. During previous experiments, 100 Hz groups did not induce large differences in fluid shear, mineralization and cell proliferation. During short term mRNA experiments we employed only 30Hz signals, providing broader range of fluid shear values compared to 100Hz. Cells were vibrated at 0.15g, 1g or 2g accelerations. Under normal culture medium conditions RUNX-2 and OPG were not significantly different than control groups (Fig. 3.4a-b). RANKL expression significantly increased in all groups ($p < 0.01$) but did not correlate with fluid shear (Fig.3.4c).

To reveal fluid shear regulation, we increased the fluid shear 2.8-fold independent of vibration parameters via increasing fluid viscosity. Cells remain viable after viscosity treatment as determined by a live/dead cell assay. The 2.8-fold increase in fluid shear was insufficient to upregulate RUNX-2 expression levels. However, increased fluid shear elevated OPG in all three groups relative to controls without any significant differences between 0.39Pa, 2.36Pa and 5.2Pa fluid shear magnitudes (Fig. 3.4b). RANKL was also elevated by 23% to 214% with increasing fluid shear. The greater increase in RANKL when compared to OPG

effectively increased the RANKL/OPG ratio and highest increase in RANKL/OPG coincided with the highest fluid shear (Fig. 3.4c).

The fact that RUNX-2 was not up-regulated in either normal nor elevated fluid shear levels across different accelerations (0.15g, 1g, 2g) raised the question whether increased cytoskeletal tension is required for the osteogenic commitment. LPA increased the number of actin stress fibers after two hours of incubation (Fig. 3.4). Mechanical signals were able to stimulate RUNX-2 expression when exposed to LPA (Fig. 3.4). The largest response relative to non-vibrated controls was 32% ($p < 0.001$) at 0.15g which was significantly greater than both 1g ($p < 0.01$) and 2g ($p < 0.05$), not correlating with fluid shear. OPG expression was also higher compared to non-LPA. OPG expression was the greatest in the 0.15g group; 36% greater than the non-vibrated control ($p < 0.001$) (Fig. 3.4b). RANKL expression showed no response to vibration compared to non-vibrated control.

Mechanically induced cytoskeletal remodeling is modulated by accelerations

Since cell pre-stress, but not fluid shear, enabled mechanical signals to modulate osteogenic mRNA expression, we further explored the connection between cytoskeletal development and vibrations by utilizing a PCR array to quantify 84 key cytoskeleton regulator genes. We treated cells with osteo-inductive medium

for 6 days in which cells were also vibrated at 0.15g, 1g and 2g accelerations at frequencies of 100Hz and 30Hz. A total of 25 genes showed a response to vibrations (>2-fold). Genes were further subdivided into 9 functional categories (Table 3.2). Of these 25 genes, 22 of them were related to actin remodeling. For both frequencies, there was a trend of increase in actin network regulators with increasing acceleration magnitude (Table 3.2). Largest up-regulation response was observed in Wiskott-Aldrich syndrome (WAS) protein, a critical regulator of Arp2/3 complex^{242, 153} enabling rapid actin fiber formation¹⁵²⁻¹⁵⁴ and binding newly formed actin filaments to the existing actin network^{155, 156}. Averaged across 100Hz and 30Hz groups WAS gene was up-regulated by 6.8, 27.8 and 41.5-fold by increasing acceleration magnitude. Across different frequencies, acceleration driven changes in WAS were retained despite the large differences in fluid shear

Discussion

We investigated the vibration driven osteogenesis and proliferation of MSCs using accelerations of 0.15g, 1g and 2g at frequencies of 100Hz and 30Hz. Selected vibration parameters induced fluid shear between 0.04Pa and 1.88Pa. To reveal the potential modulation of fluid shear on vibration response, fluid

shear was further increased up to 5Pa using dextran. In early cell differentiation, accelerations up to 2g and fluid shear up to 5Pa were unable to up-regulate RUNX-2 mRNA levels. MSCs became sensitive to mechanical signals after LPA induced actin stress fiber formation. Following the stress fiber formation, 0.15g group with smallest fluid shear (0.04Pa) showed the biggest increase in RUNX-2. After 6 days of vibration in osteo-inductive medium, 84 regulatory genes for cytoskeletal re-modeling was profiled. Vibrations exclusively up-regulated actin related genes (22 out of 25) and actin remodeling was positively correlated with the increases in the acceleration magnitude. After 13 days of vibration there was a significant increase in mineralization with vibrations. In 100Hz groups which elicited low fluid shear (<1Pa), all acceleration showed a similar increases in mineralization. At 30Hz that employed relatively high fluid shear values (0.14 to 1.88Pa), we saw a trend of increasing mineralization with increased acceleration and fluid shear.

Interestingly, 100Hz-0.15g and 30Hz-2g groups had large differences between fluid shear (0.04Pa vs 1.88Pa) without any apparent differences in mineralization, demonstrating that vibrations can increase the level osteogenic differentiation of MSCs independent of fluid shear. Lower mineralization were observed in 30Hz-0.15g and 30Hz-1g groups compared 100Hz-0.15g and 100Hz-1g groups, perhaps due to a cycle number dependent response.^{232, 190} However

we cannot rule out the possibility that mineralization increase 30 Hz-2g groups were influenced by relatively high fluid shear stress (1.88Pa). Unfortunately as opposed to short term experiments (1 day) during long term experiments we cannot use dextran to independently change fluid shear and accelerations. As the changes in osmotic pressure were shown to change the cell function.²⁴³ Due to this limitation we cannot reliably say if the changes in 30Hz-2g groups were influenced acceleration magnitude or the vibration induced fluid shear.

Changes in cytoskeletal remodeling induced by acceleration magnitude were not sufficient to explain mineralization results. For example at 100Hz, all acceleration magnitudes showed a similar mineralization even though the cytoskeletal remodeling was 2-fold lower in 0.15g when compared to 1g and 2g groups. Additionally cytoskeletal remodeling between 30Hz-1g and 30Hz-2g groups were similar even though mineralization of 30Hz-2g group was significantly higher than 30Hz-1g group. Our results show that increases in acceleration can explain the increases in cytoskeletal remodeling. However, interaction between acceleration magnitude and cytoskeletal remodeling the in regulating the mineralization response was not clear.

In proliferation experiments, we observed trends similar to mineralization experiments. 100Hz groups tend to show smaller differences between groups, emphasizing a frequency dependent response. Within 30Hz groups there were larger differences between groups with increasing acceleration and fluid shear. Interestingly, the sensitivity of 100Hz groups to acceleration was decreased in the presence of collagen which promoted stronger cell attachment.²⁴¹ The magnitude of the response of collagen group at 0.15g was almost doubled compared to the non-collagen group, implying that by making it easier for cells to attach via collagen, the efficacy of low magnitude vibrations could be modulated.

Without the use of any induction medium or pharmacological agents, an increase in fluid shear alone did not elicit any osteogenic mRNA expression. It is somewhat inconsistent with other flow studies. However most other studies either used either low frequency or laminar flow profiles that might be more effective compared to higher frequencies.²³⁰ Additionally we did not use any coatings such as fibronectin that might positively influence the cell signaling. When we employed LPA which resulted in rapid actin stress fiber formation, we saw an up-regulation of both RUNX-2 and OPG while there were no changes to RANKL expression. Our data shows that without osteogenic factors, high

frequency vibrations and induced fluid shear alone were not sufficient to induce osteogenic differentiation.

The RANKL/OPG ratio, reflective of the influence of MSCs on osteoclastogenesis, was increased with the application of vibrations during one day mRNA experiments. First of all, demonstrating that even though vibrations did not elicit osteogenic response, vibrations were sensed and responded by MSCs. Interestingly, opposite to osteogenic changes, vibrations increased RANKL/OPG ratio only without LPA treatment. When cytoskeletal remodeling was increased via LPA, vibrations increased RUNX-2 and OPG and RANKL expression was muted, effectively decreasing RANKL/OPG ratio. Perhaps this could represent a distinct cell response towards mechanical signals when the cell prestress is low. Suggesting that MSCs could modulate osteoblastogenesis better when attached to a stiff surface that will support increased cell tension.^{239, 246} However MSCs may be better modulating osteoclastogenesis⁶ when not committed to osteogenesis and residing in a softer substrate such as bone marrow.

The mechanism by which the actin stress fiber formation increased the positive mechanical regulation of RUNX-2 expression may be attributed to the increased tension within the cell.^{247, 248} LPA

activates RhoA mediated increase in cell tension through myosin II ¹⁵⁸ inducing osteogenic differentiation. Mechanistically, cell tension positively correlates with efficiency of force transfer^{163, 165} since a tenses cytoskeleton will provide a path of least resistance for mechanical signals. Following 6 days of vibration treatment, genes important for myosin light chain, RhoA, and ARP2/3 complex function was up-regulated. Up-regulation in cytoskeletal remodeling was dependent on acceleration magnitude, implying that vibrations may play a role in increasing the cellular mechanosensitivity.

In this study, we showed that vibrations can modulate MSC metabolism and fluid shear was not necessary for vibration induced changes. In 100Hz groups, cells responded to vibrations in the presence of negligible fluid shear stress (0.04Pa). Mechanically driven early osteogenic commitment of MSCs was regulated by the cytoskeleton. Early gene expression data shows osteogenesis was not induced by mechanical cues in the absence of actin bundling. Interestingly, we found that the signal with the smallest fluid shear produced the largest increase in RUNX-2 and OPG. After 6d of vibrations in osteo-induction medium, up-regulation in the regulatory genes for cytoskeletal remodeling correlated with acceleration but not fluid shear. However, cytoskeletal remodeling alone did not correlate with the long term mineralization. While group subjected to the greatest fluid shear elicited the highest overall response,

greatly different levels of fluid shear generated a very similar response in other vibration groups. Overall our results show that altering the level of acceleration/frequency and fluid shear results in similar responses, perhaps suggesting that all these mechanical cues trigger a common mechanism that is yet to be identified.

Acknowledgements

Funding by the National Institutes of Health (NIAMS) is gratefully acknowledged.

Technical expertise from Dr. Michael Hadjiargyrou and Lester Orlick was greatly appreciated.

Tables

Table 3.1. Peak fluid shear values during high frequency vibrations. Columns represent acceleration magnitudes where 'g' is earth gravitational field (9.81 m/s²) and rows represent signal frequency and dextran concentrations.

	0.15g	1g	2g
100Hz (no dextran)	0.04 Pa	0.28 Pa	0.56 Pa
30Hz (no dextran)	0.14 Pa	0.94 Pa	1.88 Pa
30Hz (6% dextran)	0.39Pa	2.63 Pa	5.26 Pa

Table 3.2. After 6d of vibration in osteogenic medium, 84 gene PCR array was used. Total of 25 genes showed a response to vibrations (>2-fold). Genes were subdivided into 9 functional categories. For both frequencies, greatest mRNA response was observed under 1g and 2g conditions. For clarity only genes showed a response bigger than 4-fold and functional groups shown in the table.

Genes	100Hz			30Hz		
	0.15g	1g	2g	0.15g	1g	2g
ARHGEF11	1.27	2.50	2.47	1.26	5.60	5.95
AURKC	1.75	3.03	3.80	1.57	5.61	9.62
CDC42	2.05	2.97	3.35	2.02	4.64	4.34
CDK5R1	1.58	6.87	6.20	0.77	4.70	13.53
CYFIP2	2.37	11.47	13.13	2.24	23.15	18.70
LIM-K2	1.28	2.59	2.39	1.03	3.28	6.68
MAP3K11	1.71	2.26	2.06	1.62	5.65	5.17
MARK2	1.30	3.08	3.23	0.98	3.59	4.76
NCK2	1.59	2.96	2.99	1.49	5.53	6.70
PPP1R12B	2.38	3.27	2.44	1.95	4.73	4.95
RADIXIN	2.68	4.22	3.83	2.02	3.93	3.67
WAS	N/A	26.84	39.97	6.88	27.60	43.03
WASL	2.11	2.57	2.77	1.91	4.72	3.07
Functional Categories						
<i>Actin Remodeling</i>	1.63	3.82	4.47	1.80	5.48	5.92
<i>Calmodulin / Calcineurin:</i>	1.15	1.94	1.79	1.21	4.12	3.41
<i>Cell Motility / Migration:</i>	1.58	2.18	2.21	1.45	3.26	3.10
<i>Cell Projections:</i>	1.85	3.34	3.42	1.75	5.34	4.54
<i>Cell Shape, Size, Polarity</i>	1.66	4.24	4.66	1.58	8.04	7.14

<i>Cytokinesis</i>	1.64	2.54	2.83	1.38	4.60	6.17
<i>Cytoskeleton Adaptor Activity:</i>	1.61	2.65	2.68	1.65	3.67	4.03
<i>G-Protein Signaling:</i>	1.53	4.78	5.99	1.98	7.10	7.52
<i>Kinases & Phosphatases:</i>	1.57	2.27	2.25	1.46	3.55	3.99
<i>Microtubules:</i>	1.58	6.87	6.20	0.77	4.70	13.53
Overall mRNA Activity	1.58	3.46	3.65	1.50	4.99	5.93

Figures

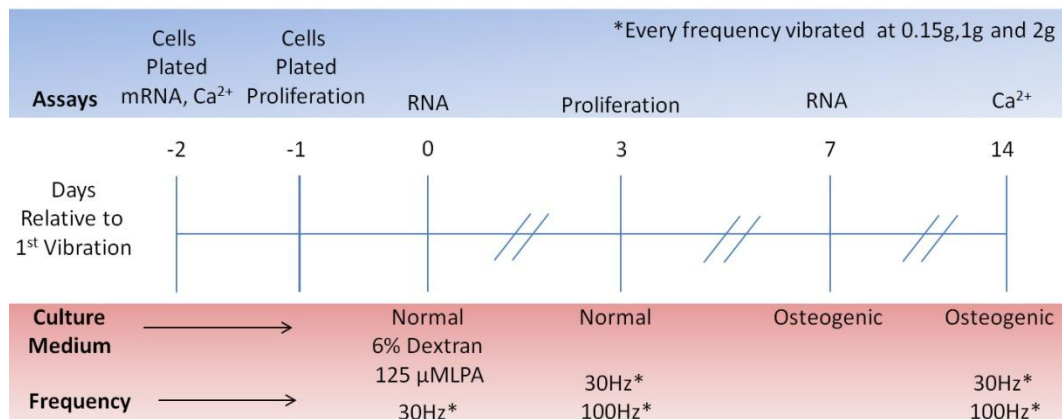


Figure 3.1. For mRNA and mineralization (Ca²⁺) experiments cells were plated at 18,000cell/cm² and for proliferation cells were plated at 750cells/cm². Vibration effects on early osteogenesis at day 1, proliferation at day 3, cytoskeletal remodeling at day 7 and mineralization at day 13 were assessed.

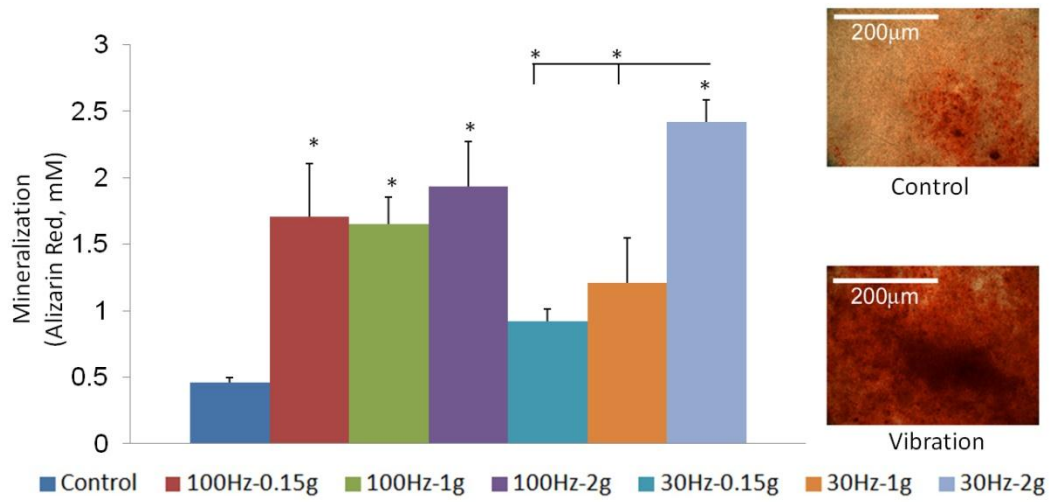


Figure 3.2. Calcification of cells were determined by alizarin red staining at day 16 after 13 days of vibration. Cells were kept in osteo-inductive medium for 14 days and were vibrated with seven different vibration parameters. $p < 0.05$: *against non-vibrated control.

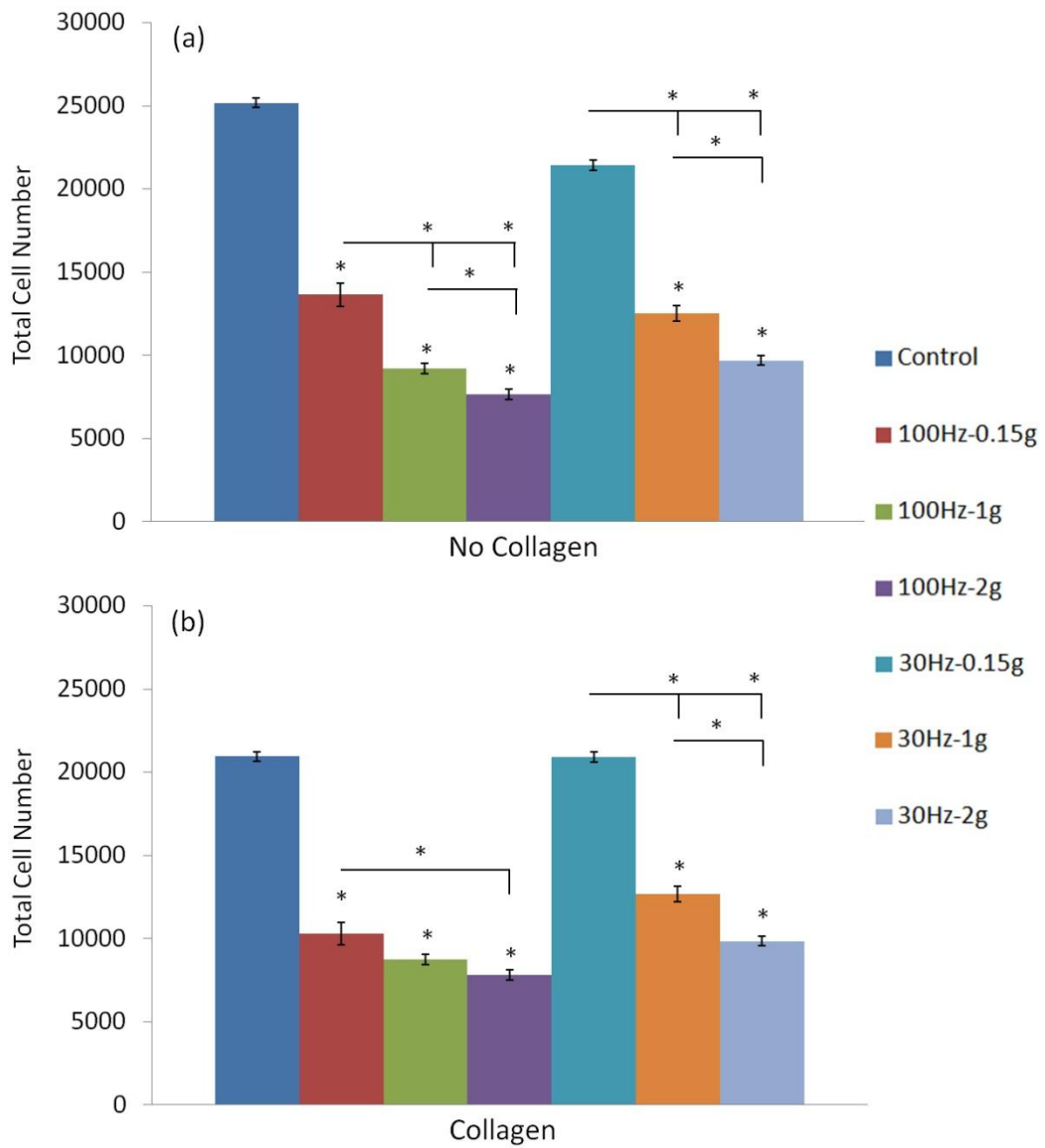


Figure 3.3. Cell proliferation characterized by total cell number at day three after two days of vibration. Culture plates were not coated (a) or coated with 0.15mg/ml collagen (b). $p < 0.05$: *against non-vibrated control.

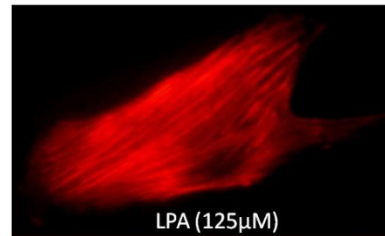
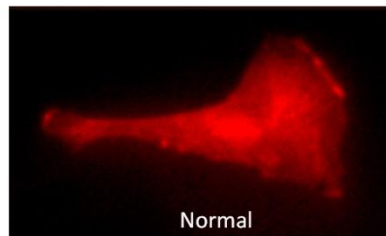
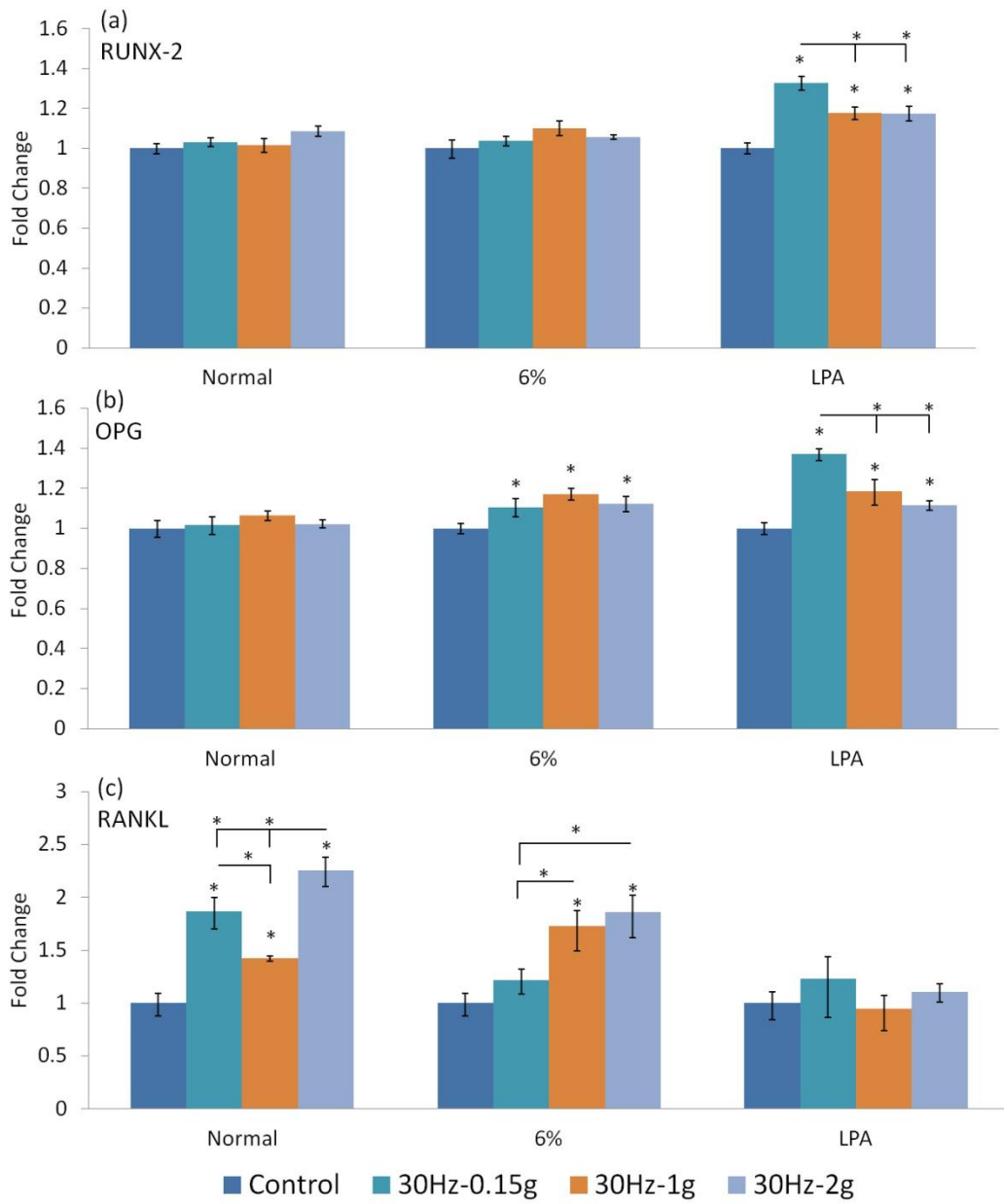


Figure 3.4. Gene expression after one day of vibration: Change in RUNX-2(a), OPG(b) and RANKL(c) expression of MC3T3-E1 cells exposed to three different mechanical signals under low-shear (Normal) and high-shear (6% dextran) and increased cell prestress (LPA) conditions. $p < 0.05$: *against non-vibrated control.

Chapter 4

VIBRATIONS INCREASE GAP JUNCTIONAL

COMMUNICATION IN OSTEOCYTES

INDEPENDENT OF FLUID SHEAR

Abstract

When applied at high frequencies, bone can sense and respond to mechanical signals of extremely small magnitude. During the application of vibrations, cell populations within the bone will be subjected not only to acceleratory motions but also to fluid shear as a result of fluid-cell interactions. We studied whether vibrations can induce cellular deformations that are different from fluid shear and whether those vibrations can affect osteocyte communication independent of fluid shear. A finite element (FE) model of a cell was used to estimate the cellular deformation during dynamic vibration and fluid shear events. Different vibration parameters were selected to vary accelerations between 0.15g to 1g and frequencies between 30Hz to 100Hz. Vibration parameters can modulate the mechanical environment of cells, including vibration induced fluid shear, as a function of acceleration/frequency. Osteocyte like MLO-Y4 cells were subjected to four different vibrations and effects of increased fluid shear on gap junctional intracellular communication (GJIC) were investigated. FE model showed that the dynamic acceleration caused larger relative nucleus motions when compared to fluid shear. On average, vibrations increased GJIC communication between osteocytes by 25%. Observed effects of vibration were independent of fluid shear as there were no differences in GJIC between the different vibrated

groups. Vibration induced increases in GJIC were not associated with altered connexin 43(Cx43) mRNA and protein levels but were dependent on Akt activation. These results demonstrate that vibrations enhanced GJIC independent of fluid shear stress. During vibrations, accelerations induced larger nucleus motions when compared to fluid shear stress. Observed increases in GJIC were not correlated with the magnitude of nucleus motions or fluid shear stress, suggesting that osteocytes were highly sensitive to low magnitude vibrations.

Introduction

Functional communication between resident bone cells is critical for the coordination of bone remodeling. This coordination is in-part facilitated by gap junctions that connect intracellular domains of adjacent cells via transmembrane channels. By enabling ions and intracellular signaling molecules to pass through, gap junctions play an important role in cell signaling and tissue function in various organ systems.²⁴⁹⁻²⁵³ Connexins regulate signaling among various bone cell populations and modulate overall osteogenic potential.^{254, 255} Connexin 43 (Cx43) is the most common connexin in bone, found virtually in all bone cells including osteoblasts, osteoclasts, marrow stromal cells and osteocytes.²⁵⁶⁻²⁵⁸ For example, osteoblasts isolated from calvaria of Cx43-null mice display reduced differentiation and mineralization.²⁵⁹ Additionally Cx43 can be found as open ended hemi-channels that can secrete molecules such as NO, PGE₂ and Ca²⁺.^{260, 261}

Gap junctional intercellular communication (GJIC) is important during cell mechanotransduction. Both fluid shear stress and mechanical strain were shown to increase GJIC between bone cells.^{262, 263, 245} Osteocytes, the most abundant bone cells that are present throughout the matrix, are well positioned to effectively use GJIC to communicate mechanically derived responses. Consistent

with this hypothesis of osteocytes being sensory cells that orchestrate the responses of the osteoblastic and osteoclastic effector cells^{46, 264, 265}, mechanical perturbation of osteocytes has been shown to regulate osteoblast function through gap junctions.²⁶⁶ This result suggest that GJIC plays an important role relaying the mechanically derived signals to other cells such as osteoblasts⁴⁸ or vice versa.

Although mechanical signals can directly modulate Cx43 function through integrin connections,²⁶⁷ fluid flow and mechanical stretch also increase Cx43 protein levels and phosphorylation.²⁶⁸⁻²⁷¹ Mechanical regulation of Cx43 appears to be largely mediated through β -catenin signaling. In bone, GJIC activity on osteocytes was ERK1/2 dependent⁴⁷ and ERK1/2 activity was sufficient to phosphorylate LRP6 and induce β -catenin²⁷² Additionally fluid flow²⁷³ has been shown to inhibit glycogen synthase kinase-3 (GSK-3), a critical component of the β -catenin degradation complex, which leads to upregulation of COX-2 and PGE₂ activity through Akt signaling.²⁷³ Akt activation is regulated through integrins²⁷⁴ and focal adhesion kinase (FAK)²⁷⁵ in response to mechanical signals. Interestingly, vibrations also regulate β -catenin levels through inhibition of GSK-3 independent of Wnt/Lrp signaling.¹⁸¹ These results suggest vibrations have a potential to protect β -catenin degradation through Akt dependent pathway which could in turn modulate GJIC.

Although vibrations have been shown to be anabolic or anti/catabolic to bone,^{71, 190, 186, 7, 181} the specific physical mechanism by which vibrations are sensed is unknown. Vibrations create a complex mechanical environment as a function of acceleration magnitude and frequency. Among other mechanical effects, vibrations induce significant fluid shear on trabecular bone surfaces^{103, 105} in the absence of significant matrix strain levels.^{71, 192} We previously showed that the fluid shear stresses during *in vitro* vibrations depend on peak velocity which is a function of frequency and acceleration.²³⁴ In addition to fluid shear, dynamic accelerations were implicated to cause out of phase motions of the nucleus.⁷¹ Consistent with the hypothesis that vibrations can be sensed through nuclear motions, when fluid shear was eliminated, PGE₂ and NO responses of pre-osteoblast cells were shown to be acceleration rate dependent.¹⁸² However it is not clear how the specific components of vibrations affect the cellular response when applied simultaneously. Here we investigated if the vibrations increase GJIC and whether the changes are related to a specific component of the vibrations. We hypothesized that application of high frequency accelerations induce larger relative nucleus motions compared to fluid shear and will increase the GJIC independent of fluid shear through Akt dependent pathway.

Materials and Methods

Experimental design

We asked whether vibrations could induce cellular deformations that are different from fluid shear and whether those vibrations could affect osteocyte communication independent of fluid shear. Finite element (FE) model of an adherent cell was used to estimate the relative nucleus motions during dynamic accelerations and vibration induced fluid shear. Vibrations were applied at accelerations of 0.15g and 1g and at frequencies of 30Hz and 100Hz. We used previously established methods to quantify vibration induced fluid shear stresses²³⁴. Fluid shear stresses corresponding to vibration parameters were of 0.04Pa, 0.14Pa, 0.28Pa and 0.94Pa (Table 4.1). Computational data were then used to correlate cellular responses with vibration induced nuclear deformations. In our *in vitro* cell model we used osteocyte like MLO-Y4 cells. To investigate whether vibrations increase the GJIC in osteocyte like MLO-Y4 cells, we used a dye transfer assay by parachuting²⁷¹ calcein stained MC3T3 cells. MC3T3 cells were used as donor cells due to their ability to create functional gap junctions with MLO-Y4 cells within 15 minutes.⁴⁸ Cells were vibrated using same parameters used in FE simulations. Following the vibrations, the percentage of total GJIC positive MLO-Y4 cells (GJIC+) and Cx43 protein levels were compared

to non-vibrated controls using flow cytometry analysis. Cell to cell communication through gap junctions were verified with a gap junction inhibitor 18 α -glycyrrhetic acid (18 α -GA) and microscope. Furthermore, to assess the involvement of Akt activation in the mechanical regulation in GJC, osteocytes were transfected with AKT-1 siRNA prior to vibrations.

Finite element modeling of a cell

FEM (Abaqus 6.9.1, Simula, RI) was used to model an adherent cell and estimate nuclear deformations during vibrations via dynamic stress analysis. The cell geometry was adopted from previous models of adherent cells.^{80, 165} The cell contact radius was 19.2 μ m, cell height was 7.6 μ m. The nucleus was modeled as an ellipsoid with major axis of 7.5 μ m and minor axis of 2.5 μ m. Selected cell dimensions were comparable to the confocal images of osteocytes within the lacunar–canalicular network.²⁷⁶

The modeled cell was comprised of three parts: the cell membrane, cytoplasm and nucleus. Since the mechanical vibrations applied at a frequency of 30Hz or higher, well below measured viscoelastic relaxation times of about 40s,²⁷⁷ material properties were assumed to be elastic. Density ratios (1:1.2:0.4) were approximated from refractive index measurements between the cytoplasm,

nucleus and cell membrane (triglyceride), respectively.^{278, 279} The density of the cytoplasm was assumed to be 50% greater than that of water (1500kg/m^3). The bending modulus of cell membrane was $1.17 \times 10^{-19}\text{N.m}$.²⁸⁰ Nuclear stiffness was set at 6kPa ²⁷⁷ based on atomic force microscopy (AFM) measurements on osteoblast. Since the nucleus was found to be four time stiffer than the cytoplasm,²⁸¹ cytoplasm stiffness was set to 1.5kPa . Simulations were also repeated for 50% and 300% of original material properties.

To estimate the nucleus motion under accelerations and fluid shear stress, two different sets of simulations were used (Fig. 4.1). During acceleration simulations, the surface of cell attachment was subjected to sinusoidal motions in a horizontal plane with the accelerations of $0.15g$ and $1g$ at frequencies of 30Hz and 100Hz . For fluid shear simulations, the surface of cell attachment was fixed so that it could not move. Dynamic forces with a sinusoidal profile corresponding to the vibration induced fluid shear magnitudes (Table 4.1) were applied to the cell membrane. Total force applied to the cell membrane was estimated from the fluid shear stress. At 0.94Pa fluid shear, for example, the total tangential force acting on the cell surface was $0.94\text{pN}/\mu\text{m}^2 \times 1470\mu\text{m}^2 = 1381.8\text{pN}$, where $1470\mu\text{m}^2$ is the total surface area of the cell. Total force was equally divided between all 5768 elements on the cell membrane. Nuclear motion was selected as an outcome variable and defined as the relative motion

between the nucleus center and the cell contact surface in the direction of the vibration motion (horizontal).

Cell culture

MLO-Y4 cells were graciously donated by Dr. Lynda F. Bonewald. Cells were cultured in 75cm² cell culture flasks (BD Biosciences, San Jose, CA) at a density of 5000cell/cm². α -MEM (Invitrogen, NY) supplemented with 2.5% fetal bovine serum (FBS, Gibco, CA), 2.5%bovine calf serum (BCS, Thermo Scientific, IL) and 1% Penicillin-Streptomycin (PS, Gibco, CA) was used as cell culture medium. MC3T3 cells were plated at 5000cell/cm² in 100mm cell culture dishes (Corning Inc., NY) and maintained in α -MEM supplemented with 10%FBS and 1%PS. All cells were maintained at 37°C and 5% CO₂ and passaged at 70% confluency.

Application of high-frequency oscillations and determination of fluid shear

The horizontal vibration system supplying the various mechanical signals is described in detail elsewhere.²⁴⁰ Briefly, an actuator was attached to a linear frictionless slide. This system can simultaneously vibrate up to three 24-well cell culture plates. Vibrations applied at peak magnitudes of 0.15 or 1g were combined with either a 30 or 100Hz frequency to result in four distinct

mechanical regimes. Cells were exposed to each of these regimes for 30min at room temperature. Control samples were handled exactly the same except that the actuator was not turned on. During vibrations, out-of-phase sloshing of cell culture medium within the well was determined using an experimentally validated finite element model.²³⁴ The differences between cell culture well and fluid velocities was utilized to estimate fluid shear stress at the cell surface. Fluid shear stresses corresponding to vibration parameters were 0.04Pa (100Hz-0.15g), 0.14Pa (30Hz-0.15g), 0.28Pa (100Hz-1g) and 0.94Pa (30 Hz-1g).

Parachute assay

MLO-Y4 cells were seeded in 24-well plates (CLS3527, Corning Inc.) coated with 0.15mg/ml rat tail Collagen I (Cell Applications Inc., CA) using 0.5ml of culture medium at a density of 10,000 cell/cm². Cells were incubated for 72 hours to reach 80-90% confluency. Four hours prior to vibration treatment, MC3T3 cells (70% confluent) were stained with 1 μ M calcein AM for 30min according to the manufacturer's instructions (L-3224, Invitrogen) and returned to the incubator. MLO-Y4 cells were vibrated for 30min. Immediately after vibration, donor MC3T3 cells were parachuted on top of MLO-Y4 cells with a ratio of 1:500 in 0.5ml of MLO-Y4 culture medium. Plates were returned to the incubator for 1hr

to allow GJIC. After 1hr cells were processed for either flow cytometry or RNA extraction. Experiments were repeated at least three times with a sample size of six per group. Analysis were done after results from individual experiments were pooled (minimum n=18/group).

Flow cytometry

After 1 hr incubation of donor and acceptor cells, 24-well plates were trypsinized (Gibco) using 0.3ml for 4 minutes and the reaction was stopped by adding equal volume of culture medium. Cells in suspension were stored on ice and immediately carried to flow cytometry for processing. For flow cytometry readings, FACScan (BD) capable of reading calcein (495/515 nm) spectra was used. A total of 5000 live cells were read. Along the fluorescence intensity scale cells who fell between negative controls (no calcein) and positive controls (only donor cells) were selected as GJIC positive cells (GJIC+). The effects of vibration treatment were quantified by obtaining the % difference of total GJIC+ between vibration groups and non-vibrated controls. Flow cytometry analysis were done using Flowjo software package (Tree Star Inc., OR). Results were also validated with an inverted fluorescent microscope (Zeiss, NY).

18 α -glycyrrhetic acid

For the experiments using gap junction blocker 18 α -GA (G8503, Sigma, MO), 10mM stock solutions were prepared in DMSO. Prior to experiments gap junction activity of both MLO-Y4 and MC3T3 cells were blocked for three hours using 75 μ M 18 α -GA diluted in culture medium. Groups with blocker were maintained in cell culture mediums containing 75 μ M 18 α -GA at all times (n=6/group). After that point the samples were treated the same as normal experimental groups.

Connexin 43 protein levels

To quantify the changes in the unphosphorylated Cx43 levels following the vibration treatment, unstained MC3T3 cells were parachuted using the same parachute assay protocol. 1hr after the vibration cells were re-suspended in DPBS and incubated with 10 μ M Cx43 mouse monoclonal antibody conjugated with Alexa Fluor 488 (138388, Invitrogen) for 1hr at 37 $^{\circ}$ C. FACScan (BD) flow cytometer were used to quantify total number of labeled cells compared to non-vibrated controls (n=5/group).

Blocking Akt activity with siRNA

siRNA duplex-Lipofectamine RNAiMAX complexes were prepared by mixing 6 pmol AKT-1 siRNA duplex (s659, Ambion, NY) and 1 μ l Lipofectamine RNAiMAX (13778030, invitrogen) in 98 μ l Opti-MEM (Gibco) and incubating at room temperature for 20 minutes. 24 hr after plating MLO-Y4 cells according to experimental protocol, cell medium was supplemented with 100 μ l siRNA complex making the final concentration of siRNA 6nM and incubated for 48 hours(n=6/group). After that point the samples were treated the same as normal experimental groups.

RNA extraction and qPCR

Cells were lysed with 600ml of TRIzol (Ambion, TX) and stored at -80°C. Total RNA was isolated (RNeasy Mini Kit, Qiagen, CA) and its quality and concentration were determined (NanodropND-1000, Thermo Scientific, NY). Upon reverse transcription (High Capacity RNA to cDNA kit, Applied Biosystems, CA), RT-PCR was performed (Step-One Plus, Applied Biosystems, CA) using Taqman primer probes (Applied Biosystems, CA) for, C-FOS, Cx43 (GJA-1), RANKL, SOST and GAPDH that served as referent. Expression levels were quantified with the delta-delta CT method²¹⁸ and results were reported relative to non-vibrated control.

Statistical analysis

Results were presented as mean \pm SEM. Differences between groups were identified by one-way analysis of variance (ANOVA) followed by Newman-Keuls post-hoc tests. P-values of less than 0.05 were considered significant.

Results

Vibrations induced nuclear motions are frequency, acceleration and stiffness dependant

We estimated the level of nuclear motion using an FE model of an adherent cell. Nuclear motions were estimated for both acceleration magnitude and vibration induced fluid shear (Table 4.2). The nuclear motion of the cell was acceleration magnitude dependent. When averaged over 30Hz and 100Hz, nucleus motion was 127nm in 0.15g and 780nm in 1g groups. Compared across two frequencies, the difference between 30Hz-0.15g and 30 Hz-1g was 27% larger when compared to 100Hz counterparts which implies some degree of frequency dependency. Nuclear motion was inversely proportional to the cell stiffness. When averaged across all groups, decreasing the cell stiffness 50% increased the nuclear motion 229% \pm 17.3 while increasing the stiffness 300% decreased the

nuclear motion by $67.4\% \pm 2.61$. Additionally relative differences between groups were stiffness dependent. At 6kPa nucleus stiffness, 30Hz-1g group had 17% more nuclear motion than 100Hz-1g; when stiffness was decreased 50% or increased 300%, 100Hz-1g was 16% and 21% larger than 30Hz-1g, respectively. The nuclear motions caused by vibration induced fluid shear were much smaller compared to accelerations. At 30Hz-1g a group with largest fluid shear (0.94Pa) nuclear motion caused by fluid shear was 80-fold smaller than acceleration induced nuclear motion. At 100Hz-0.15g, the group with smallest fluid shear (0.004Pa), acceleration based nuclear motion was 3000-fold bigger than fluid shear induced nuclear motion.

Vibration increases GJIC in osteoblastic cells

The total number of calcein positive cells was measured after 1h incubation following 30min of vibration exposure. Cells were vibrated at four different conditions: 0.15g and 1g acceleration magnitude at either 30Hz or 100Hz frequency. Vibrations significantly increased the number of GJIC+ cells in all groups ($p < 0.001$) compared to non-vibrated controls (Fig. 4.2a). Compared to controls, 30Hz-1g group showed the biggest increase ($33.2\% \pm 4.87$, $p < 0.001$). When differences between vibration groups were compared, no significant

differences were observed. Results from qualitative microscope images showed that with vibration treatment, GJIC+ cells were located further away from the donor cells (Fig. 4.2b), suggesting a vibration induced increase in the transfer efficiency of gap junctions. Observed increases in GJIC were accompanied by a decrease in C-FOS mRNA expression ($p < 0.001$). RANKL was only significantly higher in 100 Hz-1g group ($p < 0.05$) with an increase of 20% compared to control. SOST gene was detected in control group but not in vibration groups (Fig. 4.3). We confirmed that the observed GJIC was facilitated through gap junctions by blocking gap junctions for three hours with 18 α -GA gap junction blocker. Blocking the gap junction function effectively blocked the observed GJIC ($p < 0.0001$) (Fig. 4.4).

Vibration induced GJIC is not dependent on Cx43 expression but controlled by Akt signaling

We tested whether the observed increase in GJIC was related to an increase in Cx43 mRNA or protein levels. 1hr after vibration treatment, mRNA expression for Cx43 was unchanged compared to non-vibrated controls (Fig. 4.5a). Quantifying unphosphorylated Cx43 between control and vibration groups showed that the

Cx43 protein levels were not significantly different between vibration and control groups (Fig. 4.5b).

We asked the question whether the vibration induced GJIC signaling influenced by Akt signaling. The AKT-1 gene was knocked out from MLO-Y4 cells using siRNA. Vibrations were applied at the two conditions that showed the largest response in previous experiments (30Hz-1g and 100Hz-1g). After knocking out the AKT-1 gene from only MLO-Y4 cells, when averaged over two groups, GJIC+ cells decreased 35% compared with non-vibrated, normal controls ($p < 0.001$) (Fig. 4.6a-b). After siRNA application there was no difference between vibration and control groups, demonstrating that silencing Akt signaling abolished the vibration induced increase in GJIC.

Results were further confirmed in a separate experiment using the 30Hz-1g group. Gap junctions were blocked in MLO-Y4 cells by 18α -GA. When only MLO-Y4 cells were blocked there was a $35\% \pm 3$ decrease in control ($p < 0.001$) and $26\% \pm 2.2$ in vibration ($p < 0.01$) groups when compared to non-blocked counterparts. Interestingly, vibrated 18α -GA group, had $28\% \pm 2.4$ higher ($p < 0.01$) GJIC+ cells compared to non-vibrated 18α -GA group. (Fig. 4.6c) This suggests that the vibration induced increase in GJIC was controlled by Akt activation since blocking Cx43 function by 18α -GA only reduced the overall response but did

not diminished the vibration induced differences between control and vibration groups.

Vibration induced GJIC does not does not correlate with fluid shear

Although the number of GJIC+ cells were not significantly different between vibration groups, we tested which outcome variable best explain the observed differences. We correlated the results from GJIC experiments with mechanical variables from our in vitro system. Mechanical variables include vibration induced fluid shear, accelerations magnitude and nuclear motions estimated from both acceleration and fluid shear FE simulations. Non parametric Spearman Rank correlation tests were used to assess the statistical dependence between two variables. Nuclear motion from accelerations were significantly correlated with the observed GJIC differences between groups ($\rho=0.28$, $p=0.016$). Although the correlation coefficient was very small, none of the other variables were significantly correlated with GJIC experiments.

Discussion

We investigated the effects of vibrations on the osteocyte GJIC. During the vibration treatment cells were subjected to both accelerations and fluid

shear.^{103, 234} We included vibration groups that created fluid shear up to 0.94Pa, which is a widely used fluid shear value for fluid flow experiments.^{42, 51, 98, 282} An FE model of an adherent cell was used to compare nucleus motions caused by accelerations and fluid shear. Accelerations induced much larger nucleus motions compared to fluid shear stress. All the vibration groups showed significant increases in GJIC activity compared to non-vibrated controls. The additional mechanical input from fluid shear did not change the increases in GJIC+ cells between groups. For example GJIC+ cells were not significantly different between lowest fluid shear group (0.04Pa, 100Hz-0.15g) and highest fluid shear group (0.94Pa, 30Hz-1g). These results demonstrate that accelerations can active cell mechanotransduction when fluid shear is negligible.

We previously reported using pre-osteoblasts that changing the frequency or fluid shear independently can change the level of cellular response.²⁴⁰ However using osteocytes, we did not find any GJIC differences between different frequencies or fluid shear values. If one considers mechanotransduction as a response to forces generated within the cells whether it is result of fluid shear or nuclear motions, osteocytes appear to have a lower threshold for mechaniosensing. Consistent with this hypothesis, osteocytes have been shown to be more responsive to fluid shear when compared to less differentiated cells⁵³. Although the reason for this increased sensitivity is not

clear, our FE model show decreased nuclear motions as the stiffness increases, perhaps a measure of how much energy is absorbed by cytoskeleton. Osteocytes have more extensively developed cytoskeleton compared to pre-osteoblasts and MSCs and are therefore stiffer.²⁷⁷ In fact stiffer cytoskeleton transfer the forces more effectively into the nucleus,¹⁶³ suggesting that osteocytes are not only better at sensing fluid shear, but also other mechanical signals because they facilitate a more efficient force transfer through cytoskeleton.

A dynamic FE model of an adherent cell was used to understand the cellular deformations during vibrations. However there were many simplifications and assumptions regarding the geometry and material properties of the cell. For example the large difference between fluid shear and acceleration induced nuclear motions could change significantly based on nucleus size, geometry and density. Our results at best provide a first approximation in identifying dynamic deformations within the cell during vibrations.

Nuclear motions predicted by the FE model can also induce forces on the cytoskeleton which in turn might activate mechanotransduction pathways including integrin related signaling. Akt signaling plays an important role in activating cytoskeleton related cellular sensing and preserving cellular β -catenin levels in response to mechanical signals.^{43, 92, 283, 275, 160, 284} Previously, it has been

shown that the increase in β -catenin levels can increase Cx43 levels. Our results suggest that the vibration related increase in GJIC was independent of Cx43 protein or mRNA levels. When gap junction function was blocked in osteocytes, there was a decrease in overall GJIC but the differences between the vibration and control groups were not diminished. The differences between vibration and control were only diminished when Akt signaling was knocked down with siRNA treatment. This implies that the vibrations can increase Cx43 function as a downstream of Akt signaling. Previously, retention of β -catenin shown to increase gap junction related Ca^{2+} wave propagation speed in myocytes, which happened simultaneously with Cx43/ β -catenin colocalization.²⁸⁵ Perhaps similar mechanisms play a role in enhancing Cx43 function in osteocytes.

In this study we showed that independent of the changes in the fluid shear, vibrations can change GJIC in osteocytes. This increase was dependent on the increase in Cx43 function through Akt signaling. Our results imply an increased communication between bone cells with vibrations. Interestingly previous studies shown that vibrations can increase the cell sensitivity to other mechanical⁷⁵ as well as biochemical signals³⁹, suggesting that in addition to anabolic¹⁸⁷ and anti-catabolic¹⁸¹ effects of vibration they can also provide more efficient signaling within bone tissue.

Acknowledgements

Funding by the National Institutes of Health (NIAMS) is gratefully acknowledged.

Tables

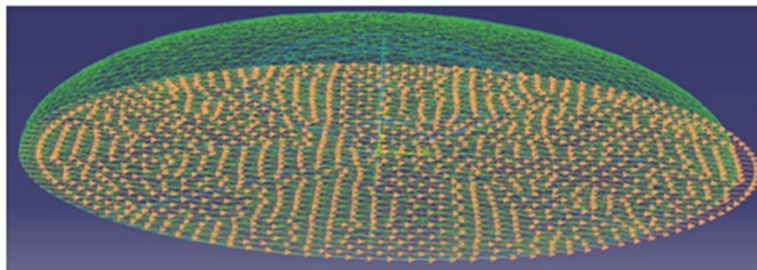
Table 4.1. Peak fluid shear values during high frequency vibrations. Columns represent acceleration magnitudes where 'g' is Earth gravitational field (9.81 m/s²) and rows represent signal frequency.

	0.15g	1g
100Hz	0.04 Pa	0.28 Pa
30Hz	0.14 Pa	0.94 Pa

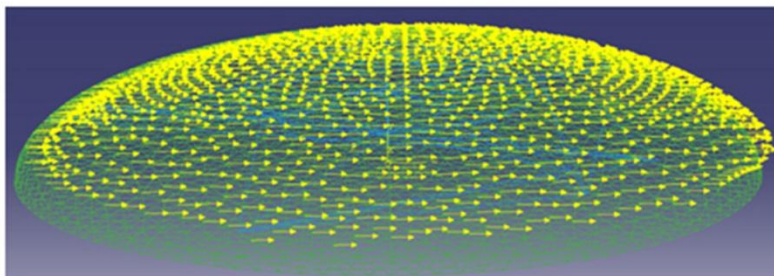
Table 4.2. Relative nuclear motions predicted by FE model. Nuclear motions during vibrations were estimated for both acceleration magnitudes and the fluid shear stress using two different dynamic simulations. Accelerations create larger nucleus deformation when compared to fluid shear. Nucleus motions depend on frequency and cell stiffness and amplitude.

Frequency	Nucleus stiffness	Acceleration magnitude		Fluid shear stress			
		0.15g	1g	0.04Pa	0.14Pa	0.28Pa	0.94Pa
100Hz	3kPa	352nm	1840nm	0.096nm	-	6.72nm	-
	6kPa	137nm	717nm	0.044nm	-	3.08nm	-
	18kPa	45nm	283nm	0.013nm	-	0.924nm	-
30Hz	3kPa	258nm	1554nm	-	3.36nm	-	22.50nm
	6kPa	117nm	844nm	-	1.54nm	-	10.34nm
	18kPa	37nm	226nm	-	0.46nm	-	3.10nm

Figures



Acceleration



Fluid Shear

Figure 4.1. FE model of an adherent cell was constructed to predict the vibration induced nucleus motions. Vibration induced accelerations and fluid shear were evaluated in separate dynamic simulations to compare the nucleus motions induced. During fluid shear simulations contact surface was fixed and forces applied to membrane in a sinusoidal manner. During acceleration simulations contact surface was subjected to dynamic sinusoidal accelerations the horizontal plane.

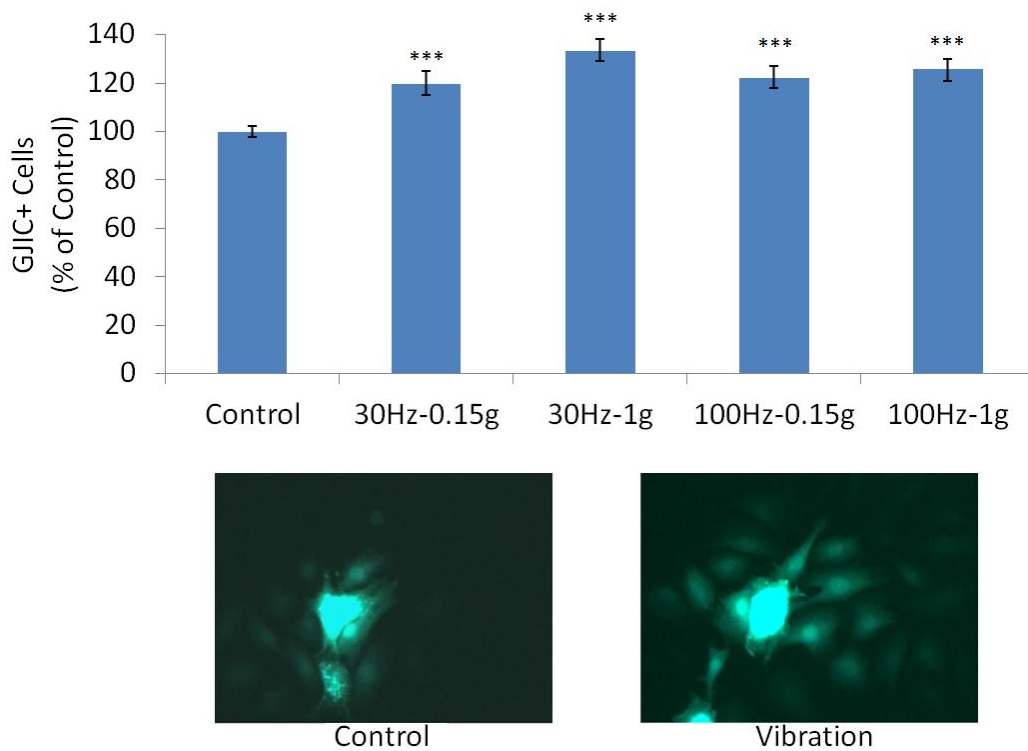


Figure 4.2. MLO-Y4 cells were vibrated with four different vibration parameters. (a) GJIC+ cells were determined via flow cytometry following 1hr of incubation at 37°C in 5%CO². (b) Vibrated MLO-Y4 cells can communicate farther as determined by microscope images. p<0.001: ***against non-vibrated control.

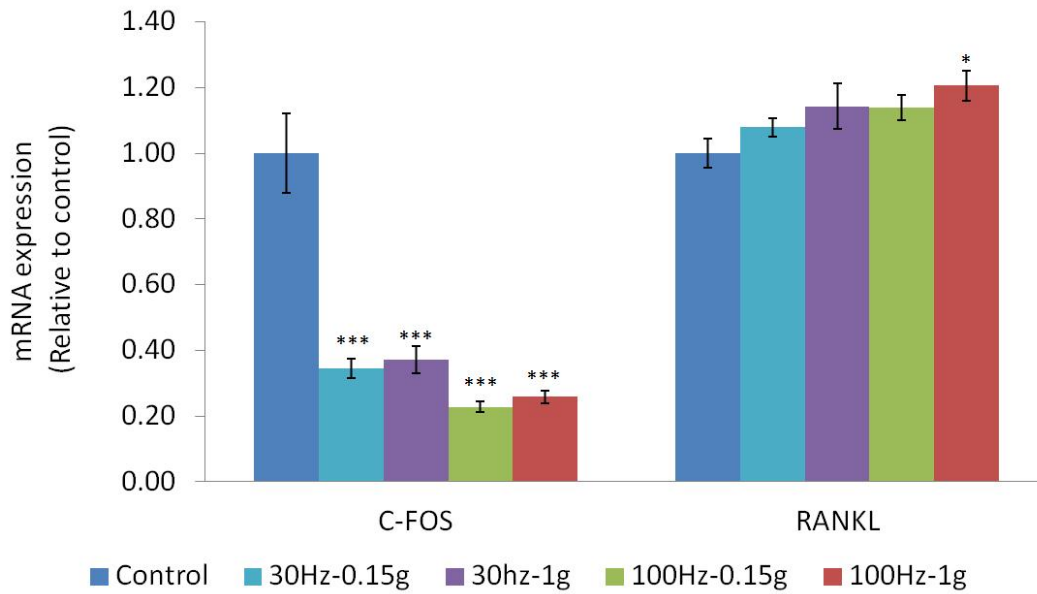


Figure 4.3. mRNA expression determined 1hr after cell communication. Vibration induced increases in GJIC were accompanied by decreases in C-FOS and increases in RANKL. $p < 0.05$: *against non-vibrated control. $p < 0.001$: ***against non-vibrated control.

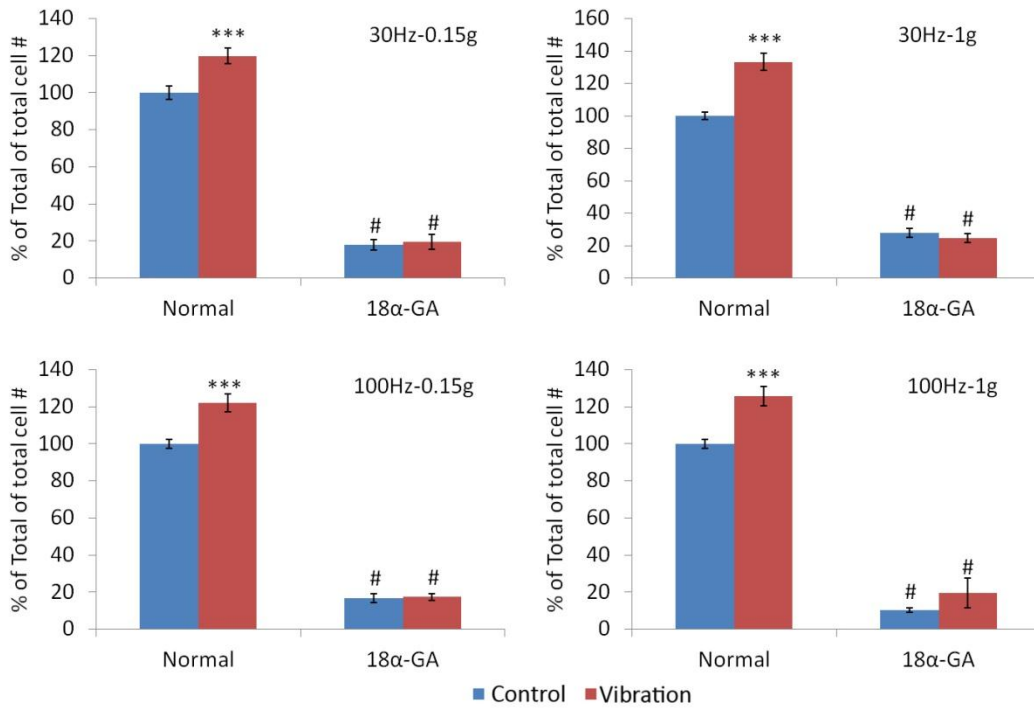


Figure 4.4. Gap junction function in both donor (MC3T3) and acceptor (MLO-Y4) cells were blocked by 75μM of 18α-GA. Compared to non-blocked groups (Normal), groups treated with 18α-GA showed significant decreases in GJIC+ cell number. $p < 0.001$: *** against non-vibrated control, $p < 0.0001$: # against non-vibrated control.

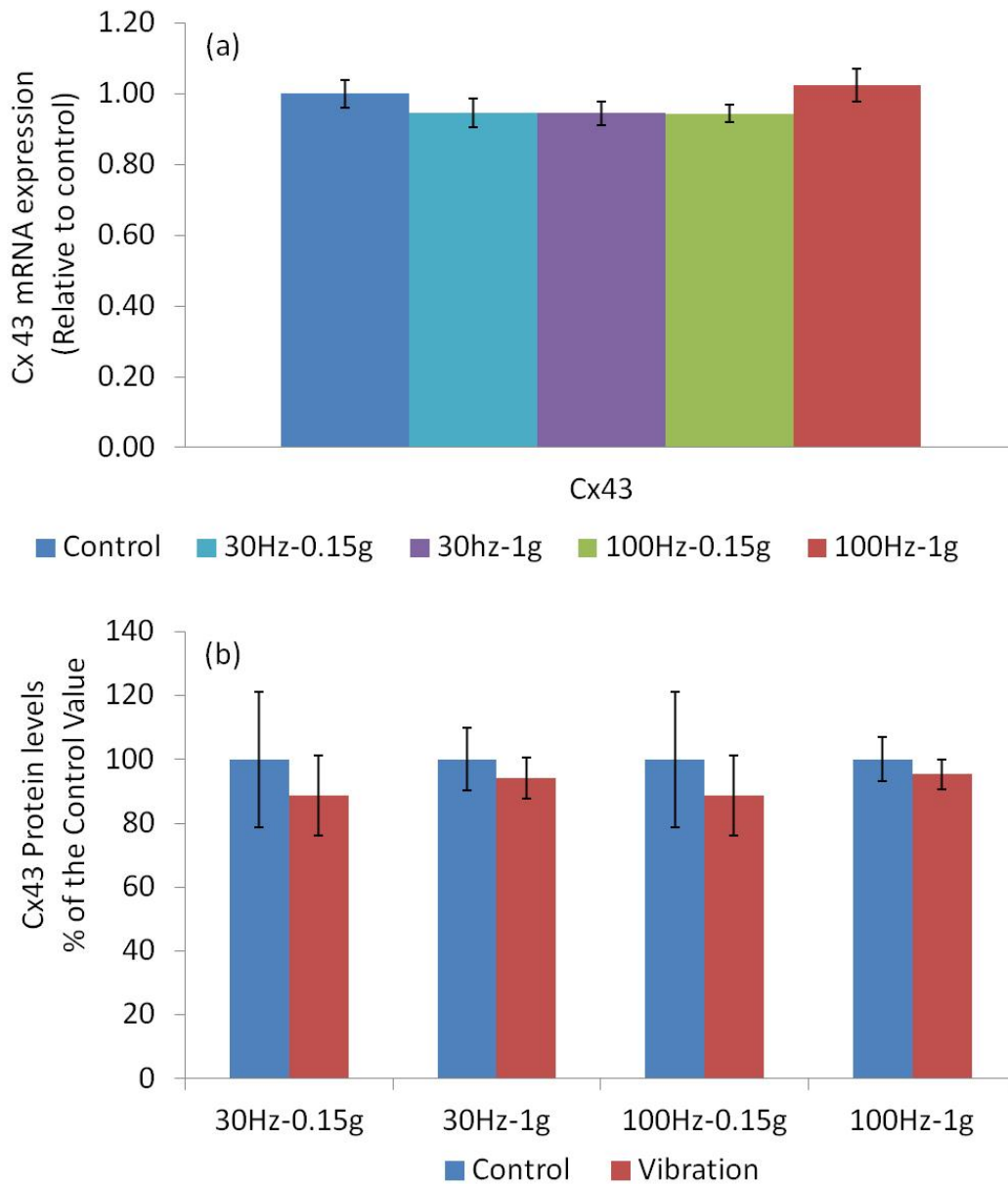


Figure 4.5. mRNA and protein levels of Cx43 were determined 1hr after vibration treatment. Following vibration treatment no changes were observed in mRNA or protein levels of Cx43.

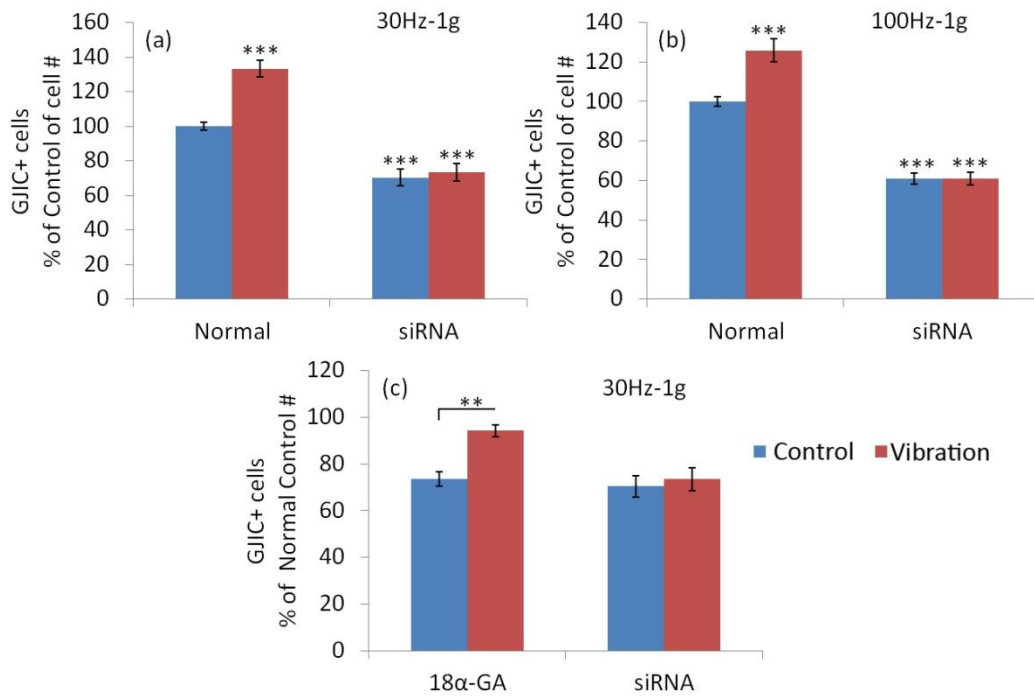


Figure 4.6. Akt signaling was blocked in MLO-Y4 cells with siRNA two days prior to vibration treatment. Following either (a) 30Hz-1g or (b) 100Hz-1g there was no difference between vibrated and control siRNA groups. (c) Blocking gap junction function only in MLO-Y4 cells decreased the GJIC similarly but the difference between control and vibration samples were preserved. $p < 0.01$: ** against non-vibrated control. $p < 0.001$: *** against non-vibrated control.

Chapter 5

CONCLUSIONS

Summary

Vibrations are an integral part of healthy bone homeostasis. Clinical studies as well as animal and cell models showed that cells can respond to vibrations. Mechanical information provided by vibrations is complex and should be represented by multitude of parameters. Therefore, during vibrations cells not only subjected to accelerations and frequency but also secondary mechanical signals such as vibration induced fluid shear. This notion brings up an important question of what is the primary mechanical information carried by vibrations and how this information is sensed? However, lack of standard terminology within the literature, makes it difficult to paint a unified picture for the efficacy and cellular sensing mechanisms of vibration therapy. In this dissertation I examined mechanical information carried by vibrations both macro and cellular level. Furthermore, premise of interactions between vibration induced mechanical signals that would modulate the cellular mechanotransduction was tested across different bone cells.

In **second chapter** using experimental and computational methods we characterized the vibration induced fluid shear as a function of acceleration and frequency. We separated the fluid shear component from acceleration and

frequency by modulating fluid viscosity. Therefore, during horizontal vibrations we determined the exact fluid shear stress distribution at any given vibration parameter. Osteoblast responded to vibration in a frequency dependant manner by increasing mechanically inducible COX-2 mRNA levels. Increasing fluid shear reversed the frequency dependency. Neither frequency nor fluid shear consistently accounted for the observed changes, emphasizing that other variables including out-of-phase motions of the nucleus may play a role in the cellular response to vibrations.

Results from **third chapter** showed that actin cytoskeleton plays a critical role in regulating mechanically induced osteogenesis. Undifferentiated MSCs sensed and responded to vibrations. However, no immediate osteogenic response was observed prior to actin remodeling. When studied over long term cultures, cytoskeletal remodeling in response to vibration treatment were largely predicted by the acceleration. Comparing low and high fluid shear groups demonstrated that fluid shear was not necessary for the mineralization and proliferation responses of MSCs. Additionally, cell proliferation and mineralization showed a decrease when vibration frequency was decreased. Interestingly, frequency dependent decreases in proliferation and mineralization were compensated by the increases acceleration and fluid shear.

During **fourth chapter**, we hypothesized that application of accelerations induce larger relative nucleus motions compared to fluid shear and will increase the GJIC independent of fluid shear. We compared the nuclear motions caused by dynamic fluid shear or acceleration events within a cell *in silico*. Results show that accelerations induce larger nucleus motions compared to fluid shear. There was no measurable differences between low (0.04Pa) and high (1.88Pa) fluid shear treatments, suggesting that accelerations alone were sufficient to increase the intracellular communication. The increases in the cellular communication were dependent on Akt pathway. Interestingly, the cellular responses were independent of both acceleration and fluid shear magnitude, suggesting that osteocytes were more mechanosensitive compared to less differentiated cells.

Limitations of the *in vitro* and Computational Model

In this dissertation we employed an *in vitro* model which imposes a number of simplifications when compared to *in vivo*. Cell culture mediums used in our model were unable to adequately replicate the complex biochemical environment and paracrine interactions between cells within bone. Similarly

possible interactions between ECM and mechanical signals were omitted. For example, matrix produced by osteoblasts under the vibration treatment were shown to push of MSCs further down on the osteogenesis when compared to non-vibrated controls.¹⁸³ Finally, *in vitro* model does not incorporate realistic 3D environments which known to change cell behavior when compared to 2D cultures.^{286, 287}

In chapter two, we characterized vibration induced fluid shear. Experimental observations were accomplished via PIV, where particle motions at different fluid depths were quantified during vibrations. We measured the shear rate down to 37.5 μm . A typical height of osteoblasts *in vitro* is about 3 μm ,²⁸⁸ showing that the shear rate measurements were done approximately 35 μm away from actual cell surface. Given that the trabecular spacing in humans can be in order of millimeters, our measurements may provide a first approximation. However, in small micro channels ($\leq 30 \mu\text{m}$) variations in cell shape are sufficient to alter fluid shear gradients.²²³ This shows that there are local fluid shear variations in the immediate vicinity of cells (3 to 5 microns) that were beyond our measurement capabilities. These limitations likely underestimated the fluid shear stress over cells. Our inability to measure the shear rate at a higher accuracy was caused by several factors. During vibrations, tracking the particle

path requires visualizing an area larger than the total travel of the microscope slide which limits the largest magnification to 20X. At this magnification depth of focus is $\sim 20\mu\text{m}$, further limiting the accuracy of the positioning. A possible way to overcome this difficulty would be to utilize mirrors to visualize planes perpendicular to focal plane, ultimately providing a greater spatial resolution of the space over the cell surface.²⁸⁹

In our in vitro system the viscosity of the medium was used control fluid shear independent of the vibration parameters. However changing the viscosity of the medium from 1cP to 3.5cP also changed the osmolarity of the medium. Osteoblasts express transient receptor potential (TRP) superfamily of ion channels.²⁹⁰ TRP vanilloid 4 (TRPV4) is a Ca^{2+} permeable nonselective cation channel. Interestingly, TRPV4 is sensitive to both hypotonic cell swelling and fluid shear.^{291, 292} Swelling induced changes appear to be uncoupled from mechanical stretch but related to increases in phospholipase A₂ (PLA₂) and arachidonic acid production,^{293, 294} showing that the increases in osmolarity (viscosity) can alter the response of osteoblasts.²⁴³ These results are significant because in the second chapter we measured COX-2 mRNA levels which play an important role in converting arachidonic acid to PGE₂. These finding suggest that our ability to

accurately measure the COX-2 mRNA response might have been confounded by osmolarity.

Though the dissertation we referred to the viscosity of the bone marrow. Bone marrow is not a homogenous medium but a mixture of cells, solid structures and fluids.²²⁶ Additionally, bone marrow and bone surfaces, share cellular as well as vascular connections through the bone structure. These direct mechanical connections cannot be encompassed by a simple viscosity measurement. The reported viscosity is in reality an apparent viscosity after whole contents of the bone is virtually homogenized in the viscometer.¹⁰⁸ To our knowledge there are no methods available to reliably measure real apparent viscosity of the bone marrow *in vivo*.

During chapter four, we presented a dynamic FEM of an adherent cell and estimated vibration induced nucleus motions. As clearly indicated by our results, nucleus motions entirely depend on material properties and cell geometry. In a real cell, microtubules and actin cytoskeleton considerably limits the level of nucleus motions.¹²⁵ Therefore due to lack of cytoskeleton, nucleus motions during dynamic accelerations were likely overestimated. During the course of model development we included a simple tensegrity structure to represent the cytoskeleton. Inclusion of a cytoskeleton decreased the nuclear

motions when direct force applied to nucleus in static, one step simulations. However due to due to dynamic nature of the vibration signal, cytoskeleton caused instabilities during dynamic simulations and had to be excluded from the model. One way to include cytoskeleton into the cell model would be using static simulations. However, unlike the fluid shear, we do not know level of deformation and force subjected to nucleus by accelerations. Further experiments are needed to measure nuclear motions experimentally in order to run more realistic simulations.

Vibration as a Therapeutic Agent of Bone Formation

Results in this dissertation demonstrated that at the cellular level, MSCs, osteoblasts and osteocytes responded to vibration treatment. Osteoblasts and MSCs were able to increase bone formation markers, showing that vibrations may affect the local cell populations within bone. Osteocytes on the other hand increased the cellular communication. These results regarding osteocyte communication were significant. Our results imply that vibrations not only affect specific cell populations but the through gap junctional communication, may

spread the local mechanical or biochemical stimuli through lacunar-canalicular network and affect the whole bone.

Another interesting implication of the results presented in this dissertation is that vibration's potential to amplify mechanosensitivity of bone. Mechanical strain and subsequent fluid flow have been shown to affect the bone formation.^{88, 99} Inherently large deformations are very site specific because the peak strains created at structurally weak or buckling points. Vibrations on the other hand can be transferred to whole body from head to toe.^{295, 203} Additional to anabolic effects of vibrations, they can also increase the effectiveness of low frequency large magnitude deformations through increasing cellular communication.

Mechanosensitivity of a Bone Cells to Vibration

In this dissertation we investigated which of the specific mechanical information created by vibrations influenced bone cell metabolism the most. We divided the vibration induced forces into three main components, frequency, acceleration

and vibration induced fluid shear stress. Vibration responses for osteoblasts and MSCs were frequency dependant. Except the groups with really high fluid shear ($\geq 2\text{Pa}$), increases in frequency indicated a trend of increase in cellular response through the chapter two and three. Since all the vibrations were delivered for a fixed time (30 min), higher frequency signals apply more cycle per vibration period. Results were consistent with the literature that mechanical response of bone is cycle number dependant.^{296, 190, 297} However, osteocytes studied at chapter four were not responsive to frequency changes, even though all the vibration groups were significantly higher than controls. These results suggest that cells have an ability to change their cellular sensitivity to vibrations perhaps through differentiation.

As bone cells differentiate from MSC to osteocyte their environment becomes progressively stiffer, from marrow to calcified bone. It is known that increases in stiffness supports osteogenesis and may advance cytoskeletal remodeling, prestress²³⁹ and efficiency of force transfer into the nucleus.¹⁶³ Our results from chapter three showed that without actin fiber formation there were no osteogenic effects of vibrations. When osteogenic differentiation was initiated using osteogenic cell culture medium, vibrations were able to increase level of cytoskeletal remodeling and mineralization compared to controls. It is

possible that cycle number and cytoskeletal development has an interaction during vibration response. For example during MSC mineralization, 100Hz signals showed a consistent increase in all acceleration magnitudes even though level of cytoskeletal remodeling was different between groups. Mineralization within 30Hz signals however, correlated well with the level of cytoskeletal development. These results may indicate that as cell differentiates from MSC to osteocyte they develop more extensive cytoskeleton which in turn increases their sensitivity to mechanical signals. Cytoskeleton is directly connected to the mechanosensitive sites such as focal adhesions. Increase in cytoskeletal proteins reflects the fact that there are more cytoskeletal elements within the cell, creating a higher level of connectivity. This might indicate that upon vibration treatment there will be more focal adhesion sites that are connected within the cell and respond more robustly to mechanical signals. Not surprisingly, inserting refractory periods shown to increase the cellular response to vibrations, indicating an elevated responsiveness.

Although it is not entirely clear, if the increased mineralization response of MSCs at 30Hz groups was due to increased cellular sensitivity or increased signal strength. When actin stress fiber formation was induced using LPA, increases in acceleration magnitude and fluid shear failed to increase the RUNX-

2 expression. In fact lowest acceleration magnitude produced the highest RUNX-2 increase. These results imply that during cellular differentiation, mechanosensitivity is modulated by level of cytoskeletal development but not the signal strength. We observed similar results in chapter four. When we used osteocyte like cells, that possess a more developed cytoskeleton compared to undifferentiated MSCs, changes in signal magnitude did not change the cellular response, suggesting that osteocytes may be more sensitive to mechanical signals.

Fluid shear magnitude did not have a profound effect on the overall vibration response. Consistently across all the experiments performed in this dissertation, groups with lower fluid shear stress elicited higher or equal responses when compared to groups with higher fluid shear. When compared to accelerations, fluid shear induced smaller cellular deformations. These results are consistent with the hypothesis that mechanotransduction response of cells converge on the forces created on the cytoskeleton, rather than independently affecting the cellular response. However, we cannot rule out the competition between the forces created by fluid shear and accelerations. For example, during second chapter, increasing the fluid viscosity and therefore increasing fluid shear inverted the COX-2 frequency response. Groups with lower frequency and higher

fluid shear (up to $\sim 8\text{Pa}$) elicited higher mRNA expressions, suggesting that trends of change in cellular response could be dominated by fluid shear if the forces created by fluid shear are bigger or comparable to accelerations.

Optimization of Patient Specific Outcomes by Controlling Mechanical Signals

With the end of decade old human genome project²⁹⁸ a new trend towards personalized medicine is apparent including the bone field.²⁹⁹⁻³⁰² Results presented in this dissertation show that vibration induced mechanical forces can be tailored toward specific cell populations or cell functions. For example, in a number of preliminary experiments that were not presented in the previous chapters, we used either osteolife (Lifeline cell technologies) or α -MEM (Gibco) for culturing MSCs. When compared the growth rates of cell under this two medium we found that osteolife produced 3 to 4 times faster growth rates, likely through addition of factors that were not disclosed in the product sheet. Interestingly, upon vibration treatment, proliferation response was increasing under α -MEM³⁰³ while decreasing under osteolife conditions (chapter 3). These

results point to two important facts. First, based on the chemical environment vibrations can either increase or decrease the proliferation of same cell population. Second, when proliferation increased with addition of chemical factors (osteolife medium) vibrations can interfere with that response in a dose dependent manner. Previously we also observed dose dependent response of osteoblast proliferation to signal magnitude.³⁰⁴ Although directly translating results presented in this dissertation into a clinical setting is a big leap of faith. Let's suppose a hypothetical case of a patient with a fracture. It might be possible to deliver the vibration therapy in a certain fashion for the optimal recovery of the patient. For example, in early fracture, safe low magnitude signals would support osteoblast and MSC proliferation and as the healing process continues higher magnitude signals could be used to reduce proliferation and support cytoskeletal development in cells on the fracture surface.

Although the scope of this dissertation falls short, some important pointers can be taken regarding the cell specific signals. For example, we found that osteocytes do not differentiate between vibration parameters while MSCs and osteocyte show frequency specific responses. More specifically, both MSCs and osteoblasts show increased response with increasing frequency. During

vibration treatment, patient specific frequencies may be selected to maximize osteocyte response while minimizing other cell responses. Regardless of the challenges, future studies regarding the personalized mechanical therapies will create new and complete understanding in cellular mechanosensitivity and communication within bone environment.

Conclusions

In conclusion, results presented in this dissertation indicated that cells can exclusively sense and respond to accelerations in the presence of fluid shear stresses. There exists a relationship between frequency, signal strength and cytoskeletal adaptation. To understand vibration driven mechano-adaptation, future studies investigating the interactions between different cells as well as cellular response and extracellular matrix environment are needed. Perhaps it is possible to direct the cellular response to vibrations within bone that will benefit patient specific outcomes.

BIBLIOGRAPHY

1. Huang, Y., et al., *Gravity, a regulation factor in the differentiation of rat bone marrow mesenchymal stem cells*. J Biomed Sci, 2009. **16**: p. 87.
2. Kearney, E.M., et al., *Tensile strain as a regulator of mesenchymal stem cell osteogenesis*. Ann Biomed Eng. **38**(5): p. 1767-79.
3. Wagner, D.R., et al., *Hydrostatic pressure enhances chondrogenic differentiation of human bone marrow stromal cells in osteochondrogenic medium*. Ann Biomed Eng, 2008. **36**(5): p. 813-20.
4. Fukuda, K. and J. Fujita, *Mesenchymal, but not hematopoietic, stem cells can be mobilized and differentiate into cardiomyocytes after myocardial infarction in mice*. Kidney Int, 2005. **68**(5): p. 1940-3.
5. Mendez-Ferrer, S., et al., *Mesenchymal and haematopoietic stem cells form a unique bone marrow niche*. Nature, 2010. **466**(7308): p. 829-834.
6. Galli, C., et al., *Commitment to the Osteoblast Lineage Is Not Required for RANKL Gene Expression*. Journal of Biological Chemistry, 2009. **284**(19): p. 12654-12662.
7. Ozcivici, E., et al., *Low-level vibrations retain bone marrow's osteogenic potential and augment recovery of trabecular bone during reambulation*. PLoS One, 2010. **5**(6): p. e11178.
8. Zayzafoon, M., W.E. Gathings, and J.M. McDonald, *Modeled Microgravity Inhibits Osteogenic Differentiation of Human Mesenchymal Stem Cells and Increases Adipogenesis*. Endocrinology, 2004. **145**(5): p. 2421-2432.
9. Haudenschild, A.K., et al., *Pressure and distortion regulate human mesenchymal stem cell gene expression*. Ann Biomed Eng, 2009. **37**(3): p. 492-502.
10. Doyle, A.M., R.M. Nerem, and T. Ahsan, *Human mesenchymal stem cells form multicellular structures in response to applied cyclic strain*. Ann Biomed Eng, 2009. **37**(4): p. 783-93.
11. Huang, C.H., et al., *Interactive effects of mechanical stretching and extracellular matrix proteins on initiating osteogenic differentiation of human mesenchymal stem cells*. J Cell Biochem, 2009. **108**(6): p. 1263-73.
12. Zheng, W., et al., *Fluid flow stress induced contraction and re-spread of mesenchymal stem cells: a microfluidic study*. Integrative Biology, 2012. **4**(9): p. 1102-1111.
13. Ducy, P., et al., *A Cbfa1-dependent genetic pathway controls bone formation beyond embryonic development*. Genes & Development, 1999. **13**(8): p. 1025-1036.
14. Nakashima, K., et al., *The Novel Zinc Finger-Containing Transcription Factor Osterix Is Required for Osteoblast Differentiation and Bone Formation*. Cell, 2002. **108**(1): p. 17-29.

15. Feng, Z., et al., *Effect of cytoskeleton inhibitors on deadhesion kinetics of HepG2 cells on biomimetic surface*. Colloids Surf B Biointerfaces. **75**(1): p. 67-74.
16. Luu, Y.K., et al., *Mechanical Stimulation of Mesenchymal Stem Cell Proliferation and Differentiation Promotes Osteogenesis While Preventing Dietary-Induced Obesity*. Journal of Bone and Mineral Research, 2009. **24**(1): p. 50-61.
17. Ducy, P., *CBFA1: A molecular switch in osteoblast biology*. Developmental Dynamics, 2000. **219**(4): p. 461-471.
18. Brown, J.R., et al., *Fos Family Members Induce Cell Cycle Entry by Activating Cyclin D1*. Molecular and Cellular Biology, 1998. **18**(9): p. 5609-5619.
19. Lian, J.B., et al., *Phenotype suppression: A postulated molecular mechanism for mediating the relationship of proliferation and differentiation by Fos/Jun interactions at AP-1 sites in steroid responsive promoter elements of tissue-specific genes*. Journal of Cellular Biochemistry, 1991. **45**(1): p. 9-14.
20. Owen, T.A., et al., *Coordinate occupancy of AP-1 sites in the vitamin D-responsive and CCAAT box elements by Fos-Jun in the osteocalcin gene: model for phenotype suppression of transcription*. Proceedings of the National Academy of Sciences, 1990. **87**(24): p. 9990-9994.
21. Sunter, A., et al., *Accelerated cell cycle progression in osteoblasts overexpressing the c-fos proto-oncogene - Induction of cyclin A and enhanced CDK2 activity*. Journal of Biological Chemistry, 2004. **279**(11): p. 9882-9891.
22. Xiong, J., et al., *Matrix-embedded cells control osteoclast formation*. Nat Med, 2011. **17**(10): p. 1235-1241.
23. Moursi, A.M., et al., *Fibronectin regulates calvarial osteoblast differentiation*. Journal of Cell Science, 1996. **109**(6): p. 1369-1380.
24. Moursi, A.M., R.K. Globus, and C.H. Damsky, *Interactions between integrin receptors and fibronectin are required for calvarial osteoblast differentiation in vitro*. Journal of Cell Science, 1997. **110**(18): p. 2187-2196.
25. Glimcher, M.J., *Mechanism of calcification: Role of collagen fibrils and collagen-phosphoprotein complexes in vitro and in vivo*. The Anatomical Record, 1989. **224**(2): p. 139-153.
26. Lian, J.B. and G.S. Stein, *Concepts of Osteoblast Growth and Differentiation: Basis for Modulation of Bone Cell Development and Tissue*

- Formation*. Critical Reviews in Oral Biology & Medicine, 1992. **3**(3): p. 269-305.
27. Hauschka, P.V., et al., *Osteocalcin and matrix Gla protein: vitamin K-dependent proteins in bone*. Physiological Reviews, 1989. **69**(3): p. 990-1047.
 28. Ogata, Y., *Bone sialoprotein and its transcriptional regulatory mechanism*. Journal of Periodontal Research, 2008. **43**(2): p. 127-135.
 29. Torii, Y., et al., *Demonstration of alkaline phosphatase participation in the mineralization of osteoblasts by antisense RNA approach*. Cell Biology International, 1996. **20**(7): p. 459-464.
 30. Wetterwald, A., et al., *Characterization and cloning of the E11 antigen, a marker expressed by rat osteoblasts and osteocytes*. Bone, 1996. **18**(2): p. 125-32.
 31. Bezooijen, R.L.v., et al., *SOST/sclerostin, an osteocyte-derived negative regulator of bone formation*. Cytokine & Growth Factor Reviews, 2005. **16**(3): p. 319-327.
 32. van Bezooijen, R.L., et al., *Sclerostin is an osteocyte-expressed negative regulator of bone formation, but not a classical BMP antagonist*. J Exp Med, 2004. **199**(6): p. 805-14.
 33. Zhang, K.Q., et al., *E11/gp38 selective expression in osteocytes: Regulation by mechanical strain and role in dendrite elongation*. Molecular and Cellular Biology, 2006. **26**(12): p. 4539-4552.
 34. Chen, N.X., et al., *Ca²⁺ regulates fluid shear-induced cytoskeletal reorganization and gene expression in osteoblasts*. American Journal of Physiology-Cell Physiology, 2000. **278**(5): p. C989-C997.
 35. Jacobs, C.R., et al., *Differential effect of steady versus oscillating flow on bone cells*. Journal of Biomechanics, 1998. **31**(11): p. 969-976.
 36. Pavalko, F.M., et al., *Fluid shear-induced mechanical signaling in MC3T3-E1 osteoblasts requires cytoskeleton-integrin interactions*. Am J Physiol Cell Physiol, 1998. **275**(6): p. C1591-1601.
 37. Harter, L.V., K.A. Hruska, and R.L. Duncan, *Human osteoblast-like cells respond to mechanical strain with increased bone matrix protein production independent of hormonal regulation*. Endocrinology, 1995. **136**(2): p. 528-535.
 38. Rubin, J., et al., *Activation of extracellular signal-regulated kinase is involved in mechanical strain inhibition of RANKL expression in bone stromal cells*. Journal of Bone and Mineral Research, 2002. **17**(8): p. 1452-1460.

39. Patel, M.J., et al., *Low Magnitude and High Frequency Mechanical Loading Prevents Decreased Bone Formation Responses of 2T3 Preosteoblasts*. Journal of Cellular Biochemistry, 2009. **106**(2): p. 306-316.
40. Rosenberg, N., M. Levy, and M. Francis, *Experimental model for stimulation of cultured human osteoblast-like cells by high frequency vibration*. Cytotechnology, 2002. **39**(3): p. 125-130.
41. Kapur, S., D.J. Baylink, and K.H.W. Lau, *Fluid flow shear stress stimulates human osteoblast proliferation and differentiation through multiple interacting and competing signal transduction pathways*. Bone, 2003. **32**(3): p. 241-251.
42. Bancroft, G.N., et al., *Fluid flow increases mineralized matrix deposition in 3D perfusion culture of marrow stromal osteoblasts in a dose-dependent manner*. Proceedings of the National Academy of Sciences of the United States of America, 2002. **99**(20): p. 12600-12605.
43. Case, N., et al., *β -Catenin Levels Influence Rapid Mechanical Responses in Osteoblasts*. Journal of Biological Chemistry, 2008. **283**(43): p. 29196-29205.
44. Reich, K.M., C.V. Gay, and J.A. Frangos, *Fluid shear stress as a mediator of osteoblast cyclic adenosine monophosphate production*. Journal of Cellular Physiology, 1990. **143**(1): p. 100-104.
45. Robinson, J.A., et al., *Wnt/ β -Catenin Signaling Is a Normal Physiological Response to Mechanical Loading in Bone*. Journal of Biological Chemistry, 2006. **281**(42): p. 31720-31728.
46. Klein-Nulend, J., P.J. Nijweide, and E.H. Burger, *Osteocyte and bone structure*. Curr Osteoporos Rep, 2003. **1**(1): p. 5-10.
47. Alford, A.I., C.R. Jacobs, and H.J. Donahue, *Oscillating fluid flow regulates gap junction communication in osteocytic MLO-Y4 cells by an ERK1/2 MAP kinase-dependent mechanism*. Bone, 2003. **33**(1): p. 64-70.
48. Yellowley, C.E., et al., *Functional Gap Junctions Between Osteocytic and Osteoblastic Cells*. Journal of Bone and Mineral Research, 2000. **15**(2): p. 209-217.
49. Jiang, J.X., A.J. Siller-Jackson, and S. Burra, *Roles of gap junctions and hemichannels in bone cell functions and in signal transmission of mechanical stress*. Frontiers in Bioscience, 2007. **12**: p. 1450-1462.
50. Nakashima, T., et al., *Evidence for osteocyte regulation of bone homeostasis through RANKL expression*. Nat Med, 2011. **17**(10): p. 1231-1234.
51. BURGER, E.H. and J. KLEIN-NULEND, *Mechanotransduction in bone—role of the lacuno-canalicular network*. FASEB J., 1999. **13**(9001): p. 101-112.

52. Weinbaum, S., S.C. Cowin, and Y. Zeng, *A model for the excitation of osteocytes by mechanical loading-induced bone fluid shear stresses*. Journal of Biomechanics, 1994. **27**(3): p. 339-360.
53. Klein-Nulend, J., et al., *Sensitivity of osteocytes to biomechanical stress in vitro*. FASEB J, 1995. **9**(5): p. 441-5.
54. Santos, A., A. Bakker, and J. Klein-Nulend, *The role of osteocytes in bone mechanotransduction*. Osteoporosis International, 2009. **20**(6): p. 1027-1031.
55. Takahashi, N., et al., *Osteoclast-like cell formation and its regulation by osteotropic hormones in mouse bone marrow cultures*. Endocrinology, 1988. **122**(4): p. 1373-82.
56. Lacey, D.L., et al., *Osteoprotegerin Ligand Is a Cytokine that Regulates Osteoclast Differentiation and Activation*. Cell, 1998. **93**(2): p. 165-176.
57. Yasuda, H., et al., *Osteoclast differentiation factor is a ligand for osteoprotegerin/osteoclastogenesis-inhibitory factor and is identical to TRANCE/RANKL*. Proceedings of the National Academy of Sciences, 1998. **95**(7): p. 3597-3602.
58. Hsu, H., et al., *Tumor necrosis factor receptor family member RANK mediates osteoclast differentiation and activation induced by osteoprotegerin ligand*. Proceedings of the National Academy of Sciences, 1999. **96**(7): p. 3540-3545.
59. Grigoriadis, A., et al., *c-Fos: a key regulator of osteoclast-macrophage lineage determination and bone remodeling*. Science, 1994. **266**(5184): p. 443-448.
60. Matsuo, K., et al., *Nuclear factor of activated T-cells (NFAT) rescues osteoclastogenesis in precursors lacking c-Fos*. J Biol Chem, 2004. **279**(25): p. 26475-80.
61. Boyle, W.J., W.S. Simonet, and D.L. Lacey, *Osteoclast differentiation and activation*. Nature, 2003. **423**(6937): p. 337-342.
62. Simonet, W.S., et al., *Osteoprotegerin: a novel secreted protein involved in the regulation of bone density*. Cell, 1997. **89**(2): p. 309-19.
63. Yasuda, H., et al., *Identity of osteoclastogenesis inhibitory factor (OCIF) and osteoprotegerin (OPG): a mechanism by which OPG/OCIF inhibits osteoclastogenesis in vitro*. Endocrinology, 1998. **139**(3): p. 1329-37.
64. Boyce, B.F. and L. Xing, *Functions of RANKL/RANK/OPG in bone modeling and remodeling*. Archives of Biochemistry and Biophysics, 2008. **473**(2): p. 139-146.

65. Thomas, G.P., et al., *Changing RANKL/OPG mRNA expression in differentiating murine primary osteoblasts*. J Endocrinol, 2001. **170**(2): p. 451-60.
66. O'Connor, J.A., L.E. Lanyon, and H. MacFie, *The influence of strain rate on adaptive bone remodelling*. J Biomech, 1982. **15**(10): p. 767-81.
67. Poliachik, S.L., et al., *32 wk old C3H/HeJ mice actively respond to mechanical loading*. Bone, 2008. **42**(4): p. 653-659.
68. Rath, B., et al., *Compressive forces induce osteogenic gene expression in calvarial osteoblasts*. Journal of Biomechanics, 2008. **41**(5): p. 1095-1103.
69. Rubin, C.T. and L.E. Lanyon, *Regulation of bone formation by applied dynamic loads*. J Bone Joint Surg Am, 1984. **66**(3): p. 397-402.
70. Rubin, C.T. and L.E. Lanyon, *Regulation of bone mass by mechanical strain magnitude*. Calcif Tissue Int, 1985. **37**(4): p. 411-7.
71. Garman, R., et al., *Low-level Accelerations applied in the absence of weight bearing can enhance trabecular bone formation*. Journal of Orthopaedic Research, 2007. **25**(6): p. 732-740.
72. Oxlund, B.S., et al., *Low-intensity, high-frequency vibration appears to prevent the decrease in strength of the femur and tibia associated with ovariectomy of adult rats*. Bone, 2003. **32**(1): p. 69-77.
73. Pre, D., et al., *The differentiation of human adipose-derived stem cells (hASCs) into osteoblasts is promoted by low amplitude, high frequency vibration treatment*. Bone, 2011. **49**(2): p. 295-303.
74. Rubin, C., et al., *Anabolism. Low mechanical signals strengthen long bones*. Nature, 2001. **412**(6847): p. 603-4.
75. Tanaka, S.M., et al., *Effects of broad frequency vibration on cultured osteoblasts*. Journal of Biomechanics, 2003. **36**(1): p. 73-80.
76. Wren, T.A.L., et al., *Effect of High-frequency, Low-magnitude Vibration on Bone and Muscle in Children With Cerebral Palsy*. Journal of Pediatric Orthopaedics, 2010. **30**(7): p. 732-738.
77. Judex, S. and C.T. Rubin, *Is bone formation induced by high-frequency mechanical signals modulated by muscle activity?* Journal of Musculoskeletal & Neuronal Interactions, 2010. **10**(1): p. 3-11.
78. Robinson, T.L., et al., *Gymnasts exhibit higher bone mass than runners despite similar prevalence of amenorrhea and oligomenorrhea*. Journal of Bone and Mineral Research, 1995. **10**(1): p. 26-35.
79. Verschueren, S.M.P., et al., *Effect of 6-month whole body vibration training on hip density, muscle strength, and postural control in postmenopausal women: A randomized controlled pilot study*. Journal of Bone and Mineral Research, 2004. **19**(3): p. 352-359.

80. McGarry, J.G., et al., *A comparison of strain and fluid shear stress in stimulating bone cell responses - a computational and experimental study*. *Faseb Journal*, 2004. **18**(15): p. 482-+.
81. Sikavitsas, V.I., et al., *Mineralized matrix deposition by marrow stromal osteoblasts in 3D perfusion culture increases with increasing fluid shear forces*. *Proceedings of the National Academy of Sciences of the United States of America*, 2003. **100**(25): p. 14683-14688.
82. Qin, Y.X. and M. Hu, *Intramedullary pressure induced by dynamic hydraulic pressure stimulation and its potential in treatment of osteopenia*. *Bone*, 2011. **48**: p. S186-S186.
83. Qin, Y.X. and H.Y. Lam, *Intramedullary pressure and matrix strain induced by oscillatory skeletal muscle stimulation and its potential in adaptation*. *Journal of Biomechanics*, 2009. **42**(2): p. 140-145.
84. Zhang, P., et al., *Knee loading dynamically alters intramedullary pressure in mouse femora*. *Bone*, 2007. **40**(2): p. 538-543.
85. Rubin, C.T. and L.E. Lanyon, *REGULATION OF BONE-FORMATION BY APPLIED DYNAMIC LOADS*. *Journal of Bone and Joint Surgery-American Volume*, 1984. **66A**(3): p. 397-402.
86. Ehrlich, P.J. and L.E. Lanyon, *Mechanical strain and bone cell function: A review*. *Osteoporosis International*, 2002. **13**(9): p. 688-700.
87. Kearney, E., et al., *Tensile Strain as a Regulator of Mesenchymal Stem Cell Osteogenesis*. *Annals of Biomedical Engineering*, 2010. **38**(5): p. 1767-1779.
88. Mosley, J.R. and L.E. Lanyon, *Strain rate as a controlling influence on adaptive modeling in response to dynamic loading of the ulna in growing male rats*. *Bone*, 1998. **23**(4): p. 313-318.
89. Tenenbaum, H.C., *Cellular Origins and Theories of Differentiation of Bone-Forming Cells*, in *Bone: The Osteoblast and Osteocyte*, B.K. Hall, Editor 1992, CRC Press: Boca Raton, FL. p. 41-69.
90. Blatnik, J.S., L.P.A. Sung, and G.W. Schmid-Schonbein, *The influence of fluid shear stress on the remodeling of the embryonic primary capillary plexus*. *Biomechanics and Modeling in Mechanobiology*, 2005. **4**(4): p. 211-220.
91. Patwari, P. and R.T. Lee, *Mechanical control of tissue morphogenesis*. *Circulation Research*, 2008. **103**(3): p. 234-243.
92. Dimmeler, S., et al., *Activation of nitric oxide synthase in endothelial cells by Akt-dependent phosphorylation*. *Nature*, 1999. **399**(6736): p. 601-605.
93. Topper, J.N., et al., *Identification of vascular endothelial genes differentially responsive to fluid mechanical stimuli: Cyclooxygenase-2,*

- manganese superoxide dismutase, and endothelial cell nitric oxide synthase are selectively up-regulated by steady laminar shear stress.* Proceedings of the National Academy of Sciences of the United States of America, 1996. **93**(19): p. 10417-10422.
94. Kim, M., et al., *Mechanical stimulation activates G alpha q signaling pathways and 5-hydroxytryptamine release from human carcinoid BON cells.* Journal of Clinical Investigation, 2001. **108**(7): p. 1051-1059.
 95. Pavalko, F.M., et al., *Fluid shear stress inhibits TNF-alpha-induced apoptosis in osteoblasts: A role for fluid shear stress-induced activation of P13-kinase and inhibition of caspase-3.* Journal of Cellular Physiology, 2003. **194**(2): p. 194-205.
 96. Zhang, B., et al., *The physiological response of osteoblasts to pulsatile fluid flow shear stress in vitro.* Sheng wu yi xue gong cheng xue za zhi = Journal of biomedical engineering = Shengwu yixue gongchengxue zazhi, 2008. **25**(4): p. 845-8.
 97. Li, P., et al., *Fluid flow-induced calcium response in early or late differentiated osteoclasts.* Annals of Biomedical Engineering, 2012. **40**(9): p. 1874-83.
 98. KleinNulend, J., et al., *Pulsating fluid flow increases nitric oxide (NO) synthesis by osteocytes but not periosteal fibroblasts - Correlation with prostaglandin upregulation.* Biochemical and Biophysical Research Communications, 1995. **217**(2): p. 640-648.
 99. Price, C., et al., *Real-Time Measurement of Solute Transport Within the Lacunar-Canalicular System of Mechanically Loaded Bone: Direct Evidence for Load-Induced Fluid Flow.* Journal of Bone and Mineral Research, 2011. **26**(2): p. 277-285.
 100. Han, Y., et al., *Mechanotransduction and strain amplification in osteocyte cell processes.* Proc Natl Acad Sci U S A, 2004. **101**(47): p. 16689-94.
 101. Christophis, C., et al., *Shear Stress Regulates Adhesion and Rolling of CD44+ Leukemic and Hematopoietic Progenitor Cells on Hyaluronan.* Biophysical Journal, 2011. **101**(3): p. 585-593.
 102. Lasky, L.C. and B. Sullenbarger, *Manipulation of Oxygenation and Flow-Induced Shear Stress Can Increase the In Vitro Yield of Platelets from Cord Blood.* Tissue Engineering Part C-Methods, 2011. **17**(11): p. 1081-1088.
 103. Coughlin, T.R. and G.L. Niebur, *Fluid shear stress in trabecular bone marrow due to low-magnitude high-frequency vibration.* Journal of Biomechanics, 2012. **45**(13): p. 2222-2229.

104. Fritton, S.P., K.J. McLeod, and C.T. Rubin, *Quantifying the strain history of bone: spatial uniformity and self-similarity of low-magnitude strains*. Journal of Biomechanics, 2000. **33**(3): p. 317-325.
105. Dickerson, D.A., E.A. Sander, and E.A. Nauman, *Modeling the mechanical consequences of vibratory loading in the vertebral body: microscale effects*. Biomechanics and Modeling in Mechanobiology, 2008. **7**(3): p. 191-202.
106. Cabrita, G.J.M., et al., *Hematopoietic stem cells: from the bone to the bioreactor*. Trends in Biotechnology, 2003. **21**(5): p. 233-240.
107. Gordon, M., *Stem Cells Handbook*. Bone Marrow Transplant, 2004. **33**(11): p. 1165-1165.
108. Bryant, J.D., et al., *Rheology of bovine bone marrow*. Proc Inst Mech Eng H, 1989. **203**(2): p. 71-5.
109. Blecha, L.D., et al., *Mechanical interaction between cells and fluid for bone tissue engineering scaffold: Modulation of the interfacial shear stress*. Journal of Biomechanics, 2010. **43**(5): p. 933-937.
110. Gimble, J.M., et al., *The function of adipocytes in the bone marrow stroma: an update*. Bone, 1996. **19**(5): p. 421-428.
111. Justesen, J., et al., *Adipocyte tissue volume in bone marrow is increased with aging and in patients with osteoporosis*. Biogerontology, 2001. **2**(3): p. 165-171.
112. Li, S., et al., *Distinct roles for the small GTPases Cdc42 and Rho in endothelial responses to shear stress*. The Journal of Clinical Investigation, 1999. **103**(8): p. 1141-1150.
113. Shyy, J.Y.-J. and S. Chien, *Role of Integrins in Endothelial Mechanosensing of Shear Stress*. Circulation Research, 2002. **91**(9): p. 769-775.
114. Wung, B.S., et al., *Modulation of Ras/Raf/Extracellular Signal-Regulated Kinase Pathway by Reactive Oxygen Species Is Involved in Cyclic Strain-Induced Early Growth Response-1 Gene Expression in Endothelial Cells*. Circulation Research, 1999. **84**(7): p. 804-812.
115. Aikawa, R., et al., *Integrins Play a Critical Role in Mechanical Stress-Induced p38 MAPK Activation*. Hypertension, 2002. **39**(2): p. 233-238.
116. Li, C., et al., *Cyclic Strain Stress-induced Mitogen-activated Protein Kinase (MAPK) Phosphatase 1 Expression in Vascular Smooth Muscle Cells Is Regulated by Ras/Rac-MAPK Pathways*. Journal of Biological Chemistry, 1999. **274**(36): p. 25273-25280.
117. Millward-Sadler, S.J. and D.M. Salter, *Integrin-Dependent Signal Cascades in Chondrocyte Mechanotransduction*. Annals of Biomedical Engineering, 2004. **32**(3): p. 435-446.

118. Wang, G.Y., et al., *RhoA/ROCK signaling suppresses hypertrophic chondrocyte differentiation*. Journal of Biological Chemistry, 2004. **279**(13): p. 13205-13214.
119. Tadokoro, S., et al., *Talin Binding to Integrin β Tails: A Final Common Step in Integrin Activation*. Science, 2003. **302**(5642): p. 103-106.
120. Hirakata, M., et al., *Tyrosine kinase dependent expression of TGF-[beta] induced by stretch in mesangial cells*. Kidney Int, 1997. **51**(4): p. 1028-1036.
121. Kulik, T.J. and S.P. Alvarado, *Effect of stretch on growth and collagen synthesis in cultured rat and lamb pulmonary arterial smooth muscle cells*. Journal of Cellular Physiology, 1993. **157**(3): p. 615-624.
122. Hynes, R.O., *The emergence of integrins: a personal and historical perspective*. Matrix Biology, 2004. **23**(6): p. 333-340.
123. Baker, E.L. and M.H. Zaman, *The biomechanical integrin*. Journal of Biomechanics, 2010. **43**(1): p. 38-44.
124. Zimmerman, D., et al., *Impaired Bone Formation in Transgenic Mice Resulting from Altered Integrin Function in Osteoblasts*. Developmental Biology, 2000. **220**(1): p. 2-15.
125. Maniotis, A.J., C.S. Chen, and D.E. Ingber, *Demonstration of mechanical connections between integrins cytoskeletal filaments, and nucleoplasm that stabilize nuclear structure*. Proceedings of the National Academy of Sciences of the United States of America, 1997. **94**(3): p. 849-854.
126. Boettiger, D., *Mechanical control of integrin-mediated adhesion and signaling*. Current Opinion in Cell Biology, (0).
127. Rezaia, A. and K.E. Healy, *Integrin subunits responsible for adhesion of human osteoblast-like cells to biomimetic peptide surfaces*. Journal of Orthopaedic Research, 1999. **17**(4): p. 615-623.
128. Pelham, R.J. and Y.-l. Wang, *Cell locomotion and focal adhesions are regulated by substrate flexibility*. Proceedings of the National Academy of Sciences, 1997. **94**(25): p. 13661-13665.
129. Geiger, B., et al., *Transmembrane crosstalk between the extracellular matrix and the cytoskeleton*. Nat Rev Mol Cell Biol, 2001. **2**(11): p. 793-805.
130. Weyts, F.A.A., et al., *ERK activation and $\alpha\beta3$ integrin signaling through Shc recruitment in response to mechanical stimulation in human osteoblasts*. Journal of Cellular Biochemistry, 2002. **87**(1): p. 85-92.
131. Petit, V. and J.-P. Thiery, *Focal adhesions: Structure and dynamics*. Biology of the Cell, 2000. **92**(7): p. 477-494.

132. Schaller, M.D., *The focal adhesion kinase*. Journal of Endocrinology, 1996. **150**(1): p. 1-7.
133. Schlaepfer, D.D., C.R. Hauck, and D.J. Sieg, *Signaling through focal adhesion kinase*. Progress in Biophysics and Molecular Biology, 1999. **71**(3-4): p. 435-478.
134. Subauste, M.C., et al., *Vinculin modulation of paxillin-FAK interactions regulates ERK to control survival and motility*. The Journal of Cell Biology, 2004. **165**(3): p. 371-381.
135. Furuta, Y., et al., *Mesodermal defect in late phase of gastrulation by a targeted mutation of focal adhesion kinase, FAK*. 1995. **11**(10): p. 1989-1995.
136. Hagel, M., et al., *The Adaptor Protein Paxillin Is Essential for Normal Development in the Mouse and Is a Critical Transducer of Fibronectin Signaling*. Molecular and Cellular Biology, 2002. **22**(3): p. 901-915.
137. Shen, T.-L., et al., *Conditional knockout of focal adhesion kinase in endothelial cells reveals its role in angiogenesis and vascular development in late embryogenesis*. The Journal of Cell Biology, 2005. **169**(6): p. 941-952.
138. Xu, W., H. Baribault, and E.D. Adamson, *Vinculin knockout results in heart and brain defects during embryonic development*. Development, 1998. **125**(2): p. 327-337.
139. Boutahar, N., et al., *Mechanical Strain on Osteoblasts Activates Autophosphorylation of Focal Adhesion Kinase and Proline-rich Tyrosine Kinase 2 Tyrosine Sites Involved in ERK Activation*. Journal of Biological Chemistry, 2004. **279**(29): p. 30588-30599.
140. Flitney, E.W., et al., *Insights into the mechanical properties of epithelial cells: the effects of shear stress on the assembly and remodeling of keratin intermediate filaments*. The FASEB Journal, 2009. **23**(7): p. 2110-2119.
141. Brangwynne, C.P., et al., *Microtubules can bear enhanced compressive loads in living cells because of lateral reinforcement*. The Journal of Cell Biology, 2006. **173**(5): p. 733-741.
142. Odde, D.J., et al., *Microtubule bending and breaking in living fibroblast cells*. Journal of Cell Science, 1999. **112**(19): p. 3283-3288.
143. Ingber, D.E., *Tensegrity: The architectural basis of cellular mechanotransduction*. Annual Review of Physiology, 1997. **59**: p. 575-599.
144. McGarry, J.G., J. Klein-Nulend, and P.J. Prendergast, *The effect of cytoskeletal disruption on pulsatile fluid flow-induced nitric oxide and*

- prostaglandin E2 release in osteocytes and osteoblasts*. Biochemical and Biophysical Research Communications, 2005. **330**(1): p. 341-348.
145. Norvell, S.M., et al., *Fluid shear stress induction of COX-2 protein and prostaglandin release in cultured MC3T3-E1 osteoblasts does not require intact microfilaments or microtubules*. Journal of Applied Physiology, 2004. **96**(3): p. 957-966.
 146. Naumanen, P., P. Lappalainen, and P. Hotulainen, *Mechanisms of actin stress fibre assembly*. Journal of Microscopy-Oxford, 2008. **231**(3): p. 446-454.
 147. Maritzen, T., et al., *Gadkin negatively regulates cell spreading and motility via sequestration of the actin-nucleating ARP2/3 complex*. Proceedings of the National Academy of Sciences of the United States of America, 2012. **109**(26): p. 10382-10387.
 148. Zhang, W., Y. Huang, and S.J. Gunst, *The Small GTPase RhoA Regulates the Contraction of Smooth Muscle Tissues by Catalyzing the Assembly of Cytoskeletal Signaling Complexes at Membrane Adhesion Sites*. Journal of Biological Chemistry, 2012.
 149. Zhang, X.J., et al., *Rho kinase inhibitors stimulate the migration of human cultured osteoblastic cells by regulating actomyosin activity*. Cellular & Molecular Biology Letters, 2011. **16**(2): p. 279-295.
 150. McBeath, R., et al., *Cell Shape, Cytoskeletal Tension, and RhoA Regulate Stem Cell Lineage Commitment*. Developmental Cell, 2004. **6**(4): p. 483-495.
 151. Arnsdorf, E.J., et al., *Mechanically induced osteogenic differentiation - the role of RhoA, ROCKII and cytoskeletal dynamics*. Journal of Cell Science, 2009. **122**(4): p. 546-553.
 152. Machesky, L.M. and R.H. Insall, *Scar1 and the related Wiskott–Aldrich syndrome protein, WASP, regulate the actin cytoskeleton through the Arp2/3 complex*. Current Biology, 1998. **8**(25): p. 1347-1356.
 153. Machesky, L.M., et al., *Scar, a WASP-related protein, activates nucleation of actin filaments by the Arp2/3 complex*. Proceedings of the National Academy of Sciences of the United States of America, 1999. **96**(7): p. 3739-3744.
 154. Rohatgi, R., et al., *Nck and Phosphatidylinositol 4,5-Bisphosphate Synergistically Activate Actin Polymerization through the N-WASP-Arp2/3 Pathway*. Journal of Biological Chemistry, 2001. **276**(28): p. 26448-26452.
 155. Marchand, J.-B., et al., *Interaction of WASP/Scar proteins with actin and vertebrate Arp2/3 complex*. Nat Cell Biol, 2001. **3**(1): p. 76-82.

156. Mullins, R.D., J.A. Heuser, and T.D. Pollard, *The interaction of Arp2/3 complex with actin: Nucleation, high affinity pointed end capping, and formation of branching networks of filaments*. Proceedings of the National Academy of Sciences, 1998. **95**(11): p. 6181-6186.
157. Jaffe, A.B. and A. Hall, *Rho GTPases: Biochemistry and Biology*. Annual Review of Cell & Developmental Biology, 2005. **21**(1): p. 247-269.
158. Riddick, N., K. Ohtani, and H.K. Surks, *Targeting by myosin phosphatase-RhoA interacting protein mediates RhoA/ROCK regulation of myosin phosphatase*. Journal of Cellular Biochemistry, 2008. **103**(4): p. 1158-1170.
159. Khatiwala, C.B., et al., *ECM Compliance Regulates Osteogenesis by Influencing MAPK Signaling Downstream of RhoA and ROCK*. Journal of Bone and Mineral Research, 2009. **24**(5): p. 886-898.
160. Sen, B., et al., *Mechanically induced focal adhesion assembly amplifies anti-adipogenic pathways in mesenchymal stem cells*. Stem Cells, 2011. **29**(11): p. 1829-36.
161. Horikawa, A., et al., *Morphological changes in osteoblastic cells (MC3T3-E1) due to fluid shear stress: Cellular damage by prolonged application of fluid shear stress*. Tohoku Journal of Experimental Medicine, 2000. **191**(3): p. 127-137.
162. Case, N., et al., *Steady and oscillatory fluid flows produce a similar osteogenic phenotype*. Calcif Tissue Int, 2011. **88**(3): p. 189-97.
163. Hu, S.H., et al., *Prestress mediates force propagation into the nucleus*. Biochemical and Biophysical Research Communications, 2005. **329**(2): p. 423-428.
164. Cooper, L.F., et al., *Incipient Analysis of Mesenchymal Stem-cell-derived Osteogenesis*. Journal of Dental Research, 2001. **80**(1): p. 314-320.
165. McGarry, J.G. and P.J. Prendergast, *A three-dimensional finite element model of an adherent eukaryotic cell*. European cells & materials, 2004. **7**: p. 27-33; discussion 33-4.
166. Wang, N., J.P. Butler, and D.E. Ingber, *MECHANOTRANSDUCTION ACROSS THE CELL-SURFACE AND THROUGH THE CYTOSKELETON*. Science, 1993. **260**(5111): p. 1124-1127.
167. Dahl, K.N., E.A. Booth-Gauthier, and B. Ladoux, *In the middle of it all: Mutual mechanical regulation between the nucleus and the cytoskeleton*. Journal of Biomechanics, 2010. **43**(1): p. 2-8.
168. Huang, H.D., R.D. Kamm, and R.T. Lee, *Cell mechanics and mechanotransduction: pathways, probes, and physiology*. American Journal of Physiology-Cell Physiology, 2004. **287**(1): p. C1-C11.

169. Huebsch, N., et al., *Harnessing traction-mediated manipulation of the cell/matrix interface to control stem-cell fate*. Nature Materials, 2010. **9**(6): p. 518-526.
170. Stewart-Hutchinson, P.J., et al., *Structural requirements for the assembly of LINC complexes and their function in cellular mechanical stiffness*. Experimental Cell Research, 2008. **314**(8): p. 1892-1905.
171. Philip, J.T. and K.N. Dahl, *Nuclear mechanotransduction: Response of the lamina to extracellular stress with implications in aging*. Journal of Biomechanics, 2008. **41**(15): p. 3164-3170.
172. Rubin, C.T. and L.E. Lanyon, *Limb mechanics as a function of speed and gait: a study of functional strains in the radius and tibia of horse and dog*. Journal of Experimental Biology, 1982. **101**(DEC): p. 187-211.
173. Rubin, C.T. and L.E. Lanyon, *Dynamic strain similarity in vertebrates; an alternative to allometric limb bone scaling*. Journal of Theoretical Biology, 1984. **107**(2): p. 321-327.
174. Huang, R.P., C.T. Rubin, and K.J. McLeod, *Changes in postural muscle dynamics as a function of age*. Journals of Gerontology Series a-Biological Sciences and Medical Sciences, 1999. **54**(8): p. B352-B357.
175. Snow-Harter, C., et al., *Effects of resistance and endurance exercise on bone mineral status of young women: A randomized exercise intervention trial*. Journal of Bone and Mineral Research, 1992. **7**(7): p. 761-769.
176. Gilsanz, V., et al., *Low-Level, High-Frequency Mechanical Signals Enhance Musculoskeletal Development of Young Women With Low BMD*. Journal of Bone and Mineral Research, 2006. **21**(9): p. 1464-1474.
177. Rubin, C., et al., *Prevention of postmenopausal bone loss by a low-magnitude, high-frequency mechanical stimuli: A clinical trial assessing compliance, efficacy, and safety*. Journal of Bone and Mineral Research, 2004. **19**(3): p. 343-351.
178. Muir, J., et al., *Postural instability caused by extended bed rest is alleviated by brief daily exposure to low magnitude mechanical signals*. Gait & Posture, 2011. **33**(3): p. 429-435.
179. Rubin, C., G. Xu, and S. Judex, *The anabolic activity of bone tissue, suppressed by disuse, is normalized by brief exposure to extremely low-magnitude mechanical stimuli*. The FASEB Journal, 2001. **15**(12): p. 2225-2229.
180. Chan, M.E., et al., *Bone structure and B-cell populations, crippled by obesity, are partially rescued by brief daily exposure to low-magnitude mechanical signals*. The FASEB Journal, 2012.

181. Sen, B., et al., *Mechanical signal influence on mesenchymal stem cell fate is enhanced by incorporation of refractory periods into the loading regimen*. Journal of Biomechanics, 2011. **44**(4): p. 593-599.
182. Bacabac, R.G., et al., *Bone cell responses to high-frequency vibration stress: does the nucleus oscillate within the cytoplasm?* FASEB J., 2006. **20**(7): p. 858-864.
183. Dumas, V., et al., *Extracellular Matrix Produced by Osteoblasts Cultured Under Low-Magnitude, High-Frequency Stimulation is Favourable to Osteogenic Differentiation of Mesenchymal Stem Cells*. Calcified Tissue International, 2010. **87**(4): p. 351-364.
184. Prè, D., et al., *Effects of Low-Amplitude, High-Frequency Vibrations on Proliferation and Differentiation of SAOS-2 Human Osteogenic Cell Line*. Tissue Engineering Part C: Methods, 2009. **15**(4): p. 669-679.
185. Rosenberg, N., *The role of the cytoskeleton in mechanotransduction in human osteoblastlike cells*. Human & Experimental Toxicology, 2003. **22**(5): p. 271-274.
186. Lau, E., et al., *Effect of low-magnitude, high-frequency vibration on osteocytes in the regulation of osteoclasts*. Bone, 2010. **46**(6): p. 1508-1515.
187. Tirkkonen, L., et al., *The effects of vibration loading on adipose stem cell number, viability and differentiation towards bone-forming cells*. Journal of the Royal Society Interface, 2011. **8**(65): p. 1736-1747.
188. Zhou, Y., et al., *Osteogenic differentiation of bone marrow-derived mesenchymal stromal cells on bone-derived scaffolds: effect of microvibration and role of ERK1/2 activation*. Eur Cell Mater, 2011. **22**: p. 12-25.
189. Rubin, C.T., et al., *Adipogenesis is inhibited by brief, daily exposure to high-frequency, extremely low-magnitude mechanical signals*. Proceedings of the National Academy of Sciences of the United States of America, 2007. **104**(45): p. 17879-17884.
190. Judex, S., et al., *Low-magnitude mechanical signals that stimulate bone formation in the ovariectomized rat are dependent on the applied frequency but not on the strain magnitude*. Journal of Biomechanics, 2007. **40**(6): p. 1333-1339.
191. Seeman, E. and P.D. Delmas, *Bone Quality — The Material and Structural Basis of Bone Strength and Fragility*. New England Journal of Medicine, 2006. **354**(21): p. 2250-2261.

192. Ozcivici, E., R. Garman, and S. Judex, *High-frequency oscillatory motions enhance the simulated mechanical properties of non-weight bearing trabecular bone*. Journal of Biomechanics, 2007. **40**(15): p. 3404-3411.
193. Trudel, G., et al., *Resistive exercises, with or without whole body vibration, prevent vertebral marrow fat accumulation during 60 days of head-down tilt bed rest in men*. Journal of Applied Physiology, 2012. **112**(11): p. 1824-1831.
194. Owan, I., et al., *Mechanotransduction in bone: Osteoblasts are more responsive to fluid forces than mechanical strain*. American Journal of Physiology-Cell Physiology, 1997. **273**(3): p. C810-C815.
195. Thompson, M.S., et al., *Quantification and significance of fluid shear stress field in biaxial cell stretching device*. Biomechanics and Modeling in Mechanobiology, 2011. **10**(4): p. 559-564.
196. Lau, E., et al., *Effect of low-magnitude, high-frequency vibration on osteogenic differentiation of rat mesenchymal stromal cells*. Journal of Orthopaedic Research, 2011. **29**(7): p. 1075-1080.
197. Funakoshi, M., et al., *Measurement of whole-body vibration in taxi drivers*. Journal of Occupational Health, 2004. **46**(2): p. 119-124.
198. Osawa, Y. and Y. Oguma, *Effects of whole-body vibration on resistance training for untrained adults*. Journal of Sports Science and Medicine, 2011. **10**(2): p. 328-337.
199. Goetz, C.G., *Jean-Martin Charcot and his vibratory chair for Parkinson disease*. Neurology, 2009. **73**(6): p. 475-478.
200. Mester, J., H. Kleinoder, and Z. Yue, *Vibration training: benefits and risks*. Journal of Biomechanics, 2006. **39**(6): p. 1056-1065.
201. Holguin, N., et al., *Brief Daily Exposure to low intensity Vibration Mitigates the Degredation of the Intervertebral Disc in a Frequency-specific Manner*. Journal of Applied Physiology, 2011.
202. Sandhu, E., et al., *Whole body vibration increases area and stiffness of the flexor carpi ulnaris tendon in the rat*. Journal of Biomechanics, 2011. **44**(6): p. 1189-1191.
203. Kiiski, J., et al., *Transmission of Vertical Whole Body Vibration to the Human Body*. Journal of Bone and Mineral Research, 2008. **23**(8): p. 1318-1325.
204. Xie, L., et al., *Low-level mechanical vibrations can influence bone resorption and bone formation in the growing skeleton*. Bone, 2006. **39**(5): p. 1059-66.
205. Turner, C.H., I. Owan, and Y. Takano, *Mechanotransduction in bone: role of strain rate*. Am J Physiol, 1995. **269**(3 Pt 1): p. E438-42.

206. Wang, C.Z., et al., *Low-magnitude vertical vibration enhances myotube formation in C2C12 myoblasts*. Journal of Applied Physiology, 2010. **109**(3): p. 840-848.
207. Takeuchi, R., et al., *Effects of vibration and hyaluronic acid on activation of three-dimensional cultured chondrocytes*. Arthritis & Rheumatism, 2006. **54**(6): p. 1897-1905.
208. Chow, J.W.M. and T.J. Chambers, *INDOMETHACIN HAS DISTINCT EARLY AND LATE ACTIONS ON BONE-FORMATION INDUCED BY MECHANICAL STIMULATION*. American Journal of Physiology, 1994. **267**(2): p. E287-E292.
209. Forwood, M.R., *Inducible cyclo-oxygenase (COX-2) mediates the induction of bone formation by mechanical loading in vivo*. Journal of Bone and Mineral Research, 1996. **11**(11): p. 1688-1693.
210. Romero, J.A., et al., *Analysis of lateral sloshing forces within road containers with high fill levels*. Proceedings of the Institution of Mechanical Engineers Part D-Journal of Automobile Engineering, 2006. **220**(D3): p. 303-312.
211. Tang, Y., C. Grandy, and R. Seidensticker, *Seismic response of annular cylindrical tanks*. Nuclear Engineering and Design, 2010. **240**(10): p. 2614-2625.
212. Humphrey, J.D. and S. DeLange, *An Introduction to Biomechanics* 2004: Springer.
213. Chen, D.J., et al., *Digital Speckle-Displacement Measurementt Using a Complex Spectrum Method*. Applied Optics, 1993. **32**(11): p. 1839-1849.
214. Chiang, F.P., *Evolution of white light speckle method and its application to micro/nanotechnology and heart mechanics*. Optical Engineering, 2003. **42**(5): p. 1288-1292.
215. Chiang, F.P. and G. Uzer, *Mapping full field deformation of auxetic foams using digital speckle photography*. Physica Status Solidi B-Basic Solid State Physics, 2008. **245**(11): p. 2391-2394.
216. Chen, W., M.A. Haroun, and F. Liu, *Large amplitude liquid sloshing in seismically excited tanks*. Earthquake Engineering & Structural Dynamics, 1996. **25**(7): p. 653-669.
217. Li, J., D.B. Burr, and C.H. Turner, *Suppression of prostaglandin synthesis with NS-398 has different effects on endocortical and periosteal bone formation induced by mechanical loading*. Calcified Tissue International, 2002. **70**(4): p. 320-329.

218. Livak, K.J. and T.D. Schmittgen, *Analysis of Relative Gene Expression Data Using Real-Time Quantitative PCR and the 2- $\Delta\Delta$ CT Method*. *Methods*, 2001. **25**(4): p. 402-408.
219. Bauer, H.F. and W. Eidel, *Oscillations of a viscous liquid in a cylindrical container*. *Aerospace Science and Technology*, 1997. **1**(8): p. 519-532.
220. Cox, E.A., J.P. Gleeson, and M.P. Mortell, *Nonlinear sloshing and passage through resonance in a shallow water tank*. *Zeitschrift Fur Angewandte Mathematik Und Physik*, 2005. **56**(4): p. 645-680.
221. Faltinsen, O.M., et al., *Multidimensional modal analysis of nonlinear sloshing in a rectangular tank with finite water depth*. *Journal of Fluid Mechanics*, 2000. **407**: p. 201-234.
222. Kim, Y., *A numerical study on sloshing flows coupled with ship motion - The anti-rolling tank problem*. *Journal of Ship Research*, 2002. **46**(1): p. 52-62.
223. Frame, M.D.S., et al., *Shear stress gradient over endothelial cells in a curved microchannel system*. *Biorheology*, 1998. **35**(4): p. 245-261.
224. Ito, Y., et al., *Effects of Vibration on Differentiation of Cultured PC12 Cells*. *Biotechnology and Bioengineering*, 2011. **108**(3): p. 592-599.
225. Dareing, D.W., D. Yi, and T. Thundat, *Vibration response of microcantilevers bounded by a confined fluid*. *Ultramicroscopy*, 2007. **107**(10-11): p. 1105-1110.
226. Gurkan, U.A. and O. Akkus, *The Mechanical Environment of Bone Marrow: A Review*. *Annals of Biomedical Engineering*, 2008. **36**(12): p. 1978-1991.
227. Fischer, D., et al., *In vitro cytotoxicity testing of polycations: influence of polymer structure on cell viability and hemolysis*. *Biomaterials*, 2003. **24**(7): p. 1121-31.
228. Donahue, T.L.H., et al., *Mechanosensitivity of bone cells to oscillating fluid flow induced shear stress may be modulated by chemotransport*. *Journal of Biomechanics*, 2003. **36**(9): p. 1363-1371.
229. Ponik, S.M. and F.M. Pavalko, *Formation of focal adhesions on fibronectin promotes fluid shear stress induction of COX-2 and PGE2 release in MC3T3-E1 osteoblasts*. *Journal of Applied Physiology*, 2004. **97**(1): p. 135-142.
230. Donahue, S.W., C.R. Jacobs, and H.J. Donahue, *Flow-induced calcium oscillations in rat osteoblasts are age, loading frequency, and shear stress dependent*. *American Journal of Physiology - Cell Physiology*, 2001. **281**(5): p. C1635-C1641.

231. Shafrir, Y. and G. Forgacs, *Mechanotransduction through the cytoskeleton*. American Journal of Physiology-Cell Physiology, 2002. **282**(3): p. C479-C486.
232. Holguin, N., et al., *Brief daily exposure to low-intensity vibration mitigates the degradation of the intervertebral disc in a frequency-specific manner*. J Appl Physiol, 2011. **111**(6): p. 1846-53.
233. Xie, L., et al., *Low-level mechanical vibrations can influence bone resorption and bone formation in the growing skeleton*. Bone, 2006. **39**(5): p. 1059-1066.
234. Uzer, G., et al., *Separating Fluid Shear Stress from Acceleration during Vibrations In Vitro: Identification of Mechanical Signals Modulating the Cellular Response*. Cellular and Molecular Bioengineering, 2012. **5**(3): p. 266-276.
235. Zhang, X., et al., *Cyclooxygenase-2 regulates mesenchymal cell differentiation into the osteoblast lineage and is critically involved in bone repair*. The Journal of Clinical Investigation, 2002. **109**(11): p. 1405-1415.
236. Hoey, D.A., D.J. Kelly, and C.R. Jacobs, *A role for the primary cilium in paracrine signaling between mechanically stimulated osteocytes and mesenchymal stem cells*. Biochemical and Biophysical Research Communications, 2011. **412**(1): p. 182-187.
237. Helmke, B.P. and P.F. Davies, *The Cytoskeleton Under External Fluid Mechanical Forces: Hemodynamic Forces Acting on the Endothelium*. Annals of Biomedical Engineering, 2002. **30**(3): p. 284-296.
238. Davies, P.F., et al., *Spatial relationships in early signaling events of flow-mediated endothelial mechanotransduction*. Annual Review of Physiology, 1997. **59**: p. 527-549.
239. Discher, D.E., P. Janmey, and Y.L. Wang, *Tissue cells feel and respond to the stiffness of their substrate*. Science, 2005. **310**(5751): p. 1139-1143.
240. Uzer, G., et al., *Separating Fluid Shear Stress from Acceleration during Vibrations In Vitro: Identification of Mechanical Signals Modulating the Cellular Response*. Cellular and Molecular Bioengineering: p. 1-11.
241. Hidalgo-Bastida, L.A. and S.H. Cartmell, *Mesenchymal Stem Cells, Osteoblasts and Extracellular Matrix Proteins: Enhancing Cell Adhesion and Differentiation for Bone Tissue Engineering*. Tissue Engineering Part B-Reviews, 2010. **16**(4): p. 405-412.
242. Machesky, L.M. and R.H. Insall, *Scar1 and the related Wiskott-Aldrich syndrome protein, WASP, regulate the actin cytoskeleton through the Arp2/3 complex*. Current Biology, 1998. **8**(25): p. 1347-1356.

243. Zayzafoon, M., S. Botolin, and L.R. McCabe, *p38 and Activating Transcription Factor-2 Involvement in Osteoblast Osmotic Response to Elevated Extracellular Glucose*. Journal of Biological Chemistry, 2002. **277**(40): p. 37212-37218.
244. Genetos, D.C., et al., *Oscillating fluid flow activation of gap junction hemichannels induces ATP release from MLO-Y4 osteocytes*. Journal of Cellular Physiology, 2007. **212**(1): p. 207-214.
245. Saunders, M.M., et al., *Gap junctions and fluid flow response in MC3T3-E1 cells*. American Journal of Physiology - Cell Physiology, 2001. **281**(6): p. C1917-C1925.
246. Wang, N. and D.E. Ingber, *CONTROL OF CYTOSKELETAL MECHANICS BY EXTRACELLULAR-MATRIX, CELL-SHAPE, AND MECHANICAL TENSION*. Biophysical Journal, 1994. **66**(6): p. 2181-2189.
247. Hammerick, K.E., et al., *Pulsed Direct Current Electric Fields Enhance Osteogenesis in Adipose-Derived Stromal Cells*. Tissue Engineering Part A, 2010. **16**(3): p. 917-931.
248. Wall, M.E., et al., *Human adipose-derived adult stem cells upregulate palladin during osteogenesis and in response to cyclic tensile strain*. American Journal of Physiology - Cell Physiology, 2007. **293**(5): p. C1532-C1538.
249. Bergoffen, J., et al., *Connexin mutations in X-linked Charcot-Marie-Tooth disease*. Science, 1993. **262**(5142): p. 2039-2042.
250. Britz-Cunningham, S.H., et al., *Mutations of the Connexin43 Gap-Junction Gene in Patients with Heart Malformations and Defects of Laterality*. New England Journal of Medicine, 1995. **332**(20): p. 1323-1330.
251. Kelsell, D.P., et al., *Connexin 26 mutations in hereditary non-syndromic sensorineural deafness*. Nature, 1997. **387**(6628): p. 80-83.
252. Reaume, A., et al., *Cardiac malformation in neonatal mice lacking connexin43*. Science, 1995. **267**(5205): p. 1831-1834.
253. Simon, A.M., et al., *Female infertility in mice lacking connexin 37*. Nature, 1997. **385**(6616): p. 525-529.
254. Li, Z., et al., *Inhibiting gap junctional intercellular communication alters expression of differentiation markers in osteoblastic cells*. Bone, 1999. **25**(6): p. 661-666.
255. Schiller, P.C., et al., *Gap-junctional communication is required for the maturation process of osteoblastic cells in culture*. Bone, 2001. **28**(4): p. 362-369.

256. Civitelli, R., et al., *Connexin43 mediates direct intercellular communication in human osteoblastic cell networks*. The Journal of Clinical Investigation, 1993. **91**(5): p. 1888-1896.
257. Ilvesaro, J., K. Vaananen, and J. Tuukkanen, *Bone-resorbing osteoclasts contain gap-junctional connexin-43*. Journal of Bone and Mineral Research, 2000. **15**(5): p. 919-926.
258. Schirmacher, K., et al., *Characterization of gap junctions between osteoblast-like cells in culture*. Calcified Tissue International, 1992. **51**(4): p. 285-290.
259. Lecanda, F., et al., *Connexin43 Deficiency Causes Delayed Ossification, Craniofacial Abnormalities, and Osteoblast Dysfunction*. The Journal of Cell Biology, 2000. **151**(4): p. 931-944.
260. Bacabac, R.G., et al., *Nitric oxide production by bone cells is fluid shear stress rate dependent*. Biochemical and Biophysical Research Communications, 2004. **315**(4): p. 823-829.
261. Nomura, S. and T. Takano-Yamamoto, *Molecular events caused by mechanical stress in bone*. Matrix Biology, 2000. **19**(2): p. 91-96.
262. Chan, M., et al., *A Trabecular Bone Explant Model of Osteocyte–Osteoblast Co-Culture for Bone Mechanobiology*. Cellular and Molecular Bioengineering, 2009. **2**(3): p. 405-415.
263. Grimston, S.K., et al., *Role of connexin43 in osteoblast response to physical load*, in *Skeletal Development and Remodeling in Health, Disease, and Aging*, M. Zaidi, Editor 2006, Blackwell Publishing: Oxford. p. 214-224.
264. Riddle, R.C. and H.J. Donahue, *From Streaming Potentials to Shear Stress: 25 Years of Bone Cell Mechanotransduction*. Journal of Orthopaedic Research, 2009. **27**(2): p. 143-149.
265. Turner, C.H., et al., *Do Bone Cells Behave Like a Neuronal Network?* Calcified Tissue International, 2002. **70**(6): p. 435-442.
266. Taylor, A.F., et al., *Mechanically stimulated osteocytes regulate osteoblastic activity via gap junctions*. American Journal of Physiology - Cell Physiology, 2007. **292**(1): p. C545-C552.
267. Batra, N., et al., *Mechanical stress-activated integrin alpha 5 beta 1 induces opening of connexin 43 hemichannels*. Proceedings of the National Academy of Sciences of the United States of America, 2012. **109**(9): p. 3359-3364.
268. Cheng, B., et al., *Expression of Functional Gap Junctions and Regulation by Fluid Flow in Osteocyte-Like MLO-Y4 Cells*. Journal of Bone and Mineral Research, 2001. **16**(2): p. 249-259.

269. Cherian, P.P., et al., *Effects of Mechanical Strain on the Function of Gap Junctions in Osteocytes Are Mediated through the Prostaglandin EP2 Receptor*. *Journal of Biological Chemistry*, 2003. **278**(44): p. 43146-43156.
270. Cherian, P.P., et al., *Mechanical Strain Opens Connexin 43 Hemichannels in Osteocytes: A Novel Mechanism for the Release of Prostaglandin*. *Molecular Biology of the Cell*, 2005. **16**(7): p. 3100-3106.
271. Ziambaras, K., et al., *Cyclic Stretch Enhances Gap Junctional Communication Between Osteoblastic Cells*. *Journal of Bone and Mineral Research*, 1998. **13**(2): p. 218-228.
272. Červenka, I., et al., *Mitogen-Activated Protein Kinases Promote WNT/ β -Catenin Signaling via Phosphorylation of LRP6*. *Molecular and Cellular Biology*, 2011. **31**(1): p. 179-189.
273. Xia, X.C., et al., *Prostaglandin Promotion of Osteocyte Gap Junction Function through Transcriptional Regulation of Connexin 43 by Glycogen Synthase Kinase 3/ β -Catenin Signaling*. *Molecular and Cellular Biology*, 2010. **30**(1): p. 206-219.
274. Watabe, H., et al., *Mechanotransduction activates α (5) β (1) integrin and PI3K/Akt signaling pathways in mandibular osteoblasts*. *Experimental Cell Research*, 2011. **317**(18): p. 2642-2649.
275. Rangaswami, H., et al., *Protein Kinase G and Focal Adhesion Kinase Converge on Src/Akt/ β -Catenin Signaling Module in Osteoblast Mechanotransduction*. *Journal of Biological Chemistry*, 2012. **287**(25): p. 21509-21519.
276. Verbruggen, S.W., T.J. Vaughan, and L.M. McNamara, *Strain amplification in bone mechanobiology: a computational investigation of the in vivo mechanics of osteocytes*. *Journal of the Royal Society Interface*, 2012. **9**(75): p. 2735-2744.
277. Darling, E.M., et al., *Viscoelastic properties of human mesenchymally-derived stem cells and primary osteoblasts, chondrocytes, and adipocytes*. *Journal of Biomechanics*, 2008. **41**(2): p. 454-464.
278. Dick, D.A.T., et al., *Autoradiographic demonstration of inhomogeneous distribution of sodium in single oocytes of *Bufo bufo**. *Journal of Physiology-London*, 1970. **210**(2): p. 305-&.
279. Gouw, T.H. and J.C. Vlugter, *Physical Properties of Triglycerides. I. Density and Refractive Index*. *Fette, Seifen, Anstrichmittel*, 1966. **68**(7): p. 544-549.
280. Heinrich, V. and R.E. Waugh, *A piconewton force transducer and its application to measurement of the bending stiffness of phospholipid membranes*. *Annals of Biomedical Engineering*, 1996. **24**(5): p. 595-605.

281. Guilak, F., J.R. Tedrow, and R. Burgkart, *Viscoelastic Properties of the Cell Nucleus*. Biochemical and Biophysical Research Communications, 2000. **269**(3): p. 781-786.
282. You, J., et al., *Substrate deformation levels associated with routine physical activity are less stimulatory to bone cells relative to loading-induced oscillatory fluid flow*. Journal of Biomechanical Engineering-Transactions of the Asme, 2000. **122**(4): p. 387-393.
283. Jeon, O.H., et al., *Primary Cilia-Mediated Osteogenic Response to Fluid Flow Occurs via Increases in Focal Adhesion and Akt Signaling Pathway in MC3T3-E1 Osteoblastic Cells*. Cellular and Molecular Bioengineering, 2011. **4**(3): p. 379-388.
284. Sen, B., et al., *Mechanical Strain Inhibits Adipogenesis in Mesenchymal Stem Cells by Stimulating a Durable beta-Catenin Signal*. Endocrinology, 2008. **149**(12): p. 6065-6075.
285. Ai, Z., et al., *Wnt-1 regulation of connexin43 in cardiac myocytes*. The Journal of Clinical Investigation, 2000. **105**(2): p. 161-171.
286. Birgersdotter, A., R. Sandberg, and I. Ernberg, *Gene expression perturbation in vitro—A growing case for three-dimensional (3D) culture systems*. Seminars in Cancer Biology, 2005. **15**(5): p. 405-412.
287. Tian, X.F., et al., *Comparison of osteogenesis of human embryonic stem cells within 2D and 3D culture systems*. Scandinavian Journal of Clinical & Laboratory Investigation, 2008. **68**(1): p. 58-67.
288. Andersen, L.K., et al., *Cell Volume Increase in Murine MC3T3-E1 Pre-osteoblasts Attaching onto Biocompatible Tantalum Observed by Magnetic AC Mode Atomic Force Microscopy*. European Cells and Materials
2005. **10**: p. 8.
289. Baik, A.D., et al., *Quasi-3D Cytoskeletal Dynamics of Osteocytes under Fluid Flow*. Biophysical Journal, 2010. **99**(9): p. 2812-2820.
290. Guilak, F., H.A. Leddy, and W. Liedtke, *Transient receptor potential vanilloid 4 The sixth sense of the musculoskeletal system?*, in *Skeletal Biology and Medicine*, M. Zaidi, Editor 2010, Blackwell Publishing: Oxford. p. 404-409.
291. Gao, X., L. Wu, and R.G. O'Neil, *Temperature-modulated diversity of TRPV4 channel gating - Activation by physical stresses and phorbol ester derivatives through protein kinase C-dependent and -independent pathways*. Journal of Biological Chemistry, 2003. **278**(29): p. 27129-27137.

292. O'Neil, R.G., X.C. Gao, and L. Wu, *Mechanosensitive nature of the TRPV4 channel in renal epithelia revealed by siRNA gene silencing*. FASEB Journal, 2005. **19**(5): p. A1163-A1163.
293. Basavappa, S., et al., *Swelling-induced arachidonic acid release via the 85-kDa cPLA(2) in human neuroblastoma cells*. Journal of Neurophysiology, 1998. **79**(3): p. 1441-1449.
294. Thoroed, S.M., et al., *Cell swelling activates phospholipase A(2) in Ehrlich ascites tumor cells*. Journal of Membrane Biology, 1997. **160**(1): p. 47-58.
295. Asselin, P., et al., *Transmission of low-intensity vibration through the axial skeleton of persons with spinal cord injury as a potential intervention for preservation of bone quantity and quality*. Journal of Spinal Cord Medicine, 2011. **34**(1): p. 52-59.
296. Cullen, D.M., R.T. Smith, and M.P. Akhter, *Bone-loading response varies with strain magnitude and cycle number*. Journal of Applied Physiology, 2001. **91**(5): p. 1971-1976.
297. Qin, Y.X., C.T. Rubin, and K.J. McLeod, *Nonlinear dependence of loading intensity and cycle number in the maintenance of bone mass and morphology*. J Orthop Res, 1998. **16**(4): p. 482-9.
298. Baltimore, D., *Our genome unveiled*. Nature, 2001. **409**(6822): p. 814-816.
299. Anderson, K.C., *Oncogenomics to Target Myeloma in the Bone Marrow Microenvironment*. Clinical Cancer Research, 2011. **17**(6): p. 1225-1233.
300. Baron, C., et al., *Prediction of graft-versus-host disease in humans by donor gene-expression profiling*. Plos Medicine, 2007. **4**(1): p. 69-83.
301. Mazilu, J.K. and E.R.B. McCabe, *Moving toward personalized cell-based interventions for adrenal cortical disorders: Part 1-Adrenal development and function, and roles of transcription factors and signaling proteins*. Molecular Genetics and Metabolism, 2011. **104**(1-2): p. 72-79.
302. Razzouk, S. and C. Teixeira, *Personalized implant therapy: new perspectives in bone remodeling assessment*. The New York state dental journal, 2010. **76**(4): p. 50-2.
303. Uzer, G., S. Manske, and S. Judex, *Vibration Induced Mechanical Signals that Increase Proliferation and Osteogenic Commitment of Mesenchymal Stem Cells*. J. Bone Miner. Res., 2012. **26**(Supp. 1): p. Sa0075.
304. Uzer, G., et al., *Cell proliferation is modulated by oscillatory accelerations but not by differences in fluid shear*. J. Bone Miner. Res., 2010. **25**(Supp. 1): p. Mo0049.